EPSC Abstracts
Vol. 10, EPSC2015-14, 2015
European Planetary Science Congress 2015

DAWN ARRIVES AT CERES: RESULTS OF THE SURVEY ORBIT

C. T. Russell (1), C. A. Raymond (2), A. Nathues (3), M. Hoffman(3), M. C. De Sanctis(4), E. Ammannito (1,4), T. H. Prettyman(5), A. S. Konopliv(2), R. S. Park(2), H. Y. McSween(6), C. M. Pieters(7), R. Jaumann(3), M. J. Toplis(8), S. P. Joy(1), C. A. Polanskey(2), M. D. Rayman(2), and the Dawn Science Team
(1) Institute of Geophysics and Planetary Physics, Dept. of Earth, Planetary and Space Sciences, University of California Los Angeles, Los Angeles, CA, USA, (ctrussell@igpp.ucla.edu), (2) Jet Propulsion Laboratory, California Institute of Technology, Pasadena, CA 91109, USA, (3) Max Planck Institute for Solar System Research (MPS), Justus-von-Liebig-Weg 3, 37077 Göttingen, Germany,(4) Istituto di Astrofisica e Planetologia Spaziali, Istituto Nazionale de Astrofisica, Rome, Italy, (5) Planetary Science Institute, Tucson, AZ, USA,(6) Planetary Geoscience Institute and Department of Earth & Planetary Sciences, University of Tennessee, Knoxville, Tennessee 37996–1410, USA, (7) Department of Geological Sciences, Brown University, Rhode Island, USA (8) Dynamique Terrestre et Planétaire (UMR5562), 14 Ave. E. Belin, 31400, Toulouse, France

Abstract

In September 2012 the Dawn spacecraft left Vesta the second most massive body in the asteroid main belt and set sail for Ceres the most massive. On March 6, 2015 Dawn settled into orbit around Ceres becoming the first spacecraft to orbit separately two distant solar orbiting bodies and establishing a new era in space exploration. Unlike Vesta, Ceres has remained hidden from our geochemical eyes into the origin of the asteroid belt, the analysis of meteorites. Ceres has no known associated meteorites nor a family of asteroids. The observations at Ceres return totally new information. Dawn is equipped with a framing camera with one clear and seven color filters, a visible and infrared mapping spectrometer, a gamma ray and neutron spectrometer and radiometric tracking for gravity determination.

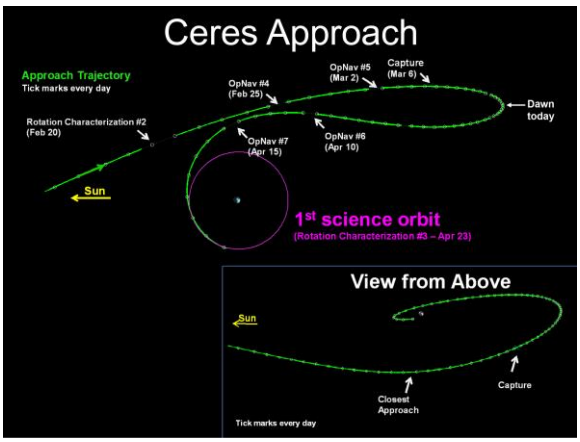

Figure 1: The trajectory that puts Dawn into the RC3 polar orbit. Top: side view. Bottom: view from above.

The approach trajectory is shown in Figure 1. A distant pass over the daylight surface was followed by a distant looping orbit over the dark side. Then in late April Dawn settled into a high altitude orbit known as Rotational Characterization (RC3). On the approach to RC3 the spacecraft found a pair of bright spots on the surface at about 240ºE longitude and 20ºN latitude shown in Figure 2. These two spots were not resolved at the distances flown during approach.

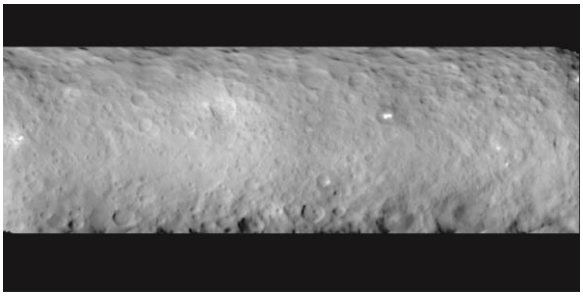

Figure 2: Mosaic of Ceres surface obtained on rotational characterization 2 showing cratered surface and two very bright neighboring spots near 240ºE longitude and 20ºN

The observation campaign in RC3 is illustrated in Figure 3. The orbit is a circular polar orbit. It

crosses the dayside and the nightside. The orbit is ideal for obtaining high phase angle scattering from any plume material emanating from the surface. It also maps the lit surface at 20 times the Hubble resolution. This orbit also provides precise data on the mass, volume and spin axis of Ceres.

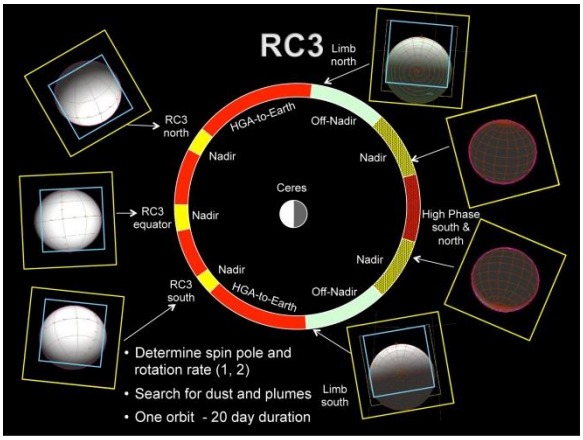

Figure 3: View of Ceres to be seen in the polar RC3 orbit.

In early June the spacecraft enters Survey orbit, optimized for the VIR mapping spectrometer. Figure 4 shows seven of the eight mapping cycles covering

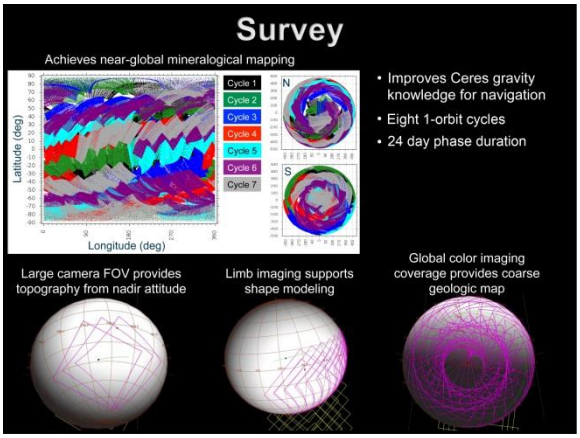

Figure 4: Mapping strategy for camera in the survey orbit.

Ceres during the ensuing three weeks. This provides a comprehensive map of the composition of Ceres' surface. This orbit provides topography shape modeling and global color maps in addition. After this mapping is complete the spacecraft descends to the High Altitude Mapping Orbit (HAMO). This orbit will not be complete by the time of the EPSC meeting.

Summary and Conclusions

Dawn has reached Ceres with sufficient resources to accomplish all its objectives. Ceres has already proven to be a most interesting body, possibly unique in the solar system.

Acknowledgements

We are grateful to NASA, Orbital-ATK and the Jet Propulsion Laboratory for their support during the development, cruise and orbital phases of the mission. Dawn's European partners have provided invaluable support: MPI, DLR, ASI, INAF and IAPS. The Dawn flight team has been particularly adept in operating the craft during its journey.

EPSC Abstracts
Vol. 10, EPSC2015-62, 2015
European Planetary Science Congress 2015

HIGH-RESOLUTION CERES SURVEY ATLAS DERIVED FROM DAWN FC IMAGES. Th. Roatsch[1], E. Kersten[1], K.-D. Matz[1], F. Preusker[1], F. Scholten[1], R. Jaumann[1], C. A. Raymond[2], and C. T. Russell[3], [1]Institute of Planetary Research, German Aerospace Center (DLR), Berlin, Germany, Thomas.Roatsch@dlr.de, [2]JetPropulsion Laboratory, California Institute of Technology, Pasadena, CA, [3]Institute of Geophysics, UCLA, Los Angeles, CA.

Introduction: NASA's *Dawn* spacecraft will orbit the dwarf planet Ceres in June 2015 with an altitude of about 4,400 km to characterize the geology, elemental and mineralogical composition, topography, shape, and internal structure of Ceres before it will be transferred to lower orbits. One of the major goals of the mission is a global mapping of Ceres.

Data: The Dawn mission will map Ceres from three different orbital heights during Survey orbit (4,424 km altitude), HAMO (High Altitude Mapping Orbit, 1474 km altitude), and LAMO (Low Altitude Mapping Orbit, 374 km altitude) [1]. The Dawn mission is equipped with a framing camera (FC) [2]. Dawn will orbited Ceres during Survey in 7 cycles in June 2015. The framing camera will take about 700 clear filter images with a resolution of about 400 m/pixel during these cycles. The images will be taken with different viewing angles and different illumination conditions. We will select the nadir looking images with similar illumination conditions for the global mosaic of Ceres.

Data Processing: The first step of the processing chain is to ortho rectify the images to the proper scale and map projection type. This process requires detailed information of Ceres' topography and will be calculated during the stereo processing of the Survey images [3]. The shape model will be used for the calculation of the ray intersection points while the map projection itself will be done onto a sphere with a mean radius of 470 km. The next step will be the mosaicking of all images to one global mosaic of Ceres, the so called basemap.

Ceres map tiles: The Ceres atlas will be produced in a scale of 1:2,000,000 and will consist of 3 tiles that conform to the subdivision of the synoptic quadrangle scheme proposed by Greeley and Batson [4] and was used e.g., for mapping Vesta in a scale of 1:1,500,000. A map scale of 1:2,000,000 guarantees a mapping at the highest available Dawn resolution in Survey and results in an acceptable printing scale for the hardcopy map of 5 pixel/mm.

Nomenclature: The Dawn team proposed to the International Astronomical Union (IAU) to use the names of gods and goddesses of agriculture and vegetation from world mythology as names for the craters and to use names of of agricultural festivals of the world for other feature names. This proposal was accepted by the IAU and the team will propose names for geological features to the IAU based on the Survey mosaic. These feature names will be applied to the map tiles as shown in Figure 1. The entire Ceres atlas consisting of 3 map tiles will become available to the public through the Dawn GIS web page [http://dawn_gis.dlr.de/atlas].

References: [1] Russell, C.T. and Raymond, C.A., Space Sci. Review, 163, DOI 10.1007/s11214-011-9836-2; [2] Sierks, et al., 2011, Space Sci. Rev., 163, DOI 10.1007/s11214-011-9745-4; [3] Preusker, F. et al., this session; [4] Greeley, R. and Batson, G., 1990, Planetary Mapping, Cambridge University Press.

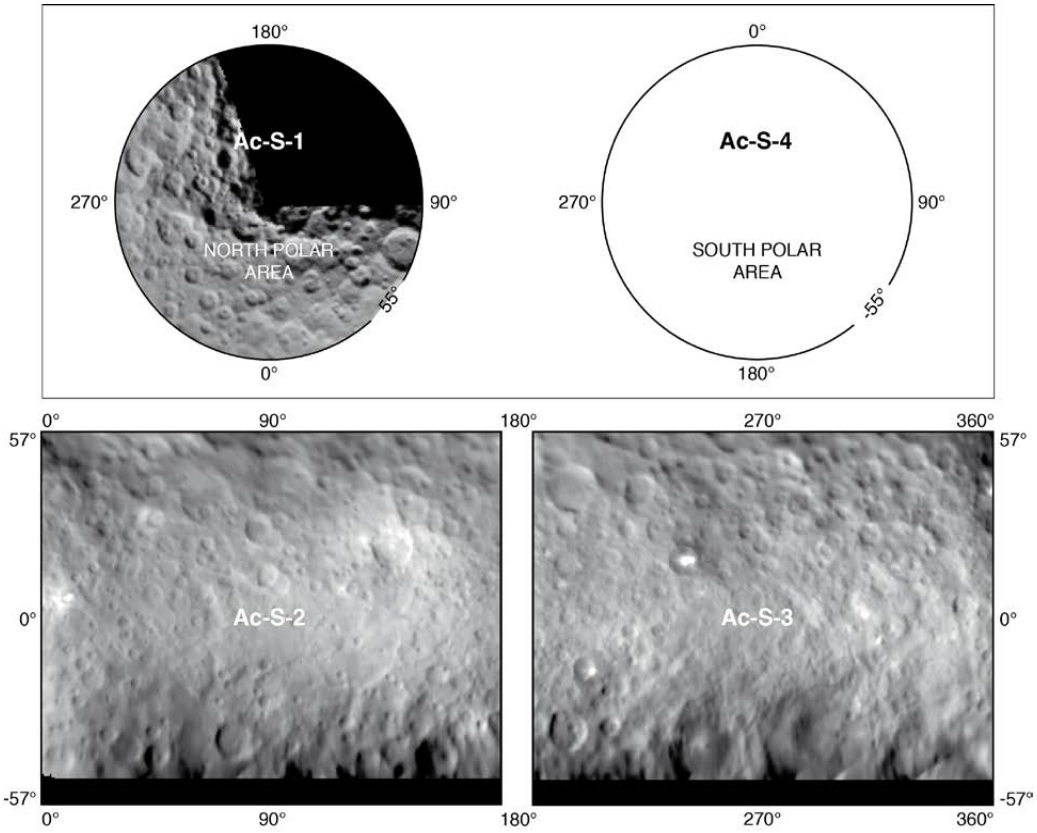

Figure 1: Subdivision of the synoptic quadrangle scheme of the Ceres Survey atlas.

EPSC Abstracts
Vol. 10, EPSC2015-65, 2015
European Planetary Science Congress 2015

The preliminary shape of Ceres

S. Elgner (1), K.-D. Matz (1), T. Roatsch (1), R. Jaumann (1), C.A. Raymond (2) and C.T. Russell (3)
(1) German Aerospace Center, Institute for Planetary Research, Germany (stephan.elgner@dlr.de), (2) Jet Propulsion Laboratory, California Institute of Technology, USA, (3) Institute of Geophysics and Planetary Physics, University of California, USA

Abstract

Methods have been developed [1, 2] to derive the global shape of an asteroid quickly with the help of limb images taken by spacecraft. Topographic profiles are found by applying a contrast-based search along the limb. By minimizing height differences at crossover locations between the individual limb profiles their locations are improved and a global network is created. We used images taken by the Dawn spacecraft during the Ceres approach in February of 2015 to derive the shape of the asteroid. 87 images from the RC1, RC2, OPNAV 4, OPNAV 6, and OPNAV 7 phases have been examined yielding a network of topographic profiles spanning from ca. 78°S to 83°N. By fitting a tri-axial ellipsoid to the data we found Ceres to be an oblate spheroid with axes significantly smaller than previously estimated [3].

1. Introduction

Several methods can be used to determine the global shape of celestial bodies, e.g. laser altimetry, stereo-photogrammetry, and stereo-photoclinometry. Another well-known procedure is the analysis of limb images [4].

2. Image data

We used 87 Dawn FC limb images from the RC1, RC2, OPNAV 4, OPNAV 6, and OPNAV 7 mission phases from February to April of 2015 (Table 1) in a combined analysis. RC1 and RC2 provide data from full rotational periods while the OPNAV limb profiles cover areas between 270°E and 120°E. The whole set of profiles spans from ca. 78°S to 83°N offering an almost global coverage of Ceres' surface (Fig. 1). To avoid bias towards the comparably dense OPNAV data, only selected profiles of these are included in the analysis ensuring a more or less uniformly built network.

Mission phase	Image count	Distance [km]	Resolution [km/px]
RC1	39	83,000	7.6 – 7.8
RC2	36	46,000	4.3
OPNAV 4	5	40,000	3.8
OPNAV 6	4	34,000	3.1
OPNAV 7	3	23,000	2.1

Table 1: Image data overview

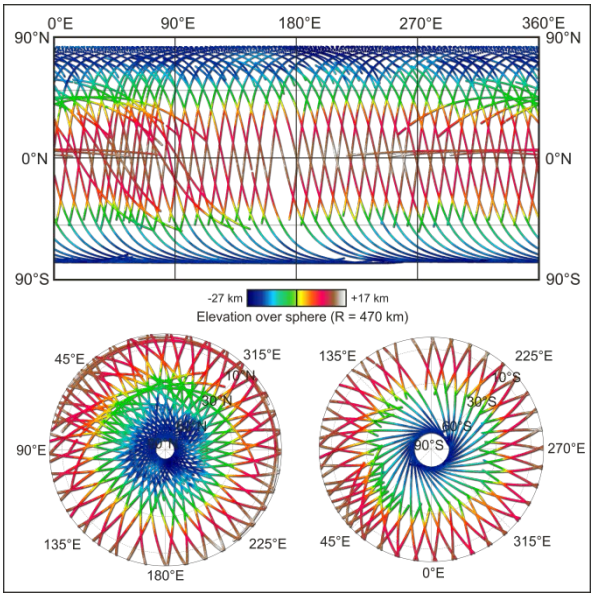

Figure 1: Ceres limb profiles in global equidistant projection (top) and in Lambert azimuthal projection for both hemispheres (bottom)

3. Method

Topographic profiles are found by applying a contrast-based search along the limb. Their locations on a reference sphere are improved by adjusting the exterior camera orientation parameters, i.e. attitude angles, for each limb image using height differences at intersections between the profiles in a least-squares-fit. The selected profiles provide almost 1,700 intersections, with the vast majority residing in the higher northern latitudes.

4. Results

We have fitted a tri-axial ellipsoid with axes of a = 481.0 ± 0.6 km, b = 479.8 ± 0.6, and c = 446.3 ± 0.4 km to the ca. 47,000 object points. The difference between the semi-major axes a and b is within error margins, therefore, Ceres can be described as an oblate spheroid with a significant polar flattening of f = 1/14. The resolution of the network is good enough to resolve large-scale (> 100 km) topographic features, e.g. large basins (Fig. 2).

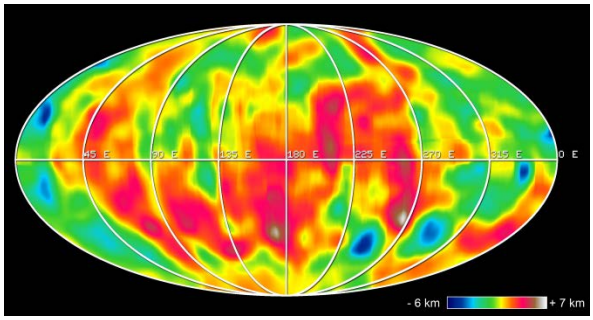

Figure 2: Interpolated digital terrain model in Mollweide projection. Heights are over a biaxial ellipsoid (a = 480 km, c = 446 km).

5. Summary and Outlook

We have derived the shape of Ceres from Dawn FC limb images. Ceres is an oblate spheroid with a significant polar flattening. Large-scale topography is visible in the limb profiles.
The introduction of additional observations from subsequent mission phases will help to further stabilize the network and refine the results. Images with higher resolutions will enable us to identify and measure topographic features at the limb.

References

[1] Elgner, S., Stark, A., Oberst, J., Perry, M.E., Zuber, M.T., Robinson, M.S., and Solomon, S.C.: Mercury's global shape and topography from MESSENGER limb images, Planet. Space Sci. 103, 299–308, 2014.

[2] Oberst, J., Elgner, S., Turner, F.S., Perry, M.E., Gaskell, R.W., Zuber, M.T., Robinson, M.S., and Solomon, S.C., Radius and limb topography of Mercury obtained from images acquired during the MESSENGER flybys. Planet. Space Sci. 59, 1918–1924, 2011.

[3] Thomas, P.C., Parker, J.W, McFadden, L.A., Russell, C.T., Stern, S.A., Sykes, M.V., and Young, E.F.: Differentiation of the asteroid Ceres as revealed by its shape, Nature 437, 224–226, 2005.

[4] Thomas, P.C., Burns, J.A., Helfenstein, P., Squyres, S., Veverka, J., Porco, C., Turtle, E.P., McEwen, A., Denk, T., Giese, B., Roatsch, T. Johnson, T.V., and Jacobson, R.A.: Shapes of the saturnian icy satellites and their significance, Icarus 190, 573–584, 2007.

EPSC Abstracts
Vol. 10, EPSC2015-77, 2015
European Planetary Science Congress 2015

First observations of Ceres by DAWN: obvious two-face tectonics, crossing lineaments, strings of “craters”.

Kochemasov G.G. IGEM of the Russian Academy of Sciences, Moscow, RF, kochem.36@mail.ru

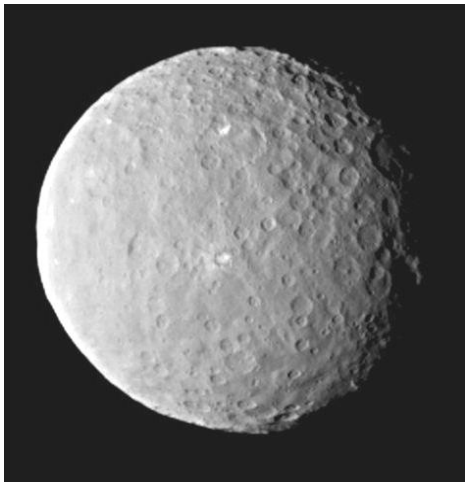

2

1

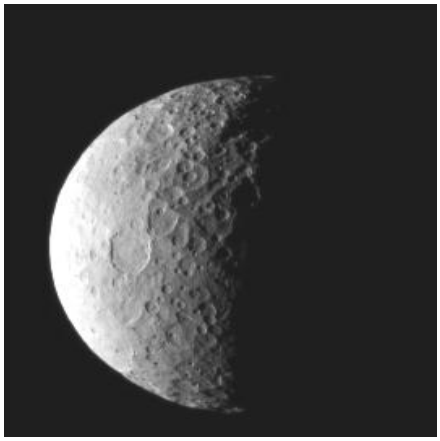

3 4

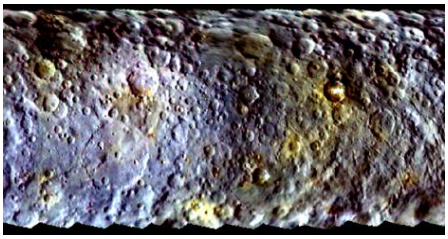

Fig .1 Ceres from 83000 km distance. February 12, 2015. 150212-PIA19056.jpg.
Fig. 2. Ceres from 46000 km distance, February 19, 2015. CeresBig_LR., PIA18923
Fig. 3. Ceres in half shadow, PIA19310_ip.jpg, Distance 40000 km, February 25, 2015.
Fig. 4. Ceres’ global relief. Pia19063
Fig. 5. Ceres’ northern hemisphere from 33000 km, April 10, PIA19064. Crosscutting lineations representing global scale waves.

5

Credit: NASA/JPL/Caltech/UCLA/MPS/DLR/IDA.

Earlier predicted tectonically dichotomous nature of Ceres is obvious even in the first distant observations of the Dawn SC (**Fig. 1-3**). Two faces of Ceres appear as relatively smooth hemisphere and surrounding it rugged with many crater forms one. Tectonically and chemically dichotomous cosmic bodies are due to their movement in keplerian non-circular orbits with periodically changing accelerations. Arising inertia-gravity forces warp the bodies by standing waves. Among them the fundamental wave 1 inevitably presses in one hemisphere and bulges out the opposite one. Thus, two faces adorn any cosmic body.

Other waves, whose lengths are inversely proportional to orbital frequencies of bodies, produce tectonic granulation [1, 2]. A scale is Earth: 1/8760 hours fr. – $\pi R/4$ granule size. Ceres' frequency is 1/106440 hr. This means too large granule-12.2πR. Making modulation of two Ceres' frequencies (rotation 1/9.07 hr and orbiting 1/106440 hr) one gets two side frequencies: 1/85212 hr & 1/965410 hr. Them correspond two granule sizes: 38.4 and 3.4 km. They both are observed in the figures: as ~ lineation spacing (Fig. 1-3, 5) and strings of small circles (Fig. 5).

References: [1] Kochemasov, G.G. Tectonic dichotomy, sectoring and granulation of Earth and other celestial bodies // Proceedings of the International Symposium on New Concepts in Global Tectonics, "NCGT-98 TSUKUBA", Geological Survey of Japan, Tsukuba, Nov 20-23, 1998, p. 144-147. **[2]** Kochemasov, G.G. Theorems of wave planetary tectonics // Geophys. Res. Abstr. 1999. V.1, №3, p. 700. **[3]** Kochemasov, G.G., 2014. From Vesta to Ceres: predicting spectacular dichotomous convexo-concave shape for the largest mini-planet in the main asteroid belt //Vesta in the light of Dawn: first exploration of a protoplanet in the Asteroid Belt, Febr. 3-4, 2014, Houston, Texas, LPI Contribution # 1773, Abstract # 2003. pdf. **[5]** Kochemasov G.G. Ceres' two-face nature: expressive success of the wave planetology // New Concepts in Global Tectonics Journal, v. 3, # 1, March 2015, 63-64.

EPSC Abstracts
Vol. 10, EPSC2015-83, 2015
European Planetary Science Congress 2015

Geomorphology of Ceres: first observations by Dawn

R. Jaumann (1,2), C.T.Russell (3), C. Raymond (4), E. Ammannito (3), D.L. Buczkowski (5), C.M. DeSanctis (6), S. Elgner (1), H. Hiesinger (7), E. Kersten (1), K. Krohn, (1), J.-Y. Li, (8), K.-D. Matz (1), T.B. McCord (9), H.Y. McSween (10), S.C. Mest (11), A. Nathues (12), K. Otto (1), F. Preusker (1) T. Roatsch, (1), P. Schenk (13), F. Scholten (1), F. Schulzeck (1), J.E.C. Scully (3), K. Stephan (1), M. Sykes (8), I. von der Gathen (1), R. Wagner (1), D.A.Williams (14).
(1) DLR, Planetary Research Berlin, Germany, Ralf.Jaumann@dlr.de; (2) Freie Universitaet Berlin, Germany; (3) UCLA, Institute of Geophysics, Los Angeles, CA, USA; (4) Jet Propulsion Laboratory, California Institute of Technology, Pasadena, CA, USA; (5) Johns Hopkins University Applied Physics Laboratory, Laurel, MD, USA; (6) Istituto Nazionale di Astrofisica, Rome, Italy; (7) Westfaelische Wilhelms-Universitaet Muenster, Germany; (8) Planetary Science Institute, Tucson, AZ, USA; (9) Bear Fight Institute, Winthrop, USA; (10) Dep. of Earth and Planetary Sciences, University of Tennessee, Knoxville, TN, USA; (11) Planetary Science Institute, Tucson, AZ, USA (12) Max Planck Institute (MPS) Göttingen, Germany; (13) Lunar and Planetary Institute, Houston, TX, USA; (14) Arizona State University, Tempe, AZ, USA.

Abstract

First observations from the Dawn mission [1] enable the derivation of Ceres' shape, facilitate investigations of the surface geology and provide the first evidence from Dawn for Ceres' geological evolution. At the time of abstract submission data had been acquired during approach to Ceres providing a set of images obtained for optical navigation and rotation characterization with resolutions of up to 3.6 km/pixel (8 times better than Hubble observations), good enough to identify large scale geological features resembling impact, tectonics and probably cryo-processes.

Introduction

Ceres is an oblate spheroidal body with a mean diameter of 950 km, a mass of $(9.43\pm0.05)\cdot10^{20}$kg, a density of about 2077kg/m^3, a rotation period of ~9 hours and an orbital period of 4.6 years [2,3]. The physical properties of Ceres are consistent with a rocky core and a thick outer mantle of water ice and possibly even an ocean of water beneath [3]. Its surface temperatures vary with latitude from 130K at the poles to 180K at the equator, reaching a maximum of 235K [4,5]. This is greater than any creep temperature for known icy compositions, implying Ceres' icy shell to be in hydrostatic equilibrium. Surface albedo determined by HST varies from ~0.07 to ~0.09 [5]. Ceres is classified according to spectral observations as a C- or G- type asteroid, sharing similarities with carbonaceous chondrites. Models constrained by the thermal and compositional conditions demonstrate that Ceres almost certainly differentiated, involving processes such as the formation of a silicate core, a liquid water mantle and a solid ice crust and crustal evolution by tectonics and probable cryovolcanism [3,4]. The Dawn spacecraft [6] reached Ceres March 6th 2015.

Major Geologic Features

Ceres exhibits smooth and rugged topography ranging from about -9 km to 8 km relative to a best-fit ellipsoidal shape with 481x481x447 km (Fig. 1). Ceres' topography has a much greater range in elevation relative to its ellipsoidal dimensions (3.2%) than the Moon and Mars (1% and 0.9%) or Earth (0.3%) but is lower compared to Vesta (15%) [7]. It is comparable to the icy satellite Iapetus (3.6%) but significantly higher than the other icy satellites of Jupiter and Saturn (< 1.8%). The topography of Ceres indicates a rigid crust manifesting a range of processes at large and small scales in the course of its geological evolution

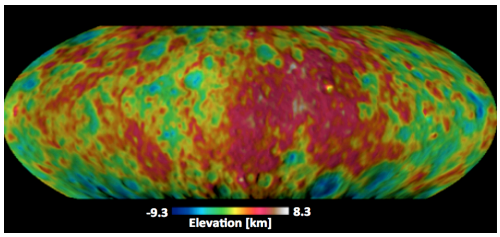

Fig 1: Large-scale topography of Ceres

Ceres's surface is characterized by impact craters, basins of > 250 km in diameter, central peaks and rings and a variety of ejecta blankets (Fig. 2 and 3), as well as lineaments, apparent infills and distinctive bright spots.

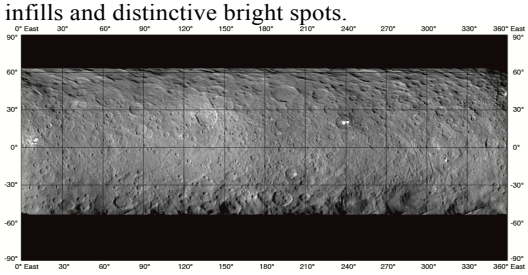

Fig 2: Mosaic of the surface of Ceres (resolution 4 km/pixel)

Impact craters range from fresh to highly degraded, comparable to that of various icy satellites, the Moon and Vesta, indicating an intensive cratering history over the age of the solar system (Fig. 3) as indicated by surface units of different ages. Some craters show upwelling dome-like structures on the crater floor.

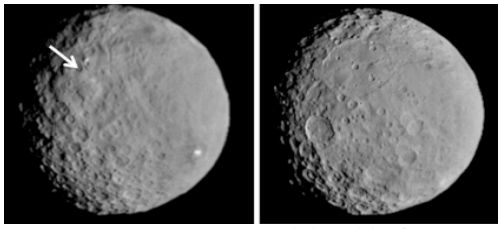

Fig 3: Impact structures and dom-like features

Bright spots occur at different locations correlated with impact structures and significantly higher albedo than the surrounding terrain. These spots seem to be independent of topography (Fig. 4) and indicate material differences and possible time variable effects related to cryo-processes either volcanic or glacial.

Trough-like features and polygonal impact crater rims indicate crustal stress that compensates by tectonic processes (Fig. 5)

According to the relatively high topography to radius ratio steep slopes and possible mass wasting is expected and observed (Fig. 6)

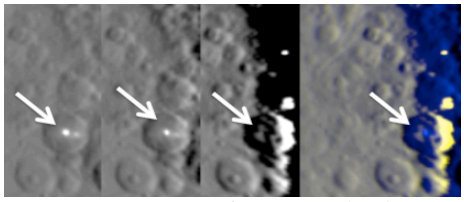

Fig 4: Sequence of rotational observations shows the bright spot at the terminator (right) to be offset of the craters' central peak.

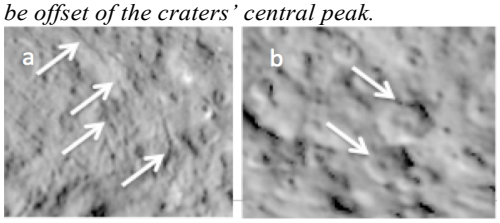

Fig 5 Crustal stress: a) trough-like lineaments, b) polygonal crater rims.

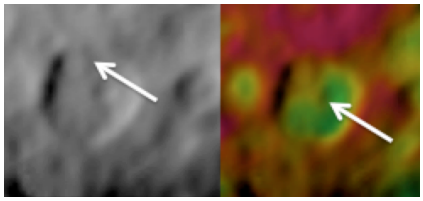

Fig 6 Possible mass wasting on Ceres.

In general, Ceres exhibits various surface features and units that indicate geological activity over time due to impact cratering, tectonics, relaxation, mass displacement and possible cryo-volcanic and/or cryo-glacial processes.

Acknowledgements: The authors gratefully acknowledge the contribution of the Dawn Science, Instruments and Operations Teams.

References: [1] Russell, C.T., Raymond, C., 2011, Space Sci. Rev., 163, p3-23, DOI 10.1007/s11214-011-9836-2; [2] Thomas, P.C. et al., 2005, Nature 437:224-226; [3] McCord, T.B., Sotin, C., 2005, J Geophys Res 110:CiteID05009; [4] Castillo-Rogez, J.C., McCord, T.B., 2009, Icarus: doi:10.1016/j.icarus.2009.04.008. [5] Li, J.-Y., et al., 2006, Icarus 182,143-160; [6] Russell, C.T., et al., 2007, Earth, Moon, and Planets 101,65-91; [7] Jaumann R. et al. (2012) *Science, 336*, 687.

EPSC Abstracts
Vol. 10, EPSC2015-98, 2015
European Planetary Science Congress 2015

Ceres hyperspectral observations by VIR on Dawn: First Results

M.C. De Sanctis[1], E. Ammannito[1,2], F. Capaccioni[1], M.T. Capria[1], G. Carrozzo[1], M. Ciarniello[1], A. Frigeri[1], S. Fonte[1], M.Giardino[1], A. Longobardo[1], G. Magni[1], S. Marchi[1,9], E. Palomba[1], A. Raponi[1], F. Tosi[1], F. Zambon[1], J-P. Combe[3], T.M. McCord[3], L.A. McFadden[4], H.McSween[5], C. M. Pieters[6] , R. Jaumann[7], J-Y Li[8], S. Joy[2], C. A. Polanskey[3], M.D. Rayman[10], C. A. Raymond[10], C. T. Russell[2] and the Dawn Science Team, [1]Istituto di Astrofisica e Planetologia Spaziali, Istituto Nazionale de Astrofisica, Rome, Italy, [2]University of California Los Angeles, Earth Planetary and Space Sciences, Los Angeles, CA-90095, USA, 3Bear Fight Institute, Winthrop, WA, USA; [4]NASA, GSFC, Greenbelt, MD, USA; [5]Department of Earth and Planetary Sciences, University of Tennessee, Knoxville, TN, [6]Institute of Planetary Research, DLR, Berlin, Germany [7]Department of Geological Sciences, Brown University, Providence, RI 02912, USA,8 Planetary Science Institute, [9]SSERVI, Southwest Research Institute , Boulder, CO. , [10]Jet Propulsion Laboratory, California Institute of Technology, 4800 Oak Grove Drive, Pasadena, CA-91109 (mariacristina.desanctis@iaps.inaf.it)

Abstract

The Dawn spacecraft [1] is at Ceres, the second of its targets. Ceres is the most massive body in the asteroid belt and was discovered in 1801 by Giuseppe Piazzi in the Palermo Observatory. It was catalogued by the IAU as a dwarf planet in 2006. Ceres (together with Vesta) represents the key to understand some important points relative to the role of the protoplanet size and the water content in determining the evolution of protoplanets and minor bodies. Ceres is thought to be differentiated, and hydrated minerals were proposed to exist on its surface [2,3]. Its low density [3] associated with the presence of transient water vapour[4], suggests a high content of ice inside the body and on its surface. Ceres seems to have been subject to differentiation and hydrothermal activity, and might host a liquid subsurface layer even today. Dawn is equipped with a Visible and InfraRed Mapping Spectrometer (VIR) [5] that fully accomplishes its scientific objectives at Ceres. Here we report about the first VIR results at Ceres

1. Introduction

VIR is an imaging spectrometer coupling high spectral and spatial resolution in the VIS (0.25-1.0 μm) and IR (0.95-5.0 μm) spectral ranges. VIR will acquire data during Approach, Survey, High Altitude Mapping (HAMO) and Low Altitude Mapping (LAMO) orbits that provided very good coverage of the surface.

2. Results

The surface composition of Ceres is poorly understood through its nearly featureless visible spectrum. Its visible reflectance spectrum has a steep UV absorption edge that begins at a relatively short wavelength, around 0.4 μm, unlike many C-type asteroids where the UV drop-off begins around 0.6 to 0.7 μm [6]. The near-IR spectrum has a strong absorption band centered at about 3-μm. The absorption features in the 3-μm region were attributed to structural water in clay minerals [7,8] but could also be ammoniated clays [9]. Moreover the presence of carbonates and iron-rich clays are reported [10].

On approach to Ceres, Dawn obtains images and hyperspectral data on different occasions, starting in January 2015. VIR data, with resolution larger than Hubble images, will reveal the first details of the Ceres' surface composition and in Fig. 1 are shown two spectra of Ceres taken from two different regions of the surface.

The spectra show large differences in the thermal emission (Fig. 1) corresponding to different temperatures of the surface.

The first data indicates an overall spectral homogeneity but some regions of the surface show spectral differences corresponding to different properties of the surface (Fig.2).

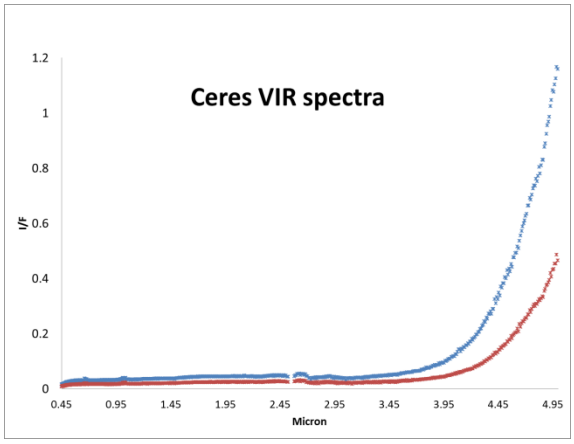

Fig.1 Two VIR spectra taken from the two different regions of Ceres.

Fig.2 RGB image obtained by VIR during the Approach using different VIS and IR color combinations. Top: Image obtained with the following color combination R= 656 nm, G = 530 nm, B = 450 nm; Bottom: Image obtained with the following color combination R = 1.6 μm, G = 2.0 μm, B = 2.4 μm

3. Conclusions

During these last months, VIR observed the surface of Ceres under different illumination conditions and at increasing spatial resolution.
The first spectra acquired show an overall global homogeneity but some differences can be seen on specific regions. VIR observed Ceres also in the thermal infrared range, deriving surface temperatures. These temperatures also show some local diversity. The study of the hyperspectral images from 0.25 to 5 μm will improve our understanding of Ceres composition and thermal properties and will do a step forward in the comprehension of the nature of this dwarf planet.
.

Acknowledgements

VIR is funded by the Italian Space Agency–ASI and was developed under the leadership of INAF-Istituto di Astrofisica e Planetologia Spaziali, Rome-Italy. The instrument was built by Selex-Galileo, Florence-Italy. The authors acknowledge the support of the Dawn Science, Instrument, and Operations Teams. This work was supported by ASI and NASA. A portion of this work was performed at the JPL/NASA.

References

[1] Russell, C.T. et al., Science, 336, 684, 2012.
[2] McCord et al., Space Science Reviews 163:63, 2011
[3] Thomas, P.C., Parker, J.Wm., McFadden, L.A., et al. Nature, 437, 224-226, 2005
[4] Kuppers et al., Nature, 505, 525–527, 2014
[5]De Sanctis M.C. et al., Space Sci. Rev., DOI 10.1007/s11214-010-9668-5 , 2010.
[6] Li et al.,Icarus, doi:10.1016/j.icarus.2005.12.012, 2006
[7] Lebofsky, L.A., Feierberg, M.A., Tokunaga, A.T., Larson, H.P., Johnson, J.R.,. Icarus 48, 453–459. 1981 [8] Feierberg, M.A., Lebofsky, L.A., Larson, H.P.,
Geochim. Cosmochim. Acta 45, 971–981, 1981
[9] King, T.V.V., Clark, R.N., Calvin, W.M., Sherman, D.M., Brown, R.H.,Science 255, 1551–1553, 1992
[10] Rivkin, A.S., Volquardsen, E.L., Clark, B.E., Icarus 185, 563–567, 2006

EPSC Abstracts
Vol. 10, EPSC2015-134, 2015
European Planetary Science Congress 2015

Preliminary Geologic Mapping of the Ac-S-2 Hemisphere of Ceres from NASA's Dawn Mission

D.A. Williams (1), D.L. Buczkowski (2), J.E.C. Scully (3), S.C. Mest (4), R. Jaumann (5), C.T. Russell (3), C.A. Raymond (6), P.M. Schenk (7), S. Marchi (8), D.P. O'Brien (4), A. Nathues (9), M. Hoffmann (9), M. Schäfer (9), T. Platz (9), R.A. Yingst (4), D.A. Crown (4), T. Roatsch (5), E. Kersten (5), F. Preusker (5).
(1) School of Earth & Space Exploration, Arizona State University, Tempe, AZ, USA, David.Williams@asu.edu; (2) Johns Hopkins University Applied Physics Laboratory, Laurel, MD, USA; (3) UCLA, Institute of Geophysics, Los Angeles, CA, USA; (4) Planetary Science Institute, Tucson, AZ, USA; (5) DLR, Planetary Research Berlin, Germany; (6) NASA Jet Propulsion Laboratory, California Institute of Technology, Pasadena, CA, USA; (7) Lunar and Planetary Institute, Houston, TX, USA; (8) Southwest Research Institute, Boulder, CO, USA; (9) Max Planck Institute for Solar System Research, Göttingen, Germany.

Abstract

NASA's Dawn spacecraft [1] was captured into orbit by the dwarf planet (1) Ceres on March 6, 2015. During the Approach phase capture was preceded and followed by a series of optical navigation and rotation characterization observations by Dawn's Framing Camera [FC, 2], which provided the first images of Ceres' surface. As was done at Vesta [3,4], the Dawn Science Team will conduct a geological mapping campaign at Ceres during the Nominal Mission, including iterative mapping using data obtained during each orbital phase. In this presentation we will describe the approach of the Ceres Mapping Campaign and discuss the preliminary geological mapping of the Ac-S-2 (0-180˚E) hemisphere of Ceres.

Ceres Geologic Mapping Campaign

1. Geologic mapping is an investigative process that goes beyond photogeologic analysis by organizing planetary features into discrete process-related map units. These units are defined and characterized based on specific physical attributes (albedo, morphology, structure, color, topography) related to the putative geologic processes that produced them (volcanism, tectonism, impact cratering, weathering-erosion-deposition). Application of stratigraphic principles (superposition, lateral continuity, cross-cutting, embayment, intrusion, etc.) are used to determine the chronologic order of emplacement of the map units. The map units can then be grouped into geologic formations, from which a geologic timescale and geologic history is determined. Thus, geologic maps are *tools* to help interpret the geologic history of a planetary surface.

2. Following on from our successful campaign to map the surface of asteroid Vesta [3,4], the Dawn Science Team will conduct a geologic mapping campaign for dwarf planet Ceres during the Nominal Mission. The goals of this campaign are two-fold: 1) to provide geologic context to the full science team of our ever-improving knowledge of the geology of Ceres with increasing FC spatial resolution during discrete orbital phases of the mission; and 2) to provide geologic context to the Visible and Infrared Spectrometer (VIR) and the Gamma-Ray and Neutron Detector (GRaND) teams to aid in interpreting their compositional information.

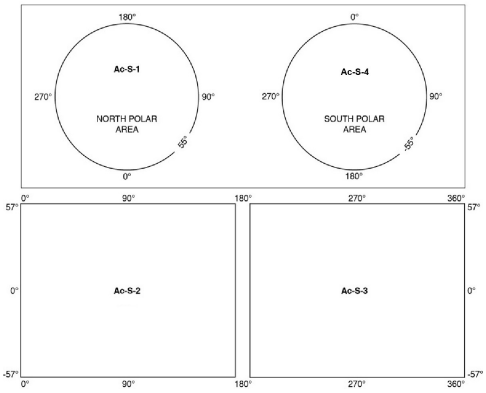

Fig 1: Hemispheric geologic mapping quadrangles for dwarf planet Ceres during the Approach and Survey orbital phases.

3. The first step of the Ceres mapping campaign is to construct a preliminary geologic map using images obtained during the Approach and Survey orbital phases. The purpose of this map is to assess the geology of Ceres at the global scale, to identify global map units and structural features, and determine the geologic processes that have affected

Ceres globally. To accomplish this we will map Ceres using a hemispheric 4-quadrangle system (Fig. 1). In this presentation we will present an overview of the geology of the Ac-S-2 (0-180˚E) hemisphere of Ceres.

First Geological Results

4. The Ac-S-2 (0-180˚E) hemisphere of Ceres shows a surface heavily modified by impact cratering, and is dominated by impact craters, including craters with central peaks at least ≥28 km diameter (Fig. 2). We see fresh, bright-rayed craters and older degraded craters at a variety of size scales. There are variations in crater abundance in different parts of this hemisphere, suggestive of some type of resurfacing process. In particular, a 280-km diameter basin centered near ~10˚S, ~123˚E, the largest impact crater positively identified at the time of this writing, contains smooth-textured (4 km/px resolution), lobate deposits on its floor. Smooth terrain also extends outside the crater to the west, perhaps indicative of a regionally extensive resurfacing process. Domical, positive relief features may also be present in this crater, but require higher resolution imaging before they can be confirmed. Putative mass wasting features have tentatively been identified, but also require confirmation with higher-resolution imaging.

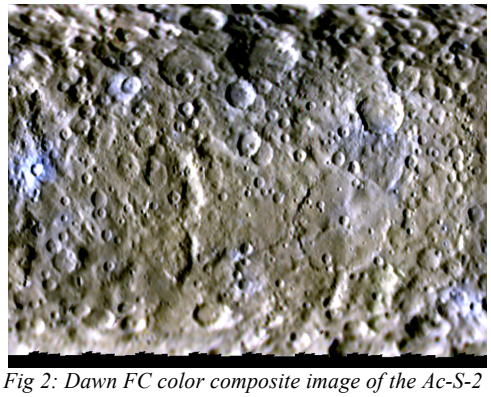

Fig 2: Dawn FC color composite image of the Ac-S-2 (0-180˚) quadrangle of Ceres. Obtained during Approach phase, Rotation Characterization 2 observation, ~4 km/pixel spatial resolution. Color composite RGB is 0.96-0.75-0.44 μm. Image processing by the MPI for Solar System Research, Germany.

5. Preliminary global map units may include Cratered Plains material, Smooth Plains material, Lobate material, Bright-rayed crater material, Crater floor material, and Central Peak material. At present spatial resolution is too low to actually map out contacts and structural features, but we expect to be able to begin constructing the maps using Rotation Characterization #3 and Survey mosaics, to be acquired in May and June 2015.

References:

[1] Russell, C.T., and Raymond, C.A., 2012, Space Sci. Rev., 163, 3-23;
[2] Sierks, H., et al., 2012, Space Sci. Rev., 163, 263-328;
[3] Williams, D.A., et al., 2014, Icarus, 244, 1-12.
[4] Yingst, R.A. et al., 2014, PSS, 103, 2-23.

EPSC Abstracts
Vol. 10, EPSC2015-186, 2015
European Planetary Science Congress 2015

Shape model and rotational state of dwarf planet Ceres from Dawn FC stereo images

Frank Preusker (1), Frank Scholten (1), Klaus-Dieter Matz (1), Thomas Roatsch (1), Stephan Elgner (1), Ralf Jaumann (1), Steve P. Joy (2), Carol A. Polanskey (3), Carol A. Raymond (4), Christopher T. Russell (2)
(1) German Aerospace Center, Institute of Planetary Research, D-12489 Berlin, Germany (Frank.Preusker@dlr.de); (2) UCLA, Institute of Geophysics, Los Angeles, CA 90095-1567, USA; (3) Bear Fight Institute, Winthrop, WA, USA; (4) Jet Propulsion Laboratory, California Institute of Technology, Pasadena, CA 91109-8099, USA

1. Introduction

In 2012, the Dawn mission completed its 14-month observation campaign at asteroid (4) Vesta and entered in March 2015 successfully into the orbit around its final target – the dwarf planet Ceres. Similar to the mapping strategy at Vesta, Ceres will be imaged in three different altitude orbits [1] Survey, High Altitude Mapping Orbit (HAMO), and Low Altitude Mapping Orbit (LAMO) using the onboard camera Dawn FC [2]. In June 2015 Dawn is going to start its Survey orbit and will acquire about 920 clear filter images with a resolution of about 400 m/pixel in eight different cycles. In each cycle Ceres will be mapped completely under similar illumination conditions (Sun elevation and azimuth), but different viewing conditions (by slewing the spacecraft off-nadir). This will allow us to analyze the images stereoscopically and to construct stereo topographic maps. The topography is particularly important because it is essential for derivation of physical properties of Ceres, precise ortho-image registration, mosaicking, and map generation of monochrome/color FC images and VIR images [3]. Furthermore we will determine a precise description of the rotational state of Ceres.

2. Methods

The stereo-photogrammetric processing for Ceres is based on a software suite that has been developed over the last decade. It has been applied successfully to several planetary image data sets [4-6]. The suite comprises photogrammetric block adjustment, multi-image matching, surface point triangulation, digital terrain model (DTM) generation, and base map production.

3. Processing and expected results

We will constrain all Survey clear filter images with our stereo requirements (Table 1) and will achieve at least triple stereo image coverage for the entire illuminated surface. Then we will apply multi-image matching for the set-up of a 3D control network. The control point network defines the input for the photogrammetric least squares adjustment where corrections for the nominal navigation data (pointing and position) will be derived. Furthermore we will refine Ceres's rotational state, formerly determined from Earth-based observations [7, 8]. Finally we will construct a global DTM (shape model) of Ceres with a lateral spacing of 16 pixels per degree (about 520 m/pixel) and a point accuracy of 70 m. As higher resolution data is obtained, the DTM will continue to improve.

4. First results from approach

In February 2015 during the Ceres Approach phase, 76 clear filter images were acquired to investigate the rotational characteristics of Ceres. During two observation sequences (RC1 and RC2) the entire illuminated surface of Ceres was mapped in visible wavelengths as a rotational movie with a nominal image scale of about 8 km/pixel and 4 km/pixel, respectively. We applied our stereo-photogrammetric processing described above and derived a 3D control point network. From that we determined the spin rate of Ceres to be 952.1532 degree/day, which perfectly matches the previous determination from ground-based data [7]. Additionally we refined Ceres's spin axis orientation to be: right ascension = 291.62° ± 0.2°, declination = 66.47° ± 0.1°, which matches within error the values formerly determined from Earth-based observations [8].

Parameters [°]	
Differences in illumination	0-10
Stereo angle	15-50
Incidence angle	0-60
Emission angle	0-60
Phase angle	5-160

Table 1. Requirements for stereo processing.

Finally we adjusted the nominal orientation and applied dense multi-image matching to compute a dense surface point cloud. From that we derived a first surface model of Ceres (see Figure 1) with a lateral spacing of about 4 km/pixel and mean point accuracy of 800 m. The reference coordinate system used to depict the shape model is defined by spin axis orientation (values above) and the prime meridian definition with W_0=170.90° [8]. This reference frame will be finally fixed using Survey orbit observations.

References

[1] Russell C.T. and Raymond C.A.: The Dawn Mission to Minor Planets 4 Vesta and 1 Ceres, Space Sci. Review, 163/1-4, 2012.

[2] Sierks H. et al: The Dawn Framing Camera, Space Science Review, 163, 263-327, 2011.

[3] Roatsch T. et al.: High-Resolution Ceres Survey atlas derived from Dawn FC images, this conference.

[4] Gwinner K. et al.: Topography of Mars from global mapping by HRSC high-resolution digital terrain models and orthoimages: Characteristics and performance, Earth Planet. Science Letters, 294, Issues 3-4, pp. 506-519, 2010.

[5] Preusker F. et al.: Stereo topographic models of Mercury after three MESSENGER flybys, Planetary Space Science, 59, 1910–1917, 2011.

[6] Scholten F. et al.: GLD100 - the near-global lunar 100 meter raster DTM from LROC WAC stereo image data, JGR, Vol. 117, 2012.

[7] Chamberlain M.A. et al.: Ceres lightcurve analysis – Period determination, Icarus 188, 451-456, 2007.

[8] Thomas P.C. et al.: Differentiation of the Asteroid Ceres as revealed by its shape, Nature 437, 224-226, 2005.

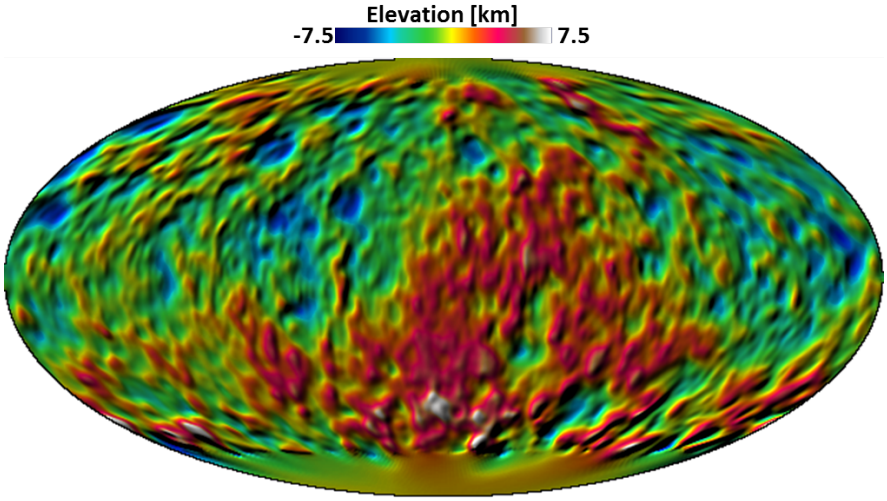

Figure 1. Global RC2 DTM of Ceres centered at 180° with a lateral spacing of about 4 km (hill-shaded color-coded heights) in Mollweide Projection (equal-area). Heights refer to a biaxial ellipsoid (482x482x445 km).

EPSC Abstracts
Vol. 10, EPSC2015-207, 2015
European Planetary Science Congress 2015

Visible and Infrared Spectroscopy of Grosvenor Mountains 95535, howardite

P. Manzari (1), S. De Angelis (1), M.C. De Sanctis (1), E. Ammannito (1,2), D. W. Mittlefehldt (3) F. Altieri (1)

[1]Institute for Space Astrophysics and Planetology, IAPS-INAF, Rome, Italy; [2]University of California Los Angeles, Earth Planetary and Space Sciences, Los Angeles, CA-90095, USA; [3]Astromaterials Research Office, NASA Johnson Space Center, 2101 NASA Parkway, Houston, TX 77058 , USA

1. Introduction

In order to strengthen the linkage between Vesta and HED spectral composition, a set of HED meteorites (33 samples) have been investigated with different laboratory setups at INAF-IAPS. Among these, the SPectral IMager facility is a laboratory VIS-IR spectrometer [1] developed to support the DAWN mission [2], which is now in orbit around Ceres. Here, we report reflectance spectral data related to powdered samples (<75μm) of one howardite, Grosvenor Mountain 95535, measured by means of the SPIM facility.

2. Petrographic description

Grosvenor Mountain 95535 (GRO95535) is an antarctic meteorite that does not show severe weathering (type A/B, [3]). It belongs to a pairing group consisting of GRO 95534, 95535, 95574 and 95581, (GRO 95602 was suggested to be paired with these, but its distinct cosmic-ray exposure age shows it is not paired with them [4]) The pairing group shows a groundmass of orthopyroxene and pigeonite and plagioclase (grains up to 0.2 mm), with a few larger mineral clasts and rare polymineralic lithic clasts up to 2.5 mm across. Microprobe analyses show a wide range in pyroxene compositions: Wo1-44, Fs14-80, En6-80, but with coarse-grained orthopyroxenes clustered around Wo1-4, Fs21-38, En60-78 [6]. Plagioclase compositions are An86-93 [3]. Monomineralic pyroxene clasts (≤ 3 mm) have mineral compositions that correspond to diogenites, basaltic eucrites and cumulate eucrites [5, 6].

3. Visible and Infrared Imaging Spectroscopy of Gro 95535

SPIM is a spare of the spectrometer on Dawn spacecraft [7]. It works in the 0.22-5.05 μm spectral range, with a spatial resolution of 38x38 μm on the target. Two bidimensional focal plane arrays, one for the visible between 0.22 and 1.05 μm (spectral resolution of 2 nm) and one for the IR between 0.95 and 5.05 μm (spectral resolution of 12 nm) allow to obtaining the spectral coverage. Thanks to the alignment of the bidimensional focal planes with the spectrometer' slit axis (the slit is 9x0.038 mm in size), it is possible to acquire the target's image of 0.038x9 mm at different wavelengths.

The chip 13 of GRO95535 [6] in form of powder with diameter <75 μm was analyzed. Ten adjacent lines (fig.1) were acquired on the powder, thus an area of 9 mm x 0.38 mm. We can observe that the average spectrum of GRO 95535 is characterized in the VNIR range by the two strong Fe^{2+} absorptions at 1 and 2 μm that are indicative of dominant pyroxene mineralogy (fig.2). The broad absorption band in the IR centered at 3 μm is due to water (likely of terrestrial origin). Several features that appear at about 1.4, 2.5 and 3.75 μm are instrumental artifacts, while the feature around 4.2 μm is due to ambient CO_2. The SPIM capability is to have a spectral image and thus to investigate pixel by pixel the single spectrum, or a spectral cluster, to better characterize the mineralogy of the sample. Although in a single pixel we can observe the effect of more mineral phases, in this case we observe on almost all these pixels the spectral features of orthopyroxene (fig.3). Furthermore, we can say that there are differences in orthopyroxene composition, in fact we observe different positions of the 1μm absorption band that represent variations of Ca and/or Fe [8,9] in M1 and M2 octahedral sites.

4. Figures

Figure 1: RGB crop image of GRO95535 powder. Ten adjacent lines have been acquired on the sample, at consecutive steps of 0.038 mm, matching the spectrometer slit width. Thus the observed area corresponds to 9x0.38 mm.

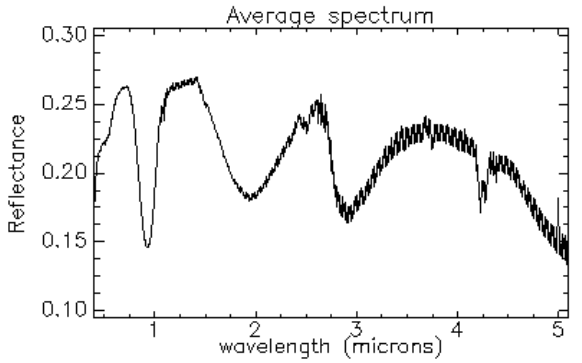

Figure 2: VIS-IR average reflectance spectrum of GRO95535 powder

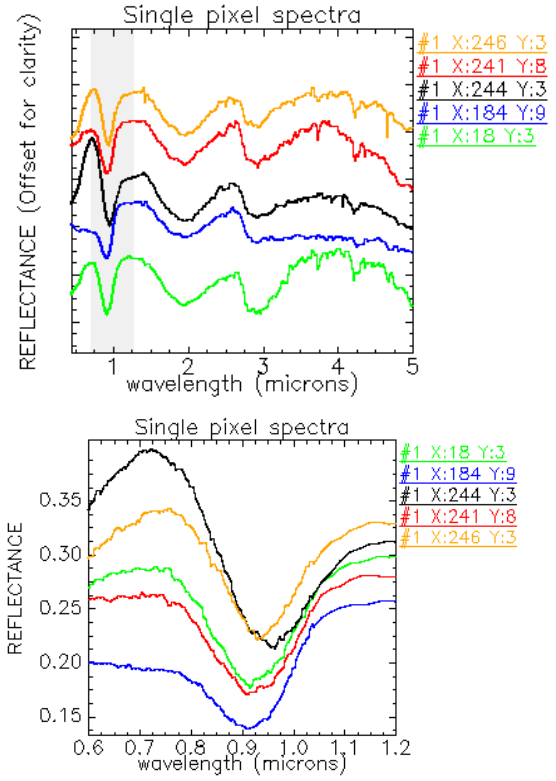

Figure 3: Single pixel spectra on GRO 95535 powder and crop of spectra at 1μm band.

5. Summary and Conclusions

The peculiarity of SPIM stands in the combination of the high spatial resolution imaging, high spectral resolution and wide spectral range. With these technical features, SPIM is capable to collect spectral images data on minerals and rock slabs hence potentially to better identify mineralogy features of components with grain size greater than 0.038 mm. In fact, although the average reflectance spectra in the 0.45-5.0 μm range show that pyroxene dominates the mineralogy of the analyzed samples, the high spatial resolution allowed to observe the spectral variability of the pyroxene. In particular, the different position of 1-micron band could be attributed to an increasing of iron or calcium in the structure.

Acknowledgements

This work is supported by the Italian Space Age Agency (ASI), ASI-INAF Contracts n. I/004/12/0.

References

[1] De Angelis S., et al., The Spectral Imaging facility: setup characterization, Rev.Sci.Instruments, submitted, (2015)

[2] Russell, C.T. et al., "Dawn: A journey in space and time". Planetary and Space Science, 52, pp 465–489, (2004).

[3] Meteoritical Bullettin Database

[4] Cartwright J.A., Ulrich O., Mittlefehldt D.W., The quest for regolithic howardites. Part 2: Surface origins highlighted by noble gases. Geochimica et Cosmochimica Acta 140, 488-508 (2014).

[5]Lunning H. Y., McSween Jr. and A. W. Beck , Heterogeneity in the vestan regolith: evidence from the Gro 95 HED pairing group. 76th Annual Meteoritical Society Meeting, 5254, (2013)

[6] Mittlefehldt David W., Herrin Jason S., Quinn Julie E., Mertzman Stanley A., Cartwright Julia A., Mertzman Karen R., Peng Zhan X., Composition and petrology of HED polymict breccias: The regolith of (4) Vesta Meteoritics & Planetary Science 48, 2105-2134 (2013).

[7] De Sanctis M.C., et al: The VIR Spectrometer, Space Sci Rev DOI 10.1007/s11214-010-9668-5, 2010.

[8] Klima Rachel L., Pieters Carle M., Dyar M. Darby Spectroscopy of synthetic Mg-Fe pyroxenes I: Spin-allowed and spin-forbidden crystal field bands in the visible and near-infrared Meteoritics & Planetary Science 42, Nr 2, 235–253 (2007)

[9] Klima Rachel L., Dyar M. Darby, Pieters Carle M. Near-infrared spectra of clinopyroxenes: Effects of calcium content and crystal structure Meteoritics & Planetary Science 46, Nr 3, 379–395 (2011)

EPSC Abstracts
Vol. 10, EPSC2015-218, 2015
European Planetary Science Congress 2015

Ceres Photometry and Albedo from Dawn Framing Camera Images

S.E. Schröder (1), S. Mottola (1), H.U. Keller (1,2), J.-Y. Li (3), K.-D. Matz (1), K. Otto (1), T. Roatsch (1), K. Stephan (1), C.A. Raymond (4), and C.T. Russell (5)
(1) Deutsches Zentrum für Luft- und Raumfahrt (DLR), 12489 Berlin, Germany (stefanus.schroeder@dlr.de), (2) Institut für Geophysik und extraterrestrische Physik (IGEP), Technische Universität Braunschweig, 38106 Braunschweig, Germany, (3) Planetary Science Institute, Tucson, AZ 85719-2395, U.S.A., (4) Jet Propulsion Laboratory (JPL), California Institute of Technology, Pasadena CA 91109, U.S.A., (5) Institute of Geophysics and Planetary Physics, University of California (UCLA), Los Angeles CA 90095, U.S.A.

1. Introduction

The Dawn spacecraft is in orbit around dwarf planet Ceres. The onboard Framing Camera (FC) [1] is mapping the surface through a clear filter and 7 narrow-band filters at various observational geometries. Generally, Ceres' appearance in these images is affected by shadows and shading, effects which become stronger for larger solar phase angles, obscuring the intrinsic reflective properties of the surface. By means of photometric modeling we attempt to remove these effects and reconstruct the surface albedo over the full visible wavelength range. Knowledge of the albedo distribution will contribute to our understanding of the physical nature and composition of the surface.

2. Photometric Modeling

The availability of images acquired at a range of illumination geometries allows the construction of photometric models for the reflectance (r_F) of the surface. We employ models that can be separated into a phase function (A_{eq}), describing the brightness as a function of phase angle (α), and a disk function (D), describing the brightness as a function of incidence and emission angles (ι, ε) [2]:

$$r_F(\iota, \varepsilon, \alpha) = A_{eq}(\alpha)\, D(\iota, \varepsilon, \alpha).$$

We evaluate various disk functions (Lambert, Lommel-Seeliger, Minnaert, Akimov) for their effectiveness and determine the phase function for each of the FC filters. We address how the photometric model parameters may provide insight into the physical properties of the surface.

3. Surface Albedo

Once a photometric model has been established, we can photometrically correct the images. This involves dividing the observed image by a model image, calculated from the photometric angles given by a shape model (Fig. 1). We use a shape model provided by JPL and project the images using the USGS ISIS software. In principle, after photometric correction the brightness distribution is governed by the intrinsic reflective properties of the surface material, i.e. the albedo. In reality we also deal with pointing inaccuracies and imperfections of the shape model and the photometric model.

Figure 1: An example of photometrically correcting a Framing Camera image of Ceres. At left the original image as acquired on approach, in the center a model image, at the right the ratio of the two, showing the albedo distribution over the surface.

On approach to Ceres, the FC imaged the surface at relatively low phase angles, for example during the RC1 phase, which favors the albedo reconstruction. We use these images to construct an albedo map of the surface. In light of the detection of water around Ceres [3], which suggests the dwarf planet is active, it is worthwhile to compare our map to previous maps made from HST [4] and Keck [5] images, and evaluate whether any surface changes occurred over the last decade. This requires degrading the FC map

resolution to match that of the other instruments, preferably by means of convolution with the point spread function.

4. Summary

We construct photometric models for the surface reflectance of Ceres. We employ these models to photometrically correct Dawn Framing Camera images and use these to map the albedo. We compare our map to existing albedo maps to identify any surface changes.

References

[1] Sierks, H., Keller, H.U., Jaumann, R., *et al*.: The Dawn Framing Camera. Space Science Reviews 163, pp. 263–327, 2011.

[2] Kaasalainen, M., Torppa, J., and Muinonen, K.: Optimization methods for asteroid lightcurve inversion. II. The complete inverse problem. Icarus 153, pp. 37–51, 2001.

[3] Küppers, M., O'Rourke, L., Bockelée-Morvan, D. *et al*.: Localized sources of water vapour on the dwarf planet (1) Ceres. Nature 505, pp. 525–527, 2014.

[4] Li, J.-Y., McFadden, L., Parker, J.W. *et al*.: Photometric analysis of 1 Ceres and surface mapping from HST observations. Icarus 182, pp. 143–160, 2006.

[5] Carry, B., Dumas, C., Fulchignoni, M. *et al*.: Near-infrared mapping and physical properties of the dwarf-planet Ceres. A&A 478, pp. 235–244, 2008.

EPSC Abstracts
Vol. 10, EPSC2015-219, 2015
European Planetary Science Congress 2015

Geomorphological related albedo features on Ceres

K. Krohn (1), K.-D. Matz (1), R. Jaumann (1,2), K. Otto (1), J.Y. Li (3), D. Buczkowski (4), M. C. De Sanctis (5), I. von der Gathen (1), E. Kersten (1), T. Kneissl (2), S. Mest (3), F. Preusker (1), T. Roatsch (1), S. Schröder (1), F. Schulzeck (1), J.E.C. Scully (6), N. Schmedemann (2), K. Stephan (1), F. Tosi (5), R.J. Wagner (1), D.A. Williams (7), C. A. Raymond (8), C. T. Russell (6)

(1) Institute of Planetary Research, German Aerospace Center (DLR), Berlin, Germany (Katrin.Krohn@dlr.de), (2) Freie Universität Berlin, Planetary Sciences and Remote Sensing, Berlin, Gemany, (3) Planetary Science Institute, Tucson, AZ, USA, (4) Johns Hopkins University Applied Physics Laboratory, Laurel, MD, USA, (5) Istituto Nazionale di Astrofisica, Rome, Italy, (6) UCLA, Institute of Geophysics, Los Angeles, CA, USA, (7) Arizona State University, Tempe, AZ, USA, (8) Jet Propulsion Laboratory, California Institute of Technology, Pasadena, CA, USA

1. Introduction

NASA's Dawn spacecraft entered orbit of Ceres on March 6, 2015, to spend one year characterizing the geology, elemental and mineralogical composition, topography, shape, and internal structure of the Ceres [1]. Ceres is supposed to be differentiated into a silicate core, a liquid water mantle and a solid ice crust with a surface temperature from 130K to 235K [2,3]. At the time of writing, the acquired image data from Ceres provide a spatial resolution of up to 2.1 km/pixel. The surface of Ceres reveals some albedo features that seem to be related to geomorphology. Those features show either a high or a low albedo compared to the surrounding.

2. Method

We measured the radiance factor of several pixels (different colored rectangles in figure 2, 3 and 5) over local time on the two bright spot features HST#1 and HST#5 and their surroundings.

3. Albedo features on Ceres

At ~11°E and 5.5°N a bright hill with a crater on the summit occurs (figure 1). The feature so far is named as HST#1 in the Hubble Space Telescope (HST) albedo map by [4] (figure 2).

Bright material also occurs as spots on crater walls and floors. The HST#5 feature at ~300°E and 20°N (figure 4) consists of both types and shows an average albedo with radiance factor of up to 0.12 over 15 km of area (figure 5).

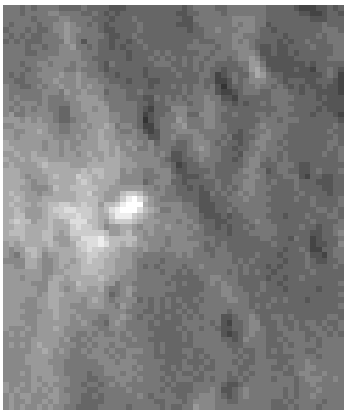

Figure 1: Bright material of HST#1.

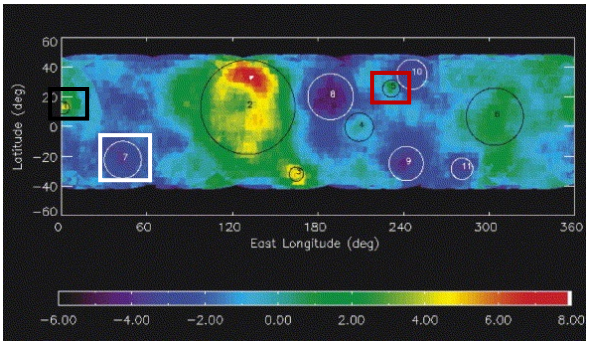

Figure 2: Albedo map from [4] showing the locations of HST#1 (black box) and HST#5 (red box) and HST#7 (white box) as identified by HST.

Bright material is distributed as radially rays around the crater. The surface radiance factor is up to 0.08 over 10 km of area(figure 3).

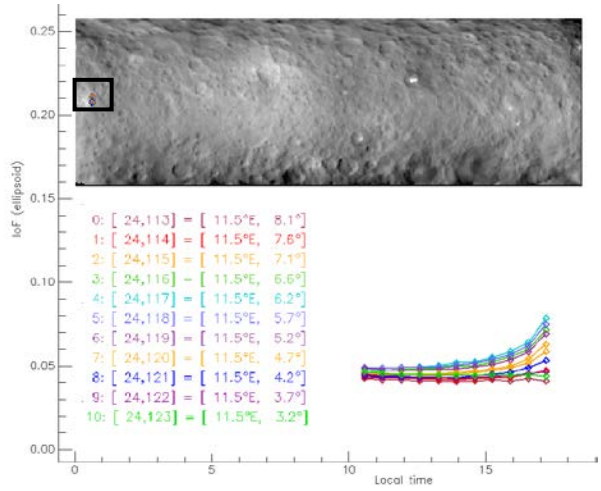

Figure 3: The figure shows the radiance factor of several pixels of HST#1 and its surroundings over the local time. The highest albedo of HST#1 (black box) is shown as light blue curve.

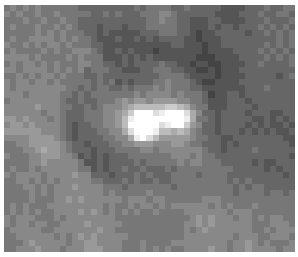

Figure 4: The two bright spots of HST#5.

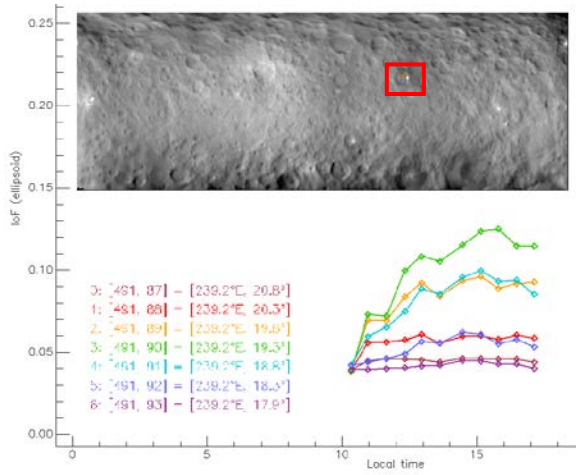

Figure 5: The figure shows the radiance factor of several pixels of HST#5 (red box) and its surroundings over the local time. The green curve shows the highest radiance factor.

Such features could be the result of exhalation of ice by cryovolcanism, or of ejected bright material, such as subsurface ice.

Ceres´ surface also reveals some darker regions. For example in the southern hemisphere between 30°E - 65°E and 25°S – 55°S darker plains, so-called HST#7 (figure 2, 6) are visible. The plains consist of smooth darker material possibly related to mass wasting.

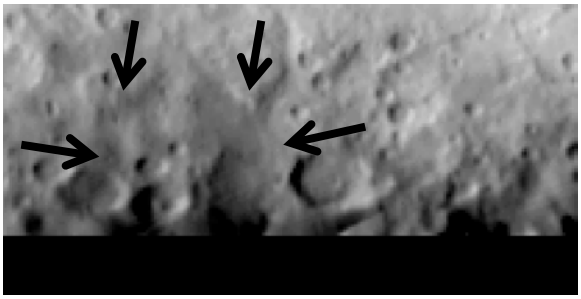

Figure 6: Darker plains of HST#7 (arrows).

In order to constrain whether the origin of the bright and dark material is endogenic or exogenic we will study the morphology and albedo parameters of these features in detail as soon as higher resolution data is available.

Acknowledgements

We thank the Dawn team for the development, cruise, orbital insertion, and operations of the Dawn spacecraft at Vesta. Dawn data are archived with the NASA Planetary Data System. K. Krohn is supported by the Helmholtz Association (HGF) through the research Helmholtz Postdoc Program.

References

[1] Russell, C.T., Raymond, C.: The Dawn Mission to Vesta and Ceres, Space Sci. Rev., Vol. 163, pp. 3-23, 2011.
[2] McCord, T.B. and Sotin, C.: Ceres: Evolution and current state, J Geophys Res, Vol. 110, E5, 2005.
[3] Castillo-Rogez, J.C. and McCord, T.B.: Ceres' evolution and present state constrained by shape data, Icarus, Vol. 205, pp. 443-459, 2010.
[4] Li, J.Y. et al.: Photometric analysis of 1 Ceres and surface mapping from HST observations, Icarus, Vol. 182, pp. 143-160, 2006.

EPSC Abstracts
Vol. 10, EPSC2015-248, 2015
European Planetary Science Congress 2015

Global stratigraphy of the dwarf planet Ceres from RC2 imaging data of the Dawn FC camera

R. J. Wagner (1), N. Schmedemann (2), T. Kneissl (2), K. Stephan (1), K. Otto (1), K. Krohn (1), S. Schröder (1), E. Kersten (1), T. Roatsch (1), R. Jaumann (1), D. A. Williams (3), R. A. Yingst (4), D. Crown (4), S. C. Mest (4), and C. T. Russell (5)
(1) Institute of Planetary Research, German Aerospace Center (DLR), Berlin, Germany (Email: roland.wagner@dlr.de); (2) Inst. of Geological Sciences, Free University Berlin, Germany; (3) School of Earth & Space Exploration, Arizona State University, Tempe/Az., USA; (4) Planetary Science Institute, Tucson, Az., USA; (5) Inst. of Geophysics & Planetary Physics, UCLA, Los Angeles, Ca., USA.

Abstract

On March 6, 2015, the Dawn spacecraft was captured into orbit around Ceres. During its approach phase since Dec. 1, 2014, imaging data returned by the framing camera (FC) have increased in spatial resolution exceeding that of the Hubble Space Telescope. In this paper, we use these first images to identify and map global geologic units and to establish a stratigraphic sequence.

1. Introduction

Since Dec. 1, 2014, the FC framing camera aboard the Dawn spacecraft [1][2] has taken several hundred images of the dwarf planet (1) Ceres with increasing spatial resolution. These images comprise optical navigation (OpNav #2 to #7) as well as rotational characterization (RC #1 & #2) sequences. For this work, images from sequence RC2 with a spatial resolution exceeding that of Hubble Space Telescope by about a factor of 7 are primarily used.

2. Methodology

Individual images as well as a global mosaic derived from the RC2 images were used for geologic mapping and crater counts. The images were processed according to the procedure described in [3]. Geologic units are identified with respect to morphology and superimposed crater frequency. In addition, topography was taken into account as a mapping criterion. The topographic information was taken from a digital terrain model (DTM) derived by [4]. Cratering model ages were obtained from crater counts in the mapped units using the cratering chronology model by Schmedemann et al. [5][6].

3. Geologic units and ages

Broadly, five units can be distinguished in terms of morphology, superimposed crater frequency and topography: (1) two generally densely cratered plains units found in a number of locations and topographic levels, designated as *cpdh* (high terrain) or *cpdl* (low terrain); (2) two sparsely cratered plains units, either topographically high (*cpsh*) or low (*cpsl*); and (3) the topographically low smooth floor of a large impact crater or basin, ~ 280 km in diameter (*bfs*). Three examples for crater counts on these units are shown in Fig. 1.

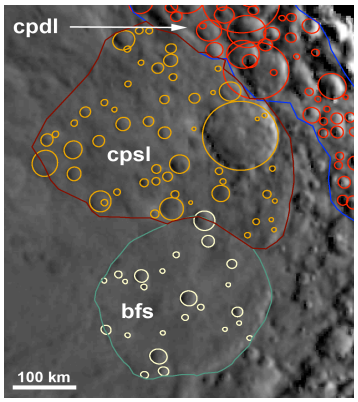

Figure 1: Detail of a geologic map with crater counts. The center of the large crater/basin (unit *bfs*) is located at lat. 11° S, long. 124° E.

Figure 2 shows the stratigraphic relationship of these units from measured crater frequencies. A sequence of geologic events forming these units can clearly be

derived from the data. Oldest units are the densely cratered plains, showing cratering model ages [6] on the order of 3.7 – 3.8 Ga. Between the higher (*cpdh*) and lower (*cpdl*) variety no clear separation in model age can be made. The sparsely cratered plains are in general younger than the densely cratered plains and seem to have a wider span in cratering model age. A topographically low area of this unit (*cpsl*), located adjacent to the north of the 280-km crater/basin, has a model age of 3.4±0.2 Ga. From the crater frequency measured on the floor of this large crater/basin (unit *bfs*), a model age of 1.8±0.6 Ga could be determined. A topographically higher area of unit *cpsh* shows a comparable model age of 2.0±0.3 Ga. These two units are the youngest found so far on Ceres.

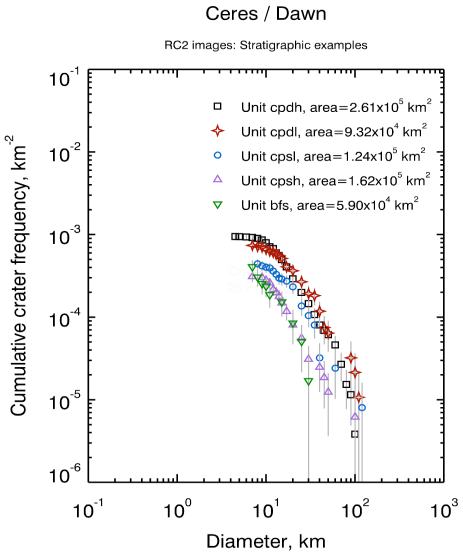

Figure 2: Cumulative crater frequency diagram of five geologic units, mapped and measured in RC2 images of the Dawn FC camera. The units are separable by their superimposed crater frequency.

4. Summary

The geologic units mapped in the RC2 images, supported by using a DTM [4], can be separated by their superimposed crater frequencies and show a clear stratigraphic sequence. Oldest units are the densely cratered plains (*cpdh*, *cpdl*), more or less independent of their topographic level. Youngest unit mapped is the smooth floor of a 280-km large crater/basin (*bfs*). The cratering model age derived on the areas of sparsely cratered plains (*cpsh*, *cpsl*) lie in between the impact feature (*bfs*) and the densely cratered plains.

The crater frequencies superposed on some of the measurement areas imply possible resurfacing processes. Slopes of the cumulative distributions become flatter below a given crater diameter on the order of ~ 30-60 km but are steeper again at craters smaller this size. This feature has to be investigated further in high-resolution data.

Further work using higher-resolution images involves the identification of stratigraphic key horizons in order to subdivide the geologic record of Ceres into a sequence of time-stratigraphic systems and, based on a cratering chronology model, into chronologic periods. The prerequisite to do this is the confirmation of suggested feature names by IAU.

References

[1] Russell, C. T., and Raymond, C. A.: The Dawn Mission to Vesta and Ceres. Space Sci. Rev. 163, 3-23, 2011.

[2] Sierks, H., et al. : The Dawn Framing Camera. Space Sci. Rev. 163, 263-327, 2011.

[3] Roatsch, T.: High-resolution Ceres Survey atlas derived from Dawn FC images. This volume, 2015.

[4] Preusker, F., et al.: Shape model and rotational state of dwarf planet (1) Ceres from Dawn FC stereo images. This volume, 2015.

[5] Schmedemann, N. et al.: The cratering record, chronology and surface ages of (4) Vesta in comparison to smaller asteroids and the ages of HED meteorites. Planet. Space Sci. 103, 104-130, 2014.

[6] Schmedemann, N. et al.: A preliminary chronology for Ceres. Lunar Planet. Sci. Conf. XLVI, abstr. #1418, 2015.

EPSC Abstracts
Vol. 10, EPSC2015-264, 2015
European Planetary Science Congress 2015

CERES STRUCTURE AND SOME TIPS FOR THE STUDY OF GRAVITATIONAL POTENTIAL BY THE DAWN MISSION

S. Voropaev (1)
(1) GEOKHI RAS, Kosygina str. 19, 119991, Moscow, Russia (voropaev@geokhi.ru)

Abstract

This study explores the geophysical implications of compositional model recently proposed for Ceres, which assume that the dwarf planet is a differentiated with low-density serpentine (core radius of about 400 km) and outer water ice layer (thickness of about 50 km). The presence of antifreezing material (ammonia) maintaining a liquid layer (thickness of about 20 km) is assumed. A major objective is to predict some of the discoveries that might be made when a spacecraft Dawn visits Ceres, and to offer some tips on the measurement results.

1. Introduction

Space mission Dawn targeted asteroid Vesta provides a number of remarkable results concerning as surface coverage as physical parameters of the surviving proto planet. It is currently in orbit about its second target at asteroid belt, the dwarf planet Ceres [1]. One of the obvious measurements to be made are main harmonics of the gravity field. When the value for J_2 is measured and assuming hydrostatic equilibrium, we can estimate value of the moment of inertia. This will put strong constraints on the internal structure of Ceres and allow us to choose among the different scenarios proposed for its thermal evolution [2]-[3].

2. Analytical procedure

If the gravitational potential of Ceres is modelled by a spherical harmonic expansion in the body-fixed reference, then the main part in second order is

$$U(r,\theta,\varphi) \approx GM/r \{1 + 1/r^2 [(A+B-2C)/2M \tfrac{1}{2}(3\cos(\theta)^2 -1) + (B-A)/4M \cos(2\varphi)\, 3\sin^2(\theta)]\},$$

where $A < B < C$ are principal moments of inertia, M is mass and G is the gravitational constant. The unnormalized coefficents (R is the reference radius of the body) are defined as

$$C - (A+B)/2 = J_2^R MR^2;$$
$$B - A = C_{22}^R\, 4MR^2.$$

Average data from the space and ground-based telescopes observations of Ceres are
major axes of the best-fit twoaxial oblate ellipsoid, a/c/R - 485/455/475 (km);
mass, M - 9.43 x 10^{20} (kg);
bulk density, ρ_b – 2080 (kg/m3);
rotation period, T - 9.075 (hours)
and B = A at second harmonic degree.
In this case, using equatorial axes **a** as the reference radius is more convenient
$C - A = J_2 Ma^2$, where $J_2 = J_2^R (R/a)^2$.
An exact analytical treatment provides for homogeneous twoaxial oblate ellipsoid (with an arbitrary bulk density)
$J_2^{(0)} = 1/5\, \varepsilon_1^2$, where eccentricity $\varepsilon_1^2 = 1 - c_1^2/a_1^2$, and if Ceres would be homogenous, $J_2^{(0)} = 0.024$ ($\varepsilon_1 = 0.346$).

In order to explore the implications of the gravity and shape for the interior structure of Ceres, simple two-layer mass-balance model was explored with an assumed core as twoaxial oblate ellipsoid with major axes $a_2 = b_2 > c_2$ and eccentricity $\varepsilon_2^2 = 1 - c_2^2/a_2^2$. In this case,

$M = M_1 + M_2$,

where $M_1 = 4\pi/3\, \rho_1 a_1^2 c_1$, ρ_1 is the outer layer density and $M_2 = 4\pi/3\, \rho_2 a_2^2 c_2$, where ρ_2 is the difference between the core's and the outer layer density. So, mass-balance provides

$$1 = \rho_1/\rho_b + \rho_2/\rho_b (a_2/a_1)^2 c_2/c_1 \qquad (1)$$

For two-layer model an exact analytical treatment provides

$$J_2^{(1)} = 1/5\, [\, M_1/M\, \varepsilon_1^2 + M_2/M\, \varepsilon_2^2 (a_2/a_1)^2\,] \qquad (2)$$

At hydrostatic equilibrium, an exact analytical treatment provides for homogeneous twoaxial oblate ellipsoid with bulk density ρ_b, eccentricity $\varepsilon^2 = 1 - c^2/a^2$ and rotation rate ω the following relation

$$\omega^2/2\pi\,\rho_b G = 1/l^3[\mathrm{arctg}(l)(3 + l^2) - 3l] = F(l), \quad (3)$$

where $l(\varepsilon) = \varepsilon/\sqrt{1 - \varepsilon^2}$ (see Fig. 1). So, for Ceres with the rotation period T = 9.075 h and bulk dencity ρ_b = 2080 (kg/m3) - $\omega^2/2\pi\,\rho_b G = 0.042$

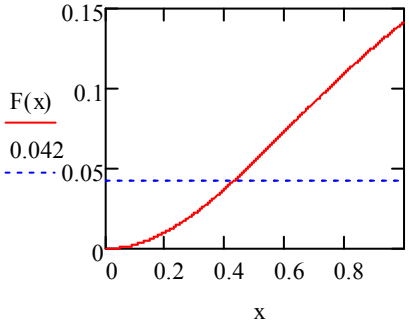

Figure 1: Relation "eccentricity/rotation" of a homogenous twoaxial oblate ellipsoid

and F(l) provides $\varepsilon^{(0)} = 0.39$ while actual Ceres eccentricity $\varepsilon_1 = 0.346$. So, $\varepsilon^{(0)} > \varepsilon_1$ is a *clear indication of the more dense core relative outer layer.*

3. Internal structure

Materials are known to fail under pressure if realistic criterion named for Tresca is met. It states that solids fracture along surfaces halfway between the axes of greatest stress σ_1 and least stress σ_3 whenever the maximum shear stress τ_{max} exceeds some constant S_0 characteristic of the material known as its *shear strength* [4]:

$$\tau_{max} = (\sigma_1 - \sigma_3)/2 > S_0$$

Experimental data for pure ice define an upper limit of shear strength S_0 at 200 K as

$$S_0 \approx 2.5\text{-}3 \text{ MPa}.$$

So, we can represent the internal structure of Ceres in the form of a serpentine core (density 2700 kg/m3) and a rigid shell of water ice (density 910 kg/m3) that can withstand gravity loads (see Figure 2). Maximum shear stress attains a peak value $\tau_{max} \approx 3$ MPa at the crust's lower boundary falling off to the surface.

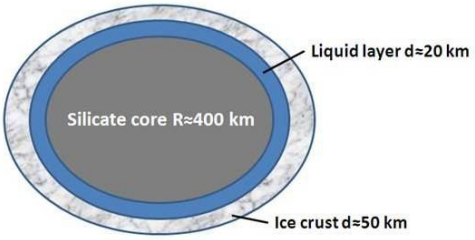

Figure 2: Estimated internal structure of Ceres

In this case, analytical treatment like (2) provides for inhomogeneous twoaxial oblate ellipsoid $J_2^{(1)}$ as

$$J_2^{(1)} = 0.02 \quad (4)$$

This value is very sensitive to the size and shape of the dwarf planet, so direct and accurate data from Dawn is very important for the next consideration.

4. Summary and Conclusions

The above discussed simple model of the internal structure provides reasonable value for the shear stress and deformation under self-gravity at the ice crust. Serpentine are currently believed to originate from olivine and pyroxene transformation by means of the warm water.

It is known that the thermal evolution of Ceres was a complex process and its initial rocks were probably experienced complex chemistry. Additional investigation of the relation between rotation rate and figure of Ceres given its heterogeneity and compare with some other nearby objects will be very interesting and promising.

References

[1] Thomas, P.C. et al.: Differentiation of the asteroid Ceres as revealed by its shape, Nature, Vol. 437, pp. 224-226, 2005.

[2] McCord T.B., Sotin, C.: Ceres: Evolution and current state, J. Geophys. Res.,, Vol. 110, E05009, 2005.

[3] Castillo-Rogez, J.C.: Ceres – Neither a porous nor salty ball, Icarus, Vol. 215, pp. 599-602, 2011.

[4] Slyuta E.N., Voropaev S.A.: Gravitational Deformation of Small Bodies of the Solar System: History of the Problem and Its Analytical Solution, Solar System Research, Vol. 49(2), pp. 123–138, 2015.

EPSC Abstracts
Vol. 10, EPSC2015-281, 2015
European Planetary Science Congress 2015

Preliminary temperature maps of dwarf planet Ceres as derived by Dawn/VIR

F. Tosi (1), M.C. De Sanctis (1), F. Zambon (1), E. Ammannito (2,1), M.T. Capria (1), F.G. Carrozzo (1), J.-Y. Li (3), A. Longobardo (1), S. Mottola (4), E. Palomba (1), A. Raponi (1), C.A. Raymond (5), C.T. Russell (2), and the Dawn/VIR team. (1) INAF-IAPS Istituto di Astrofisica e Planetologia Spaziali, Rome, Italy (federico.tosi@iaps.inaf.it), (2) University of California at Los Angeles, California, USA, (3) Planetary Science Institute, Tucson, AZ, USA, (4) Institute of Planetary Research, German Aerospace Center (DLR), Berlin, Germany, (5) NASA/Jet Propulsion Laboratory and California Institute of Technology, California, USA.

Abstract

The NASA Dawn mission [1] spacecraft was captured by the dwarf planet Ceres on March 6, 2015. During the *Approach* phase in the months preceding capture, the remote sensing instruments on the spacecraft acquired data with increasing spatial resolution. Analogous to the observation campaign planned at protoplanet Vesta during 2011-12, Dawn at Ceres proceeds in a series of orbits, carried out at increasingly lower altitudes over the mean surface, with a consequent increase of the spatial resolution.
The Visible InfraRed (VIR) mapping spectrometer onboard Dawn [2] operates in the overall spectral range 0.25-5.1 μm, with the main goal of inferring the surface composition of the target in its uppermost layer, as thick as several tens of microns [3].
Taking advantage of the wavelength range longward of 3 μm, it is possible to use VIR as a thermal mapper, i.e. as a tool to derive thermal images and spatially-resolved temperature maps. To do this, the VIR team uses a Bayesian approach to nonlinear inversion [4] that was extensively applied to the Vesta dataset, as well as to Rosetta/VIRTIS data of small bodies [e.g., 5,6].
In the case of Vesta, this capability allowed us to build both global thermal maps for each orbit phase (spatial resolution) as well as for different local solar times [7], and to investigate the thermal behavior of specific regions of interest seen at the local scale [4]. Such investigations fall well within the broad science goals that Dawn/VIR should address at Ceres.
In February 2015, still with a coarse spatial resolution (~11.4 km/px), VIR was able to obtain temperature images of Ceres that revealed the existence of differences in the thermal behavior of two bright spots seen at broad regional scale (**Figs. 1, 2**). At that time it was too early to say if this was the result of a real difference in the physical structure of the material and/or in its composition, because low resolution has the effect of averaging together very different areas.
In this work, we focus on VIR data acquired just after capture and in the first science orbit, namely the *Rotation Characterization 3 (RC3)* and *Survey* phases, yielding VIR spatial resolution of 3.4 km/px and 1.1 km/px, respectively. We derive global/broadly regional temperature maps as well as highlight thermal anomalies that may be observed at those spatial scales.
These data allow a preliminary determination of thermal properties of Ceres: in fact, thermophysical models that simulate the diurnal temperature variation for a given surface point, returning unknown quantities such as thermal conductivity and ultimately thermal inertia, may be appropriately constrained by these measurements.

1. Figures

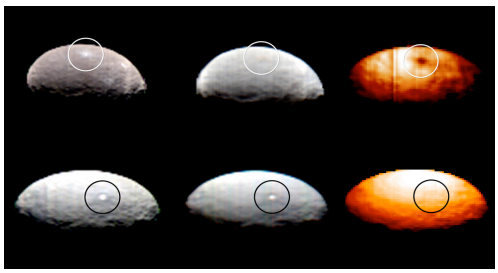

Figure 1. Region #1 (top) and Region #5 (bottom) are bright spots observed by Dawn on the surface of Ceres already in the *Approach* phase. Region #1 is located at Lon 4°N, Lon 8°E, while Region #5 is located at Lat ~20°N, 240°E. At left are images taken in visible light, close to wavelengths seen by the human eye (red = 656 nm, green = 530 nm, blue = 450 nm). The center images show the same regions of Ceres at infrared wavelengths dominated by solar reflection (red = 1.6 μm, green = 2.0 μm, blue = 2.4 μm). The right column shows Ceres in thermal infrared, where brighter colors represent higher temperatures. Region #1 corresponds to a dark spot at thermal wavelengths, which means it is cooler with respect to surrounding terrains seen under fair solar illumination (i.e., far away from the terminator). Conversely, Region #5 shows no distinct thermal behavior, which could be the result of insufficient VIR spatial resolution at the time of the observations, or the result of a different structure/composition of the surface material.
Credit: NASA/JPL-Caltech/UCLA/ASI/INAF.

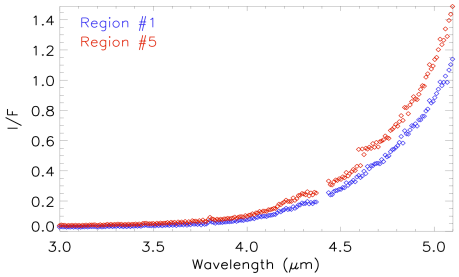

Figure 2. Spectral comparison based on VIR thermal infrared data between Region #1 (blue curve) and Region #5 (red curve). Region #1 shows a lower thermal emission compared to region #5.

Acknowledgements

This work was supported by the Italian Space Agency (ASI), ASI-INAF Contract I/004/12/0. Support of the Dawn Science, Instrument and Operations Teams is gratefully acknowledged. The computational resources used in this research have been supplied by INAF-IAPS through the DataWell project.

References

[1] Russell, C.T., et al. (2011). *The Dawn Mission to minor planets 4 Vesta and 1 Ceres*. Springer, ISBN: 978-1-4614-4902-7.

[2] De Sanctis, M.C., et al. (2011). *Space Sci. Rev.* 163 (1–4), 329-369.

[3] De Sanctis, M.C., et al. (2015). *EPSC 2015*, this conference.

[4] Tosi, F., et al. (2014). *Icarus* 240, 36-57.

[5] Coradini, A., et al. (2011). *Science* 334 (6055), 492-494.

[6] Keihm, S., et al. (2012). *Icarus* 221, 395-404.

[7] Tosi, F., et al. (2014). LPI Contribution No. 1773, p.2026.

EPSC Abstracts
Vol. 10, EPSC2015-284, 2015
European Planetary Science Congress 2015

Polygonal Craters on Dwarf-Planet Ceres

K. A. Otto (1), R. Jaumann (1,2), K. Krohn (1), D. L. Buczkowski (3), I. von der Gathen (1), E. Kersten (1), S. C. Mest (4), F. Preusker (1), T. Roatsch (1), P. M. Schenk (5), S. Schröder (1), F. Schulzeck (1), J. E. C. Scully (6), K. Stephan (1), R. Wagner (1), D. A. Williams (7), C. A. Raymond (8), C. T. Russell (6)

(1) German Aerospace Center, Institute of Planetary Research, Berlin, Germany (katharina.otto@dlr.de / Fax: +49-30-67055-402), (2) Freie Universität Berlin, Planetary Science and Remote Sensing, Germany, (3) Johns Hopkins University, Applied Physics Laboratory, Laurel, MD, USA, (4) Planetary Science Institute, Tucson, AZ, USA, (5) Lunar and Planetary Institute, Houston, TX, USA, (6) University of California LA, Institute of Geophysics, Los Angeles, CA, USA, (7) Arizona State University, Tempe, AZ, USA, (8) Jet Propulsion Laboratory, California Institute of Technology, Pasadena, CA, USA

1. Introduction

With approximately 950 km diameter and a mass of ∼1/3 of the total mass of the asteroid belt, (1) Ceres is the largest and most massive object in the Main Asteroid Belt. As an intact proto-planet, Ceres is key to understanding the origin and evolution of the terrestrial planets [1]. In particular, the role of water during planet formation is of interest, because the differentiated dwarf-planet is thought to possess a water rich mantle overlying a rocky core [2].

The Dawn space craft arrived at Ceres in March this year after completing its mission at (4) Vesta. At Ceres, the on-board Framing Camera (FC) collected image data which revealed a large variety of impact crater morphologies including polygonal craters (Figure 1). Polygonal craters show straight rim sections aligned to form an angular shape. They are commonly associated with fractures in the target material. Simple polygonal craters develop during the excavation stage when the excavation flow propagates faster along pre-existing fractures [3, 5]. Complex polygonal craters adopt their shape during the modification stage when slumping along fractures is favoured [3]. Polygonal craters are known from a variety of planetary bodies including Earth [e.g. 4], the Moon [e.g. 5], Mars [e.g. 6], Mercury [e.g. 7], Venus [e.g. 8] and outer Solar System icy satellites [e.g. 9].

2. Data

We will use FC images and a mosaic of this data set to interpret the distribution and geologic setting of polygonal craters at highest available resolution.

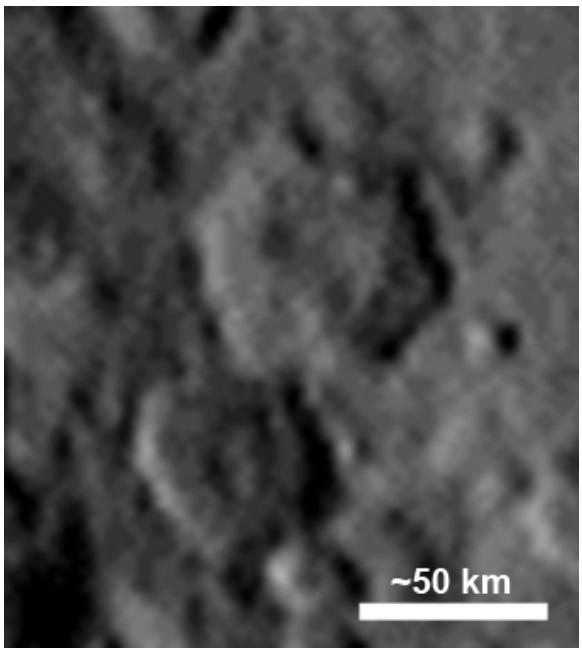

Figure 1: Polygonal craters on Ceres (reference: f2_477657691, stretched).

3. Method

By analysing the morphology and distribution of polygonal craters we aim to infer structural information on Ceres' surface material. We will analyse the geologic units with respect to polygonal crater density, orientation and morphology. Based on the assumption that polygonal craters are caused by fractures in the impacted material [5], structural regolith variations as well as tectonic conditions of surface units will be discussed.

4. Preliminary Results

On Ceres, we find polygonal craters with a size of up to 250 km in diameter and with the lower limit currently being restricted by the image resolution of $\sim$3.6 km/pixel. A preferential hexagonal shape is observed and some polygonal craters exhibit central peaks or relaxed crater floors. Areas showing an increase in polygonal crater density are observed on global scale. We will detail these findings with latest data available at the meeting.

References

[1] Russell, C. T. et al.: Dawn: A journey in space and time, PSS, Vol. 52, pp. 465-489, 2004.

[2] Thomas, P. C. et al.: Differentiation of the asteroid Ceres as revealed by its shape, *Nature*, Vol. 437, pp. 224-226, 2005.

[3] Öhman, T. et al.: Polygonal impact craters in the solar system: Observations and implications, in *Large Meteorite and Planetary Evolution IV*, GSA Special Paper 465, pp. 51-65, 2010.

[4] Poelchau, M. H. et al.: Rim uplift and crater shape in Meteor Crater: Effects of target heterogeneities and trajectory obliquity, *JGR*, Vol. 114(E01006), pp. 1-14, 2009.

[5] Eppler, D. T. et al.: Sources of shape variation in lunar impact craters: Fourier shape analysis, *GSA Bull.*, Vol. 94(2), pp. 274-291, 1983.

[6] Öhman, T. et al.: Polygonal impact craters in the Argyre region, Mars: Evidence for influence of target structure on the final crater morphology, *Meteorit. Planet. Sci*, Vol. 41(8), pp. 1163-1173, 2010.

[7] Weihs, G. T. et al.: Polygonal impact craters on Mercury, *Icarus*, in press, 2015.

[8] Aittola, M. et al.: The characteristics of polygonal impact craters on Venus, *Earth Moon Planets*, Vol. 101(1-2), pp. 41-63, 2007.

[9] Beddingfield, C. B. et al.: Testing for non-visible fractures on Dione by identifying polygonal impact craters, *46th LPSC, 16–20 March 2015, The Woodlands, TX, USA*, #1159, 2015.

EPSC Abstracts
Vol. 10, EPSC2015-298, 2015
European Planetary Science Congress 2015

Preliminary Geologic Mapping of the Ac-S-3 Hemisphere of Ceres from NASA's Dawn Mission

D.L. Buczkowski (1), R.A. Yingst (2), D.A. Williams (3), J.E.C. Scully (4), S.C. Mest (2), D.A. Crown (2), R. Jaumann (5), C.T. Russell (4), C.A. Raymond (6), P.M. Schenk (7), S. Marchi (8), D.P. O'Brien (2), A. Nathues (9), M. Hoffmann (9), M. Schäfer (9), T. Platz (9), T. Roatsch (5), E. Kersten (5), F. Preusker (5) K. Stephan (5), M.C. De Sanctis (10), A. Frigeri (10).

(1) Johns Hopkins University Applied Physics Laboratory, Laurel, MD, USA (Debra.Buczkowski@jhuapl.edu); (2) Planetary Science Institute, Tucson, AZ, USA; (3) School of Earth & Space Exploration, Arizona State University, Tempe, AZ, USA; (4) UCLA, Institute of Geophysics, Los Angeles, CA, USA; (5) Institute of Planetary Research, German Aerospace Center (DLR), Berlin, Germany; (6) NASA Jet Propulsion Laboratory, California Institute of Technology, Pasadena, CA, USA; (7) Lunar and Planetary Institute, Houston, TX, USA; (8) Southwest Research Institute, Boulder, CO, USA; (9) Max Planck Institute for Solar System Research, Göttingen, Germany; (10) Istituto di Astrofisica e Planetologia Spaziali, Istituto Nazionale de Astrofisica, Rome, Italy.

Abstract

NASA's Dawn spacecraft [1] was captured into orbit by the dwarf planet (1) Ceres on March 6, 2015. During the Approach phase capture was preceded and followed by a series of optical navigation and rotation characterization observations by Dawn's Framing Camera (FC) [2], which provided the first images of Ceres' surface. As was done at Vesta [3], the Dawn Science Team will conduct a geological mapping campaign at Ceres during the Nominal Mission, including iterative mapping using data obtained during each orbital phase. In this presentation we will describe the approach of the Ceres Mapping Campaign and discuss the preliminary geological mapping of the Ac-S-3 (180-360˚E) hemisphere of Ceres.

1. Introduction

Geologic mapping is an investigative process that organizes planetary features into discrete process-related map units, thus going beyond first-order photogeologic analysis. These units are defined and characterized based on specific physical attributes such as albedo, morphology, structure, color, and topography. These units are related to the putative geologic processes that produced them, such as volcanism, tectonism, impact cratering, deposition, weathering and/or erosion. The application of basic stratigraphic principles, including superposition, lateral continuity, cross-cutting, embayment, intrusion, etc., is used to determine the chronologic order of the map units. The map units can then be grouped into geologic formations, from which the geologic timescale and geologic history are determined. Thus, geologic maps are tools to help interpret the geologic history of a planetary surface.

2. Ceres Geologic Mapping Campaign

Following on from our successful campaign to map the surface of asteroid Vesta [3, 4], the Dawn Science Team will conduct a geologic mapping campaign for dwarf planet Ceres during the Nominal Mission. The goals of this campaign are two-fold: 1) to provide geologic context to the full science team of our ever-improving knowledge of the geology of Ceres with increasing FC spatial resolution during discrete orbital phases of the mission; and 2) to provide geologic context to the Visible and Infrared Spectrometer (VIR) and the Gamma-Ray and Neutron Detector (GRaND) teams to aid in interpreting their compositional information.

The first step of the Ceres mapping campaign is to construct a preliminary geologic map using images obtained during the Approach and Survey orbital phases. The purpose of this map is to assess the geology of Ceres at the global scale, to identify global map units and structural features, and determine the geologic processes that have affected Ceres globally. To accomplish this we will map Ceres using a hemispheric four-quadrangle system (Fig. 1).

Observations of the four hemispheric quadrangles have been considered (see section 3 below) and preliminary global map units have been contemplated. These may include, but are not restricted to, Cratered Plains material, Smooth Plains material, Lobate material, Bright-rayed crater material, Crater floor

material, and Central peak material. At present spatial resolution is too low to actually map out contacts and structural features, but we expect to be able to begin constructing the maps using Rotation Characterization #3 and Survey mosaics, to be acquired in May and June 2015.

3. First Geological Results

In this presentation we will present an overview of the geology of the Ac-S-3 (180-360˚E) hemisphere of Ceres. This region is a heavily cratered terrain, with both fresh-looking and putatively-relaxed craters evident (Fig. 2). Linear structures are also evident, but determining whether they are formed due to impact stresses or by internal activity of Ceres will require higher-resolution imaging than is available at the time of writing. Also evident in Ac-S-3 is the feature known as Spot 5; although the brightest of the "bright spots" on Ceres it is not currently observable in infrared images, unlike some of the other spots [5]. Color data (Fig. 2, bottom) indicates compositional diversity in the Ac-S-3 hemisphere, specifically around Spot 5, as well as around some of the other craters and associated with some of the linear structures. Variations in crater abundance in different parts of this hemisphere suggest that some type of resurfacing might be occurring. Domical, positive relief features may also be present in some of the craters (such as the crater to the southeast of Spot 5 that is also cut by a linear structure) but higher resolution imaging is required before they can be confirmed.

References:

[1] Russell, C.T., and Raymond, C.A., 2012, Space Sci. Rev., 163, 3-23;
[2] Sierks, H., et al., 2012, Space Sci. Rev., 163, 263-328;
[3] Yingst et al., 2014, PSS, 103, 2-23.
[4] Williams, D.A., et al., 2014, Icarus, 244, 1-12.
[5] Tosi, F. et al., 2015, EGU, abs. EGU2015-11960.

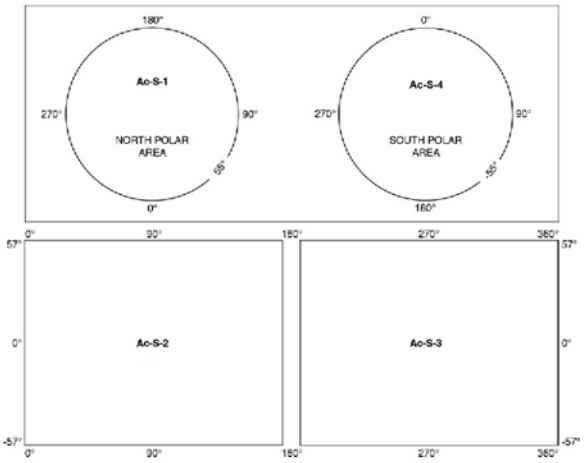

Fig 1: Hemispheric geologic mapping quadrangles for dwarf planet Ceres during the Approach and Survey orbital phases. Proposed quadrangle names have not yet been approved by the IAU.

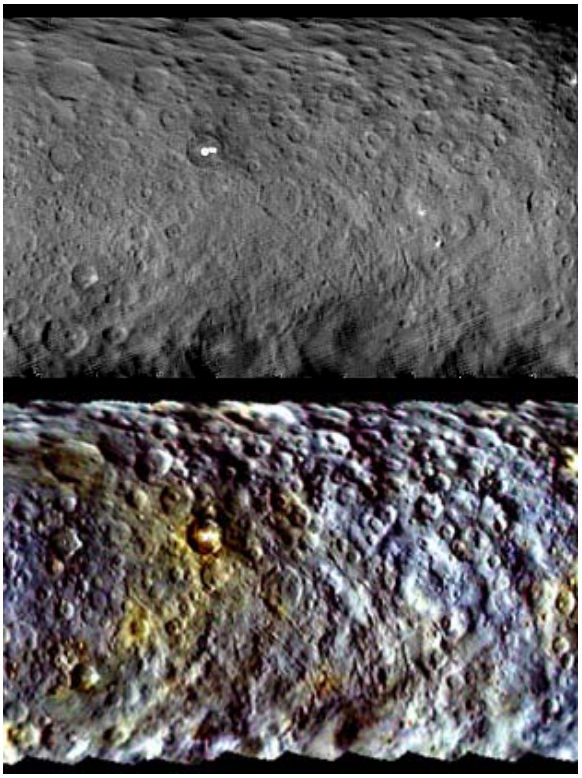

Fig 2: Dawn FC mosaic (top) and color composite image (bottom) of the Ac-S-3 (180-360˚) quadrangle of Ceres. Obtained during Approach phase, Rotation Characterization 2 observation, ~4 km/pixel spatial resolution. Color composite RGB is 0.96-0.75-0.44 μm. Image processing by the MPI for Solar System Research,Germany.

EPSC Abstracts
Vol. 10, EPSC2015-334, 2015
European Planetary Science Congress 2015

Preliminary Geologic Mapping of the Southern Hemispheric Quadrangle (Ac-S-4) of Ceres from NASA's Dawn Mission

J. E. C. Scully (1,2), D. A. Williams (3), D. L. Buczkowski (4), S. C. Mest (5), C. T. Russell (1), C. A. Raymond (2), D. A. Crown (5), R. A. Yingst (5), R. Jaumann (6), T. Roatsch (6), E. Kersten (6) and F. Preusker (6).
(1) Department of Earth, Planetary, and Space Science, University of California, Los Angeles, CA, USA (jscully@ucla.edu); (2) NASA Jet Propulsion Laboratory, California Institute of Technology, Pasadena, CA, USA; (3) School of Earth & Space Exploration, Arizona State University, Tempe, AZ, USA; (4) Johns Hopkins University Applied Physics Laboratory, Laurel, MD, USA; (5) Planetary Science Institute, Tucson, AZ, USA; (6) DLR, Planetary Research, Berlin, Germany.

Abstract

The Dawn mission visited Vesta from 2011-2012, and arrived in Ceres orbit in March 2015. For Vesta, a global geologic map at 1:500,000 scale and quadrangle maps at 1:250,000 scale were produced by the geologic mappers of the Dawn science team. A similar mapping campaign is planned for Dawn's mission at Ceres. A global geologic map will be produced based on Approach and Survey data, which will be acquired during the time period April-July 2015. For the purpose of global geologic mapping, Ceres has been divided into four hemispheric quadrangles. In this work we map the southern hemispheric quadrangle, Ac-S-4, which is located from 55-90°S and 0-360°E.

1. Introduction

The Dawn mission [1] is a NASA Discovery class mission, which visited Vesta from 2011-2012 and arrived in Ceres orbit in March 2015. Ceres and Vesta are the two most massive objects in the main asteroid belt, and are protoplanets that survived being accreted into a planet, and survived being scattered and/or ejected out of the solar system. The Dawn mission's aim is to characterize the geological, compositional and physical properties of these unique worlds, and to use these observations to learn about the formation and evolution of our solar system.

The Dawn spacecraft has three instruments: (1) the Framing Camera (FC), which provides images of the surface from the visible to the near-infrared through a clear filter and seven color filters [2]; (2) the Visible and Infrared Spectrometer (VIR), which provides hyperspectral cubes of the surface from the near-ultraviolet to mid-infrared [3] and (3) the Gamma Ray and Neutron Detector (GRaND), which measures the gamma rays and neutrons emitted from the surface [4]. The work presented here is mainly based upon Framing Camera images.

During Dawn's mission at Vesta, data were acquired by the spacecraft in six phases: (1) Approach, (2) Survey, (3) High Altitude Mapping Orbit 1 (HAMO-1), (4) Low Altitude Mapping Orbit (LAMO), (5) High Altitude Mapping Orbit 2 (HAMO-2) and (6) Departure. Four phases are planned for Dawn's mission at Ceres: (1) Approach, (2) Survey, (3) High Altitude Mapping Orbit (HAMO), and (4) Low Altitude Mapping Orbit (LAMO).

2. Methods: geological mapping

Geological mapping is a tool that is widely used to methodically observe and interpret the surfaces of planets, moons and small bodies. Systematic observations of the morphology and physical properties of these surfaces are used to define a set of geologic units. The surface of a planetary/small body is divided into these geologic units, and relative cross-cutting relationships are used to derive the stratigraphic order of the geologic units. Interpretations are made about the processes that formed the geologic units, which sometimes include the analysis of compositional properties etc. These interpretations then lead to inferences about the properties, formation and evolution of the planetary/small body on which the geologic units are located.

3. Vesta Geologic Mapping Campaign

A global geologic map of Vesta was produced with a scale of 1:500,000 [5]. In addition, to facilitate systematic geologic mapping at a higher

scale, the surface of Vesta was divided into 15 quadrangles and 1:250,000 maps were produced for each quadrangle. A team consisting of a lead mapper and mappers from neighboring quadrangles mapped each quadrangle, and the results were presented in a special issue of Icarus [6].

4. Ceres Geologic Mapping Campaign

Following the geologic mapping campaign at Vesta, a global geologic map of Ceres will be produced based on Approach and Survey data, which will be acquired during the time period April-July 2015. Subsequently, 15 quadrangle maps of Ceres will be produced at higher scale, based on HAMO and LAMO data, which will begin to be acquired in August of 2015.

For the global geologic map, which is based on Approach and Survey data, Ceres has been divided into four hemispheric quadrangles (Figure 1). In this work we map the southern hemispheric quadrangle, Ac-S-4, which is located from 55-90°S and 0-360°E.

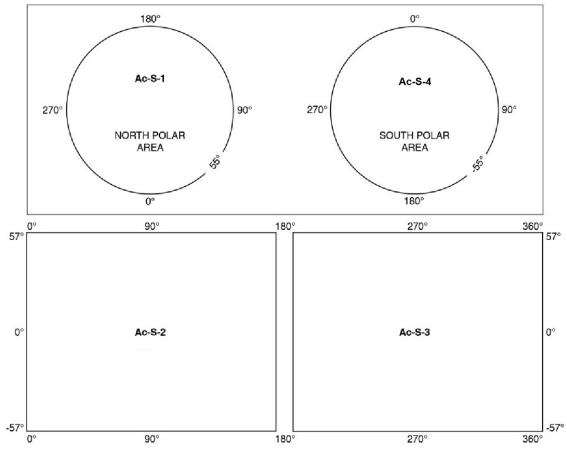

Figure 1: The four hemispheric quadrangles into which Ceres has been divided.

5. First Geological Results

As of the abstract deadline, Dawn has not yet observed Ac-S-4. Observations have been made slightly to the north of Ac-S-4, during the Rotational Characterization 2 (RC2) stage of the Approach phase (Figure 2). On the northern border of Ac-S-4, two large impact basins are visible in the RC2 data: one is located at ~43°S, ~290°E and is ~280 km in diameter, and one is located at ~45°S, ~251°E and is ~200 km in diameter. These impact basins extend into Ac-S-4 and dark lobate deposits appear to be located on their floors. There are also numerous smaller impact craters visible along the northern border of Ac-S-4. The smallest resolvable craters along this border are ~30 km in diameter. From ~45°S to ~12°N and ~236°E to ~310°E there are a set of northwest-trending grooves. It is possible that these grooves extend into Ac-S-4.

The southern hemispheric quadrangle Ac-S-4 will be observed during the Rotational Characterization 3 (RC3) stage of the Approach phase and in the Survey phase of the Dawn mission at Ceres. Based upon these data, we will construct a geologic map of this region of Ceres.

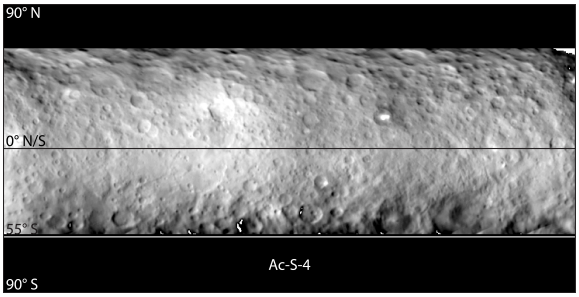

Figure 2: A Framing Camera clear filter mosaic of the surface of Ceres, obtained during RC2. The southern hemispheric quadrangle (Ac-S-4) is below the white line at 55°S. The mosaic has a simple cylindrical projection and has a resolution of ~4 km/pixel. Mosaic credit: DLR.

References

[1] Russell, C. T., and Raymond, C. A. (2011) Space Science Reviews, 163, 3-23.
[2] Sierks, H., et al. (2011) Space Science Reviews, 163, 263-328.
[3] De Sanctis, M. C., et al. (2011) Space Science Reviews, 163, 329-369.
[4] Prettyman, T. H., et al. (2011) Space Science Reviews, 163, 371-459.
[5] Yingst, R. A., et al. (2014) Planetary and Space Science, 103, 2-23.
[6] Williams, D. A., et al. (2014) Icarus, 244, 1-12.

EPSC Abstracts
Vol. 10, EPSC2015-367, 2015
European Planetary Science Congress 2015

Ceres and Rhea: Comparison of the Cratering Records of Two Icy Bodies

N. Schmedemann (1), R.J. Wagner (2), G. Michael (1), T. Kneissl (1), H. Hiesinger (3), B.A. Ivanov (4), T. Denk (1), R. Jaumann (1,2), A. Neesemann (1), C.A. Raymond (5), C.T. Russell (6)
(1) Freie Universität Berlin, Berlin, Germany (nico.schmedemann@fu-berlin.de); (2) German Aerospace Center (DLR), Institute of Planetary Research, Berlin, Germany; (3) Institut für Planetologie, Westfälische Wilhelms-Universität, Münster, Germany; (4) Institute of Dynamics of Geospheres, Moscow, Russia; (5) JPL, Caltech, Pasadena, CA, USA; (6) University of California, Los Angeles, USA.

Abstract

Early imaging data of Ceres that was acquired during Dawn's approach at Ceres allows for preliminary measurements of the Cerean crater size-frequency distribution (CSFD). In the Saturnian system, the Cassini mission already provided high resolution imaging data of the icy satellites of which Rhea shows significant physical similarities with Ceres. The direct comparison between the cratering records shows high similarities in the CSFDs of both bodies. This finding has significant implications for the understanding of the projectile populations in the outer Solar System, but requires further evaluation by upcoming high resolution imaging data of Ceres (by Dawn) and Pluto (by New Horizons).

1. Introduction

The Dawn mission [1] recently arrived at Ceres after it completed its mission at its first target Vesta in 2012. Since March 6, 2015 the Dawn spacecraft is gravitationally bound to the dwarf planet Ceres that circles the Sun in the middle asteroid Main Belt at ~2.77 AU. Initial imaging data with ground resolutions of up to ~2 km/pixels allow for reliable measurements of the cratering record down to crater diameters of ~7 km. Previous investigations of Ceres revealed significant amounts of water, thus an icy crust of substantial thickness is expected for Ceres [e.g. 2]. In the Saturnian system the Cassini spacecraft is taking high resolution imaging data since 2004 [3]. Especially the mid-sized Saturnian satellites Tethys, Dione, Rhea and Iapetus are of particular interest for the Dawn mission because all of these bodies feature an icy crust and surface gravities similar to Ceres. This does not only allow for predictions of crater morphologies, e.g. simple to complex transition, on Ceres [4] (as long as Dawn imaging data is still at comparatively low resolution), but in turn Ceres can help understanding the cratering records of the Saturnian satellites as well. It is widely believed that the main impactor source in the Saturnian system are projectiles on comet-like orbits [e.g. 5]. However, that view has been challenged by others [e.g. 6] who argue for collisionally evolved projectiles on planetocentric orbits as the main impactor source in the satellite systems of Jupiter and Saturn. Thanks to the Dawn and Cassini missions, a detailed direct comparison of the cratering records between icy bodies in the asteroid Main Belt and in the Saturnian system with very similar surface gravities becomes possible. Among the mentioned Saturnian satellites, Rhea (g~0.26 m/s²) shows the highest similarity in surface gravity with Ceres (g~0.28 m/s²).

2. Methodology

We measure crater diameters on projected imaging data in ArcGIS using the CraterTools add-in [7]. The measured data is presented in cumulative crater plots created by the craterstats software [8], following [9]. Since the absolute crater frequencies differ between Ceres and Rhea, we normalize the vertical position of the measurements as described by [10]. That improves the comparability of the data, but does not change the shape of the crater distribution. A vertical shift only accounts for different absolute projectile flux and exposure ages.

3. Measurements

For Ceres and Rhea we use one global measurement that covers the distribution of the large craters. This approach has the disadvantage to count across numerous different geologic units and various image resolutions, which usually results in shallower crater distributions. However, as long as such obstacles do not affect the crater sizes that we use for the comparison, this approach is sound. For smaller

craters, we use smaller areas that show continuously good image resolution and which are located within a single geologic unit. In Figure 1, we compare the measured crater distributions with a preliminary crater production function that has been derived for Ceres by [4]. In order to show the difference in crater scaling between basaltic and icy targets, we also show a measurement from Vesta and its respective crater production function [11]. Surface gravities as well as impact velocities on Vesta and Ceres are also similar [4].

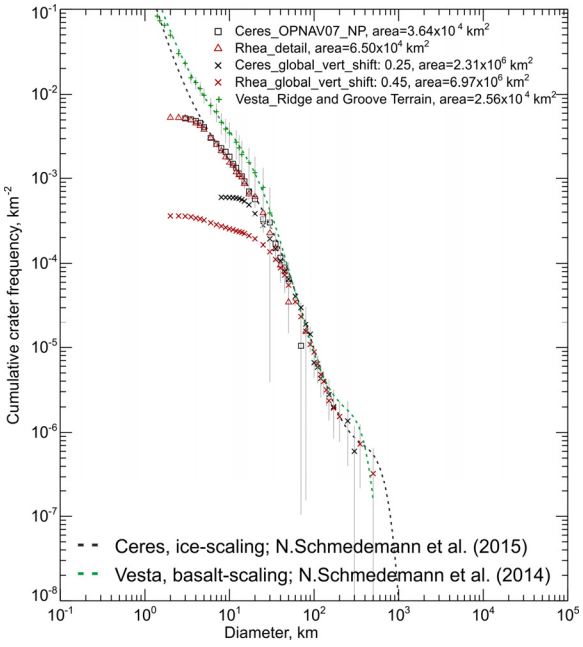

Figure 1: Measured crater distributions from Ceres and Rhea follow closely the crater production function (PF) for Ceres [4]. If vertically aligned around 100 km Vesta's crater PF is clearly different from Ceres's PF around 10 km.

4. Discussion

The different shapes of the crater size distributions on Vesta and Ceres/Rhea as well as the high similarity between Ceres and Rhea is likely caused by the fact that the impact craters on Ceres and Rhea are formed in water ice, while craters on Vesta formed in basaltic regolith with different scaling properties [4]. The very high similarity of the cratering records of Ceres and Rhea suggests a very similar projectile population that impacts both bodies even with similar velocities. According to [4] for Ceres an average impact velocity of ~4.6 km/s is expected. [6] proposes an impact velocity of 3.99 km/s for Rhea which is based on the assumption that it is impacted by planetocentric, asteroid-like projectiles with an eccentricity of 0.6. Thus, for now it appears that both, Ceres and Rhea are predominantly impacted by asteroid-like projectiles and comet-like projectiles play only a minor role. This may also be true for the other Saturnian satellites. However, although our preliminary results show a very good correlation of the cratering records of Ceres and Rhea, it cannot be ruled out, that Kuiper Belt objects show a similar collisionally evolved body size-distribution like the Main Belt asteroids. In that case it might be hard to discriminate between both projectile populations. With the fly-by of the New Horizons spacecraft at Pluto in July 2015, the Kuiper-Belt object size-frequency distribution may finally be revealed.

References

[1] Russell, C. T., and Raymond, C. A.: The Dawn Mission to Vesta and Ceres. Space Sci. Rev. 163, 3-23, 2011. [2] McCord T.B. et al.: Ceres: Its Origin, Evolution and Structure and Dawn's Potential Contribution. In: Russell, C.T, Raymond, C.A. (eds.) The Dawn Mission to Minor Planets 4 Vesta and 1 Ceres. Springer, New York, 63-76, 2012. [3] Porco, C.C. et al.: Cassini Imaging Science: Instrument Characteristics and Anticipated Scientific Investigations at Saturn, Space Science Reviews 115: 363-497, 2004. [4] Schmedemann, N. et al.: A preliminary chronology for Ceres. Lunar Planet. Sci. Conf. XLVI, abstr. #1418, 2015. [5] Zahnle et al.: Cratering rates in the outer Solar System, Icarus, 163, 263-289, 2003. [6] Neukum G.: Cratering records of the satellites of Jupiter and Saturn, Advances in Space Research, 5, 107-116, 1985. [7] Kneissl, T. et al.: Map-projection-independent crater size-frequency determination in GIS environments - New software tool for ArcGIS, Planet. Space Sci., 59, 1243–1254, 2011. [8] Michael G. et al.: Planetary surface dating from crater size-frequency distribution measurements: Partial resurfacing events and statistical age uncertainty, Earth Planet. Sci. Lett., 294, 223-229, 2010. [9] Arvidson R.E. et al.: Crater Analysis Techniques Working Group - Standard techniques for presentation and analysis of crater size-frequency data, Icarus, 467-474, 1979. [10] Neukum G. and Wise D. U.: Mars: A Standard Crater Curve and Possible New Time Scale, Science, 194, 1381-1387, 1976. [11] Schmedemann, N. et al.: The cratering record, chronology and surface ages of (4) Vesta in comparison to smaller asteroids and the ages of HED meteorites, Planet. Space Sci. 103, 104-130, 2014.

Acknowledgments: This work has been supported by the German Space Agency (DLR) on behalf of the Federal Ministry of Economic Affairs and Energy, grants 50OW1101 (NS, TK, AN) and 50QM1301 (GM). BAI is supported by Program 22 RAS.

EPSC Abstracts
Vol. 10, EPSC2015-383, 2015
European Planetary Science Congress 2015

Photometric Properties of Ceres and Comparisons with Previous HST Observations

Jian-Yang Li (1), Andreas Nathues (2), Lucille Le Corre (1), Vishnu Reddy (1), Mark V. Sykes (1), Martin Hoffmann (2), Stefano Mottola (3), Stefan E. Schröder (3), Andrea Longobardo (4), Mauro Ciarniello (4), Lucy A. McFadden (5), Carol A. Raymond (6), and Christopher T. Russell (7)
(1) Planetary Science Institute, USA, (2) Max Planck Institute for Solar System Research, Germany, (3) Deutsches Zentrum für Luft- und Raumfahrt (DLR), Germany, (4) Istituto di Astrofisica e Planetologia Spaziali, Istituto Nazionale de Astrofisica, Rome, Italy, (5) NASA Goddard Space Flight Center, USA, (6) Jet Propulsion Laboratory, California Institute of Technology, USA, (7) Institute of Geophysics and Planetary Physics, University of California, Los Angeles, USA.

1. Introduction

NASA's Dawn spacecraft entered the first science orbit around its second target, dwarf planet Ceres, in April 2015. The photometric properties of Ceres not only reveal clues about the physical state of the regolith, surface composition, and geological history, but also are important for correcting the data collected under various observing and illumination geometries to a common geometry to facilitate the interpretations of all photometric and spectral data. The Dawn data collected during its approach to Ceres cover phase angles from a few degrees to ~155º, and almost cover the full range of incidence angles and emission angles from 0º to 90º, making an excellent dataset for studying the spectrophotometric properties of Ceres. We report the analysis of the photometric properties of Ceres in the visible wavelengths using the Framing Camera (FC) [1] data through all seven color filters and one clear filter, acquired during the approach and the Survey orbit of the mission.

Although previous studies [2-4] suggested a remarkably uniform surface of Ceres, the images collected by Dawn during its approach to the target at a scale of a few km/pixel revealed some small but extremely bright spots and regions, with albedos up to >4 times the average albedo of Ceres, representing the highest contrast so far observed in all asteroids imaged from close distances by spacecraft missions. These bright spots should be geologically young, and might be related to the episodic water sublimation activity of Ceres [5-7]. We performed detailed comparisons of the albedos of these bright spots between previous Hubble Space Telescope (HST) observations and the Dawn observations that span about 10 years to search for any possible changes.

By the time of preparing this abstract, the Dawn FC has collected images at pixel scale down to 2.1 km/pixel. By June 2015, the data with a scale of 0.4 km/pixel will have been collected during the Survey Orbit phase.

2. Initial Results

We modeled the photometric data with both disk-integrated analysis and disk-resolved modeling, with the empirical models such as the IAU HG model [8] and the more recent H, G_1, G_2 model and H, G_{12} model [9], and Hapke models [10]. The disk-integrated phase function of Ceres derived from the approach images, together with some models, are shown in Fig. 1. No data within the opposition surge are available, and therefore the opposition parameters are not constrained by Dawn data, but assumed from previous studies [11]. The Hapke roughness parameter, θ, is preliminarily constrained by the disk-resolved images at 45º phase angle to be 21º. We expect to refine the analysis in all color filters in the visible wavelengths from 0.45 μm to 0.98 μm using the Survey orbit data.

The comparisons between the albedo measurements of bright spots in HST images and Dawn FC images are strongly affected by the distinctly different characteristics of the two instruments. The point-spread-function (PSF) of HST/ACS/HRC that was used to image Ceres in 2003/04 [2] has 80% of its energy encircled at 5 pixels radius. The same occurs for FC at 0.7 pixels [12]. Given that the size of many features is a few km across, smaller than the pixel scale in the HST images, Dawn images need to be convolved with the HST PSF and downsampled to comparable pixel size for a reliable comparison. The albedos of some of the most prominent bright spots

are shown to be consistent with previous HST measurements. We will use the high-resolution images collected during the Rotational Characterization 3 at a pixel scale of 1.4 km/pixel to refine these results, and also compare the color of Ceres' surface with the previous measurements from HST data.

Acknowledgements

The funding for this research was provided under the NASA Contract # NNM05AA86 through a subcontract from the University of California, Los Angeles, to Planetary Science Institute. We thank the Dawn operations teams and instrument teams for their tremendous effort to ensure the smooth operations of the spacecraft and the collection of an excellent dataset.

References

[1] Sierks, H., et al.: The Dawn Framing Camera, Space Sci. Rev. 163, 263-327, 2011.
[2] Li, J.-Y., et al.: Photometric analysis of 1 Ceres and surface mapping from HST observations, Icarus 182, 163-160, 2006.
[3] Carry, B., et al.: Near-infrared mapping and physical properties of the dwarf-planet Ceres, Astron. Astrophys. 478, 235-244, 2008.
[4] Carry, B., et al.: The remarkable surface homogeneity of the Dawn mission target (1) Ceres, Icarus 217, 20-26, 2012.
[5] A'Hearn, M.F., Feldman, P.D.: Water vaporization on Ceres, Icarus 98, 54-60, 1992.
[6] Rousselot, P., et al.: A search for water vaporization on Ceres, Astron. J. 142, 125 (6pp), 2011.
[7] Küppers, M., et al.: Localized sources of water vapour on the dwarf planet (1) Ceres, Nature 505, 525-527, 2014.
[8] Bowell, E., et al.: Application of photometric models to asteroids, in: Asteroids II, 921-945, 2002.
[9] Muinonen, K., et al.: A three-parameter magnitude phase function for asteroids, Icarus 209, 542-555, 2010.
[10] Hapke, B.: Theory of reflectance and emittance spectroscopy, 2nd Ed., Cambridge Univ. Press, Cambridge, UK, 2012.
[11] Helfenstein, P., Veverka, J.: Physical characterization of asteroid surfaces from photometric analysis, In: Asteroids II, 557-593, 2002.
[12] Schröder, S.E., et al.: In-flight calibration of the Dawn Framing Camera, Icarus 226, 1304-1317, 2013.

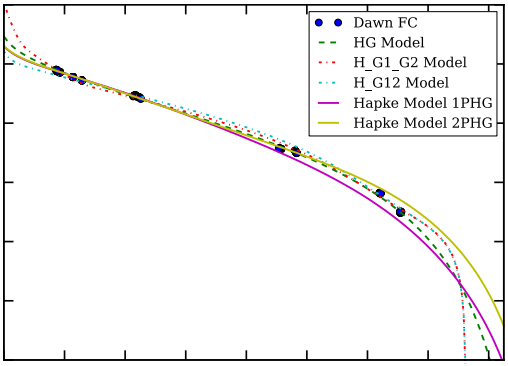

Fig. 1. The best-fit disk-integrated photometric models of Ceres with the approach data. The model parameters are: IAU HG: H=3.06, G=-0.015; IAU H, G_1, G_2: H=1.73, G_1=0.046, G_2=0.069; IAU H, G_{12}: H=3.55, G_{12}=0.23; Hapke model with 1-parameter Henyey-Greenstein (HG) single particle phase function: w=0.098, g=-0.31; Hapke 2-parameter HG function: w=0.12, b=0.35, c=0.38. B_0=1.06, h=0.06, and θ=21º are fixed for both Hapke models

EPSC Abstracts
Vol. 10, EPSC2015-385, 2015
European Planetary Science Congress 2015

Search for Dust Around Ceres

Jian-Yang Li (1), Andreas Nathues (2), Stefano Mottola (3), Mark V. Sykes (1), Carol A. Polanskey (4), Steven Joy (5), Nickolaos Mastrodemos (4), Lucy A. McFadden (6), David Skillman (6), Nargess Memarsadeghi (6), Martin Hoffman (2), Stefan E. Schröder (3), Uri Carsenty (3), Carol A. Raymond (4), and Christopher T. Russell (5)
(1) Planetary Science Institute, USA, (2) Max Planck Institute for Solar System Research, Germany, (3) Deutsches Zentrum für Luft- und Raumfahrt (DLR), Germany, (4) Jet Propulsion Laboratory, California Institute of Technology, USA, (5) Institute of Geophysics and Planetary Physics, University of California, Los Angeles, USA, (6) NASA Goddard Space Flight Center, USA

1. Introduction

Since the first but ambiguous evidence of water sublimation activity on Ceres was reported more than two decades ago [1] and the negative results in a number of follow up observations [2], water vapor has recently been unambiguously detected by the Herschel Space Observatory observations [3]. The mechanism of water sublimation on Ceres is still unclear, but the most probable mechanisms include cometary-like sublimation and cryovolcanism. Such sublimation activity could entrain dust grains in the outgassing, resulting in either a dust envelope or dust plumes above the surface of Ceres. Given the much higher escape velocity of ~0.5 km/s on the surface of Ceres compared to those on comets (a few m/s), any dust around Ceres might be short-lived, and/or close to the surface of Ceres. The implications of possible dust around Ceres motivated NASA's Dawn mission to perform a high-sensitivity, high-resolution search for dust around Ceres. The Dawn spacecraft, during its first science orbit around Ceres, will have an excellent opportunity to search for dust at a pixel scale of 1.4 km/pixel from the night-side of Ceres looking close to the direction of the Sun. This observing geometry is the most favorable to search for dust around Ceres due to the significant increase of dust brightness and decrease in the surface brightness of Ceres towards high solar phase angle. Here we report the results of this search for dust around Ceres with Dawn's Framing Camera (FC) [4].

2. Observations

Dawn's first science orbit around Ceres, the Rotational Characterization 3 (RC3) orbit, includes night-side observations of Ceres that are specifically designed to carry out a dust search. The altitude of 13,500 km of the RC3 orbit allows the whole disk of Ceres to fit within the field-of-view of the FC. The night-side observations start as the spacecraft crosses the terminator over the south pole of Ceres in a polar orbit that is within 5º of the Ceres-Sun vector, continuing until the Sun is about 25º from the camera's boresight. The observations reach a phase angle of about 155º. After the night-side equator crossing to the northern hemisphere, the observations resume from about 155º phase angle, lasting until the terminator crossing over the north pole towards the day-side of Ceres. The whole night-side observations cover 7 rotations of Ceres on each side of the equator, and the two Ceres rotations at the highest phase angles between 145º and 155º will be our primary dataset to search for dust and is the most favorable geometry for detection. Based on the characteristics and the performance of FC during the Vesta phase, we estimate the sensitivity of 10^6 particles/m^2 for a 5-σ detection of dust with 1 μm grains, an albedo of 0.1, and a phase function of typical cometary dust [5].

3. Preliminary Results

The data from the first half of the night-side observations from the south of Ceres' equator have been collected. No dust plumes or envelopes have been identified. The second half of the observations will be performed after the close of the abstract submission for this EPSC 2015 conference. The existence or otherwise lack of dust associated with the sublimation activity of water on Ceres will help put constraints on the nature and characteristics of outgassing on Ceres.

Acknowledgements

The funding for this research was provided under NASA Contract # NNM05AA86 through a

subcontract from the University of California, Los Angeles to Planetary Science Institute. We thank the Dawn operations teams and instrument teams for their tremendous effort to ensure the smooth operations of the spacecraft and the collection of an excellent dataset.

References

[1] A'Hearn, M.F., Feldman, P.D.: Water vaporization on Ceres, Icarus 98, 54-60, 1992.

[2] Rousselot, P., et al.: A search for water vaporization on Ceres, Astron. J. 142, 125 (6pp), 2011.

[3] Küppers, M., et al.: Localized sources of water vapour on the dwarf planet (1) Ceres, Nature 505, 525-527, 2014.

[4] Sierks, H., et al.: The Dawn Framing Camera, Space Sci. Rev. 163, 263-327, 2011.

[5] Schleicher, D.: 2010: Composite Dust Phase Function for Comets, http://asteroid.lowell.edu/comet/dustphase.html

EPSC Abstracts
Vol. 10, EPSC2015-400, 2015
European Planetary Science Congress 2015

Impact Craters on Ceres: Evidence for Water-Ice Mantle?

P. Schenk (1), S. Marchi (2), D. O'Brien (3), K. Otto (4), R. Jaumann (4), D. Williams (5), C. Raymond (6), and C.T. Russell (7) and the Dawn Science Team. (1) Lunar and Planetary Institute, Houston, TX, USA, (2) Southwest Res. Institute, Boulder CO, (3) Planet. Sci. Inst., Tuscon, AZ, (4) DLR, Berlin, Germany, (5) Ariz. State Univ., Tempe, AZ, (6) Jet Propulsion Lab, Pasadena, CA, (7) Univ. Calif. Los Angeles, CA (schenk@lpi.usra.edu)

Abstract

Impact craters on Ceres as revealed by the Dawn spacecraft are to first order similar in shape and morphology to those observed on Saturn's midsize icy satellites, consistent with a bulk icy composition for Ceres' outer layers. Rayed craters have been identified and cataloged. Large impact basins have a range of morphologies, some of which are indicative of post-impact modification. Subtle differences in morphology might be related to non-ice material within the crust, pending improved resolution. Additional details are expected to reveal the nature of Ceres interior as higher-resolution imaging and topography become available.

1. Introduction

Dawn's first reconnaissance of the dwarf planet 1 Ceres is now underway. This major body is likely to be ice-rich [e.g., 1,2], given its low density, and may have an icy mantle 50-100 km thick [1,2]. Dawn will investigate the internal composition and mass distribution within Ceres.

Impact crater morphologies are very sensitive to both surface gravity and to composition, as demonstrated by the major differences in morphology on icy and rocky bodies [e.g., 3]. Both rocky Vesta and the ice-rich satellites of Saturn (e.g., Dione and Tethys) have surface gravity very similar to Ceres, facilitating direct comparison of impact craters. If Ceres' outer layers are dominated by ice, then impact craters should resemble those of Saturn's moon rather than Vesta. Here we present initial findings based on initial Dawn mapping of Ceres as a test of whether Ceres has an ice mantle.

1.1 Crater Morphologies on Ceres

Approach and first orbital mapping reveals that Ceres is heavily cratered, exhibiting a wide range of preservations states and morphologies. Bright and dark ray craters up to ~100 km across are evident, which can be used to estimate the current flux of impactors. Whether the bright material is ice-rich has not yet been determined.

A test of ice composition is complex crater formation. Complex craters, in the form of central peaks, dominate on Ceres down to crater diameters of <25 km (Fig. 1). This transition is much lower than the >60 km diameter observed on Vesta [4], but almost as small as on Dione and Tethys (pending higher resolution imaging). To first order, this favors an ice-rich composition for the outer 10's of kilometers of Ceres interior. The degree to which non-ice material can mix into the mantle and still result in similar morphologies is not yet known.

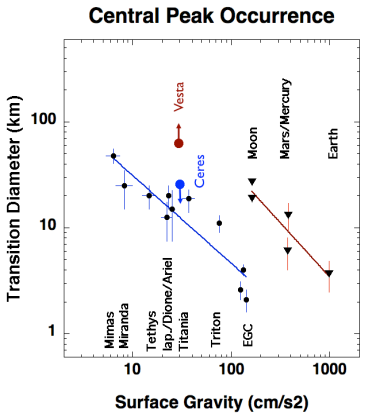

Figure 1: Preliminary simple-complex transition diameter estimate for Ceres. Icy satellite data are from White and Schenk, pers. comm).

At least 3 basins >200 km in diameter have been identified from 4-km/pxl approach imaging. The interior morphology of these structures is not yet clear but there do appear to be subtle differences between these basins and their icy satellite counterparts. A sufficiently large impact into a

thinner ice shell will also excavate into the rocky core, potentially producing anomalous landforms [5]. This hypothesis can be tested with resolved imaging and topography.

The largest of these basins, ~275 km across, has a low rim scarp and shallow but uneven topography, Several large floor mounds also occur near the rim. These are several km high and of uncertain origin. Another basin ~150-km across also exhibits similar morphology, suggesting that modification processes on Ceres have characteristics distinct from icy bodies.

Another large (~250-km-wide) basin near the South Pole exhibits a set of arcuate linear troughs extending north from the rim. While the curvature of the lineations is consistent with lateral ejecta and secondary deposition on a rotating body, their origin remains uncertain pending resolved imaging. Impact ejecta, melt distribution, boulder formation, rim angularity and ice excavation are all key features awaiting low-altitude mapping. Ejecta deposits, melt features and secondaries have all been mapped on Saturn's icy moons [6], and are expected on Ceres.

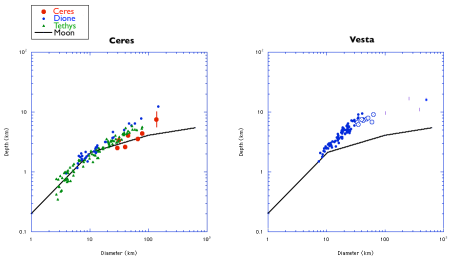

Figure 2: Preliminary crater depth measurements (left) on Ceres, from Dawn approach imaging (blue and green points are crater depths for Dione and Tethys). Fresh crater depths are shallower than on Vesta (right), as expected.

A key prediction for Ceres is that the high surface temperatures will result in flattening of impact crater topography due to 'relaxation' of topography [7,8]. Initial measurements of the most pristine craters suggest depths comparable to unmodified craters on Dione and Tethys (Fig. 2), suggesting that at least some crater have not relaxed. These craters are important for determining the magnitude of relaxation elsewhere on Ceres.

2. Summary and Conclusions

Approach and high-altitude Dawn mapping imaging of Ceres show crater morphologies that initially resemble those of the ice-rich satellites of Saturn, all of which have surface gravity similar to Ceres. Depths and transition diameters are thus far consistent with significant water ice in the outer layers of Ceres. Complicating factors include lower impact velocities on Ceres (~5 km/s), the possibility of extensive mixing of non-ice material within an outer icy layer, and layering within the outer shell. Large impact into a thin ice shell over a silicate core could also produce impact morphologies distinct from icy satellites. Detailed imaging expected later in the mapping phase of the Dawn mission should reveal key features that may provide evidence of these effects.

Acknowledgements

We thank NASA and the Dawn project for supporting this work.

References

[1] McCord, T., J. Castillo-Rogez, A. Rivkin: Ceres: Its origin, evolution and structure and Dawns potential contribution, Space Sci. Rev. 163, 63-76, 2011.

[2] Castillo- Rogez, J.: Ceres: Neither a porous nor salty ball, Icarus, 215, 599-602, 2011.

[3] Schenk, P., Schenk, P., Chapman, C., Zahnle, K., Moore, J., Ages and Interiors, The cratering record of the Galilean Satellites, in *Jupiter*, (F. Bagenal, T. Dowling and W. McKinnon, eds.), Cambridge Press, pp. 427-456, 2004.

[4] Schenk, P., and 10 others: Impact crater morphologies on Vesta in Solar System Context, Lunar Planet. Sci. Conf. 44, abstr. 2039, 2013.

[5] Bowling, T., B. Johnson, D. Blair, and J. Melosh: Large impact basins on Ceres: Probing beneath the icy mantle, AGU Fall Meeting, abstr. P51E-03, 2014.

[6] Hoogenboom, Schenk, P., and Johnson, K.: Contribution of secondary craters on the icy satellites: Results from Ganymede and Rhea, Lunar Planet. Sci. Conf. 46, abstr. 2530, 2015.

[7] Bland, M.: Predicted crater morphologies on Ceres: Probing internal structure and evolution, Icarus, 226, 510-521, 2013.

EPSC Abstracts
Vol. 10, EPSC2015-407, 2015
European Planetary Science Congress 2015

Gravity Science Investigation of Ceres from Dawn

R.S. Park (1), A.S. Konopliv (1), C.A. Raymond (1), S.W. Asmar (1), B. Bills (1), C.T. Russell (2), D.E. Smith (3), and M.T. Zuber (3)
(1) Jet Propulsion Laboratory, California Institute of Technology, Pasadena, CA, USA, (2) UCLA, Los Angeles, CA, USA, (3) Massachusetts Institute of Technology, Cambridge, MA, USA

Abstract

The Dawn gravity science investigation utilizes the DSN radiometric tracking of the spacecraft and landmark tracking from framing camera images to determine the gravity field and orientation parameters of Ceres [1,2]. The gravity science data was collected since the Dawn spacecraft entered an orbit around Ceres on March 6, 2015, and currently, a preliminary solution is available.

1. Introduction

The Dawn spacecraft acquired DSN radiometric data at X-band (8.4 GHz) since it entered an orbit around Ceres. The DSN range data typically provides ~2 m accuracy and is mainly used to determine the ephemeris of Ceres. The DSN Doppler data typically provides ~0.2 mm/s accuracy at 60s count time and is mainly used to determine the spacecraft ephemeris, gravity field, and orientation parameters of Ceres. Through an image correlation process of onboard framing camera data, a 3-dimensional shape of Ceres is created. The landmark tracking data is reduced from a global shape reconstruction process [3], which provides an additional constraint on Ceres-relative position of the Dawn spacecraft. Based on the Approach phase data, we have: GM (km^3/s^2) = 62.7±0.1, Pole R.A. (deg) = 291.8±0.1, and Pole Dec. (deg) = 67.1±0.1.

The Dawn spacecraft currently maintains its attitude by using its two remaining reactions wheels and hydrazine-powered jets. Considering this additional non-gravitational perturbation, we expected to determine the gravity field of Ceres to about degree and order 5 (see Figure 1).

Once the final gravity field is determined, it can be correlated with the gravity derived from a shape model with various interior models to provide constraints on its internal structure. For example, Figure 2 shows the radial acceleration of Ceres based on the constant-density shape model of [4]. Also, the offset between the center-of-mass and the center-of-figure can be computed for a first-order test on homogeneity, and second-degree harmonics can be used to test hydrostatic equilibrium of Ceres. Deviations from the constant density shape model at higher orders will be compared to the surface morphology to understand the subsurface structure, including impact basins.

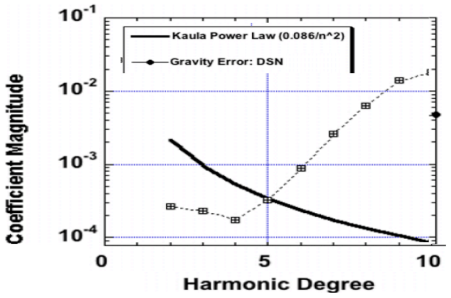

Figure 1: Expected error spectrum of Ceres gravity field at the end of gravity science investigation where harmonic degree 5 gives 300 km resolution at half-wavelength.

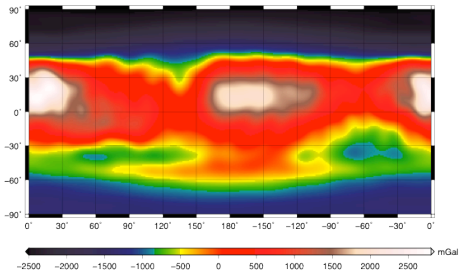

Figure 2: Radial Acceleration (mGal) computed from shape using a 20x20 spherical harmonic expansion and projected onto a sphere with 476 km radius, excluding the point-mass contribution.

Acknowledgements

This work was carried out in part at the Jet Propulsion Laboratory, California Institute of Technology, under contract with the National Aeronautics and Space Administration.

References

[1] Russell, C.T., et al. (2011). *The Dawn Mission to minor planets 4 Vesta and 1 Ceres*. Springer, ISBN: 978-1-4614-4902-7.

[2] Konopliv, A. S., S. W. Asmar, B. G. Bills, N. Mastrodemos, R. S. Park, C. A. Raymond, C. T. Russell, D. E. Smith, M. T. Zuber, "The Dawn Gravity Investigation at Ceres and Ceres," *Space Sci Rev* DOI 10.1007/s11214-011-9794-8 2011.

[3] R.W.Gaskell, "Optical Navigation Near Small Bodies." AAS paper 11-220, AAS/AIAA Space Flight Mechanics Meeting, New Orleans, LA, 2011.

[4] Thomas, P. et al., "Differntiation of the asteroid Ceres as revealed by its shape", *Nature*, 437, 224-226, 2005

EPSC Abstracts
Vol. 10, EPSC2015-428, 2015
European Planetary Science Congress 2015

Geophysics of Ceres from Dawn

C. A. Raymond[1], C. T. Russell[2], R. S. Park[1], A. S. Konopliv[1], S. W. Asmar[1], J. C. Castillo-Rogez[1], K. Hughson[2], R. Jaumann[3], T. McCord[4], F. Preusker[3], P. Schenk[5], D. E. Smith[6,7], and M. T. Zuber[6]

[1]Jet Propulsion Laboratory, California Institute of Technology, Pasadena, CA, USA (carol.a.raymond@jpl.nasa.gov), [2]UCLA, Los Angeles, CA, USA,[3]DLR, Inst. of Planetary Research, Berlin, Germany, [5]Lunar Planetary Institute, Houston, TX, USA, [6]MIT, Cambridge, MA, USA, [7]GSFC, Greenbelt, MD, USA

Abstract

Dawn's 16-month investigation of Ceres will return comprehensive data elucidating its geology and morphology, composition, and gravity field. One of the objectives of the investigation is to understand Ceres' interior structure and the possibility of communication between the subsurface ocean, thought to have existed during the first half of Ceres' evolution, and the surface. Geophysical data collected to date provide a preliminary assessment of the structure and composition of the ice shell and implications for past mobility.

1. Introduction

Data collected by the Dawn spacecraft during Approach (beginning in January 2015), RC3 (April-May 2015) and Survey (August 2015) have produced a preliminary shape model [1] and gravity field [2], as well as image mosaics and compositional maps. These data have been examined for evidence of resurfacing, which would indicate mobility of the ice shell that may have brought material from the early subsurface ocean's floor to the surface and which might be continuing to the present day. The morphology of the surface, and in particular the impact basins, constrains the thickness of the ice shell. It also reflects the percentages of ice and rock in the outermost layer of Ceres, and the composition of the icy layer. This information illuminates the degree to which the deep silicate core has communicated with the surface.

2. Crater Morphology

The degree of cratering seen on the surface of Ceres is surprising given the expectation of a thick ice shell at the surface. At Ceres' surface temperatures, pure water ice would be quite weak and would not have retained the original morphology of the ancient impact basins [e.g., 3]. The large number of craters seen on the surface indicates that the near-surface layer is not as weak as pure water ice. The diversity of crater morphologies and their lateral heterogeneity indicates variations in the underlying ice shell. It is likely that rock fragments resulting from impacts, and/or ice that have been mixed with salts can explain the strength of the shell. We employ a finite element modelling code to examine the ice shell properties that could produce the observed morphology.

We will present geophysical modeling results and the inferences obtained on the ice shell of Ceres.

Acknowledgements

This work was carried out in part at the Jet Propulsion Laboratory, California Institute of Technology, under contract with the National Aeronautics and Space Administration.

References

[1] Preusker et al., [2015], Shape model and rotational state of dwarf planet Ceres from Dawn FC stereo images, this meeting

[2] Park, R. et al, [2015]. Gravity Science Investigation of Ceres from Dawn, this meeting.

[3] Bland, M., [2013], Predicted crater morphologies on Ceres: Probing internal structure and evolution. *Icarus* 226, 510-521.

EPSC Abstracts
Vol. 10, EPSC2015-450, 2015
European Planetary Science Congress 2015

DAWN Framing Camera results from Ceres orbit

A. Nathues (1), M. Hoffmann (1), M. Schäfer (1), L. Le Corre (2/1), V. Reddy (2/1), T. Platz (1), C. T. Russell (3), J.-Y. Li (2), E. Ammannito (3), I. Buettner (1), U. Christensen (1), I. Hall (1), M. Kelley (4), P. Gutiérrez Marqués (1), T.B. McCord (5), L. A. McFadden (6), K. Mengel (7), S. Mottola (8), D. O'Brien (2), C. Pieters (9), C. Raymond (10), J. Ripken (1), T. Schäfer (1), P. Schenk (11), H. Sierks (1), M. V. Sykes (2), G. S. Thangjam (1), F. Tosi (12), J.-B. Vincent (1), D.A. Williams (13) and the Dawn Science Team.

(1) MPI for Solar System Research, Göttingen, Germany, (nathues@mps.mpg.de, +49 551 384 979 433), (2) Planetary Science Institute, Tucson, USA, (3) University of California, Institute of Geophysics, Los Angeles, USA; (4) NASA Headquarters, Washington, USA, (5) Bear Fight Center, Winthrop, USA, (6) NASA, Goddard Space Flight Center, Greenbelt, USA, (7) Clausthal University of Technology, Clausthal-Zellerfeld, Germany, (8) DLR, Institut für Planetenforschung, Berlin, Germany, (9) Brown University, Geological Science, Providence, USA, (10) Jet Propulsion Laboratory, Pasadena, USA, (11) Lunar and Planetary Institute, Houston, USA, (12) Instituto Nazionale di Astrofisica, Rome, Italy, (13) Arizona State University, Tempe, USA

1. Introduction

Having completed its investigation of Vesta in late 2012, the NASA Dawn mission [1] reached its second target, the dwarf planet Ceres on March 6, 2015. During its operational phase, Dawn is scheduled to fly four polar orbits, each with a different distance to the target. The Framing Cameras (FCs) onboard the Dawn spacecraft are mapping the dwarf planet Ceres in seven colors and a clear filter [2], covering the wavelength range between 0.4 and 1.0 µm. The FCs also conduct a number of sequences for purposes of navigation, instrument calibration, and have already performed satellite searches and three early rotational characterizations (RCs) of Ceres in February and May 2015. During the EPSC conference we intend to present the most intriguing results obtained from the Survey orbit (resolution ~400 m/pixel) as well as the first results from HAMO orbit (~140 m/pixel) focusing on the analysis of FC color data.

2. Potential water ice

FC data have been obtained during the RC phases and during several periods of optical navigation. These observations led to a number of intriguing discoveries. One of these is the detection of bright spots, especially on the floor of the 89.5 km diameter crater located at 22.6°N/239.4°E. The brightest of these spots has a geometric albedo of more than 0.4 and was not spatially resolved until RC2. Its high geometric albedo and spectral shape in VIS are consistent with water ice, but further investigations are required to rule out other potential analogue materials. One of the questions Dawn intends to answer is whether Ceres harbors a substantial subsurface reservoir of water ice. During the late approach phase, FCs spatial resolution was already sufficient to identify surface morphologies, which are dominated by the effect of relaxation. Deserving particular mention is a basin structure (Ø 260 km) centered at 13.1°S/122.7°E showing a much smoother surface compared to the rougher terrains indicated in Figure 1. Also, the determined minimum size of central peak craters is more consistent with the icy outer satellites than rocky bodies [3].

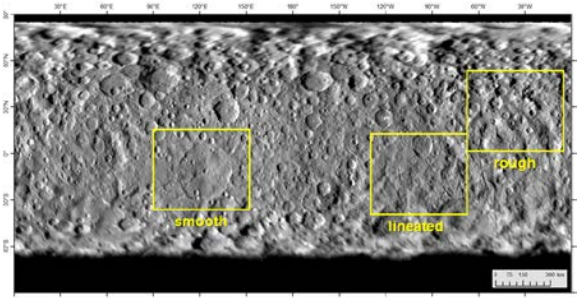

Figure 1: Clear filter mosaic of Ceres acquired by Dawn FC during RC2. Terrains of different roughness are marked. Credit: NASA/JPL-Caltech/UCLA/MPS/DLR/IDA

3. Hunting for water vapor

Near-surface water vapor was detected before arrival of Dawn at Ceres [4]. This water vapor could arise from a variety of processes including cryovolcanism, recent impacts, and sublimation-induced outgassing activity. These should be colorimetrically

distinguishable from the relatively flat and dark spectral background of the average Ceres surface. The water vapor emission observed by [4] requires surface exposures of water ice over small areas that are expected to be clearly resolved in FC images. Because the water vapor emissions seem to be episodic [4, 5], time-resolved color maps of the entire surface may reveal a history of emissions and insights into the mechanism(s) giving rise to them. Thus, the FC color data will provide an important complement to topographic and clear-filter albedo investigations to identify current and past surface processes, as well as other investigations returned by Dawn's payload instruments, to identify current and past surface processes.

4. Identifying native materials

Dawn's first target, Vesta, revealed a surface with remarkable color heterogeneities that even increased over small spatial scales [6, 7, 8]. Given Ceres' larger size, a surface similarly contaminated by exogenic material was expected but not identified so far. The color mosaics derived from RC2 show an unexpectedly high contrast across the Ceres surface (Fig. 2). The low reflectance surface units could be analogous to carbonaceous chondritic material with its low albedo and typical spectral shape [9]. Carbonaceous chondrite meteorite groups (CI, CM), containing hydrated minerals and water, show a very low overall reflectance of less than 0.1 in the visible and near-infrared range. Besides ice, we also consider evaporites, such as carbonates, sulfates and brucite as potential contributors to the brightest surface units on Ceres. These materials show overall reflectance values of more than 0.6 for relatively pure phases. Those minerals have been found in CI and CM [10] meteorites and could be derived from CI- or CM- like precursor material under aqueous conditions. Cryovolcanism or any other kind of surface or subsurface activity could cause those materials to be locally concentrated.

FC color parameters have been identified in order to discriminate the major carbonaceous chondrite groups and to narrow down ambiguities to other potential materials [9]. The FC filters are also suitable for the detection of phyllosilicate absorptions at 0.7 µm and 0.9 µm [9]. These minerals are common products of aqueous alteration of olivine and pyroxene precursor materials and are primary constituents in carbonaceous chondrites.

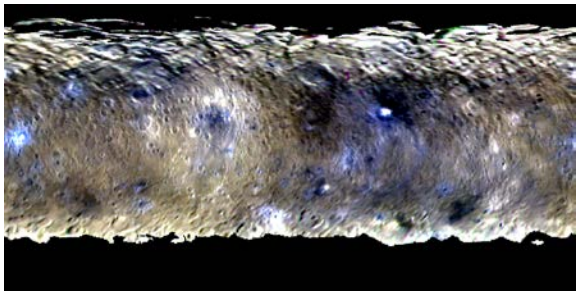

Figure 2: False color image mosaic of Ceres obtained during RC2 (same extent as Fig. 1, R – 0.96 µm, G – 0.75 µm, B – 0.44 µm). Credit: NASA/JPL-Caltech/UCLA/MPS/DLR/IDA

6. Summary and Conclusions

As of the editorial deadline, Dawn FC has acquired imagery with a spatial resolution of up to ~2 km/pixel. Color mosaics from RC2 show a world that is spectrally more diverse than expected. The geomorphology of surface features is, over large areas, consistent with surface relaxation. The discovery of the bright spots and the exploration their nature is very fascinating but requires higher resolution data, which will be on-ground by September 2015.

Acknowledgements

The Dawn FC project is financially supported by the Max Planck Society (MPS), German Aerospace Center (DLR), and NASA/JPL.

References

[1] Russell et al., The Dawn Mission to Minor Planets 4 Vesta and 1 Ceres, Space Sci. Rev., 163, 2011. [2] Sierks et al., The Dawn Framing Camera, in [1], 263-327, 2011. [3] Bray & Schenk 2015, Icarus 246, 156, 2015. [4] Küppers et al., Nature, Vol. 505, pp. 252-527, 2014. [5] Hoffmann et al., EPSC, 2015. [6] Reddy et al., Science, Vol. 336 no 6082, pp. 700-704, 2012. [7] Nathues et al., Icarus, Volume 239, p. 222-237,2014. [8] Nathues et al., Icarus, in press. [9] Schäfer et al., submitted to Icarus. [10] Johnson et al., Geoch. et Cosmoch. Acta 57, 2843–2852,1993.

EPSC Abstracts
Vol. 10, EPSC2015-466, 2015
European Planetary Science Congress 2015

Dawn Framing Camera: Morphology and morphometry of impact craters on Ceres

T. Platz (1), A. Nathues (1), M. Schäfer (1), M. Hoffmann (1), T. Kneissl (2), N. Schmedemann (2), J.-B. Vincent (1), I. Büttner (1), P. Gutierrez-Marques (1), J. Ripken (1), C. T. Russell (3), T. Schäfer (1), G.S. Thangjam (1).
(1) Max Planck Institute for Solar System Research, Göttingen, Germany (platz@mps.mpg.de); (2) Freie Universität Berlin, Berlin, Germany; (3) University of California, Los Angeles, USA.

Abstract

In the first approach images of Ceres we tried to discern the simple-to-complex transition diameter of impact craters. Limited by spatial resolution we found the smallest complex crater without central peak development to be around 21.4 km in diameter. Hence, the transition diameter is expected to be between 21.4 km and 10.6 km, the predicted transition diameter for an icy target. It appears likely that either Ceres' surface material contains a rocky component or has a laterally inhomogeneous composition ranging from icy to ice-rocky.

1. Introduction

On March 6, 2015 the Dawn spacecraft was captured by Ceres' gravity field. Several optical navigation (OpNav) and rotation characterization (RC) observations were acquired during approach phase by the Framing Camera (FC) [1, 2]. In this preliminary study we used images of RC2 and OpNav7 campaigns taken on February 19, 2015 and April 15, 2015, respectively. We present morphological observations of impact craters and provide first measurements of crater depth to diameter relationships. Then, first inferences about the simple to complex transition diameter and resulting surface property (i.e., icy vs. rocky) are made.

1.1 Data and methods

RC2 and OpNav7 images have been processed at the Max Planck Institute for Solar System Research and were resampled to resolutions of 2 km/px and 1.5 km/px, respectively. Individual images are analyzed using ESRI's GIS environment. Crater diameters and crater shadow casts were measured using the ArcGIS extension *CraterTools* [3], which helped to avoid distortions related to map projections. Crater depths are calculated following the equation:

$$d = L / \tan \theta \quad (1)$$

where d is the crater depth, L is the shadow length, and θ represents the incidence angle. For each crater, the diameter was measured 10 times while the shadow length and incidence angle were determined at five locations. For individual parameters the 2σ confidence interval is provided; the depth value includes error propagation analysis of L and θ.

2. Crater morphology

The surface of Ceres is peppered by impact craters. The largest two basins observed so far have diameters of about 270 km. The largest basin (D~273 km) is centered at 13.1°S/122.7°E and is filled by smooth-textured deposits. A central depression surrounding the central pit is noted. The basin rim resembles a pentagonal shape with the northwestern portion being partially buried and disrupted.

Complex craters feature a flat floor and often show a central peak or pit. The interior of some complex craters appear filled. Crater rims vary in shape from circular/elliptical to rectangular and penta-/hexagonal or in some cases developed a combination of semi-circular and angular (plane view) outline. A preliminary survey revealed that the smallest complex crater showing a central peak has a diameter of about 24.5 km. Due to the limited resolution craters smaller than about 20 km in diameter are difficult to classify as either simple or complex crater. However, based on shadow shape, the 17.5 km crater shown in Fig. 1 may represent a simple crater.

3. Crater morphometry

We applied the shadow cast method [e.g., 4] to estimate the depth of impact craters. In the initial

survey we were interested to discern the transitional diameter from simple to complex craters. Figure 1 shows 16 measurements for craters in the size range 17.5–124.8 km.

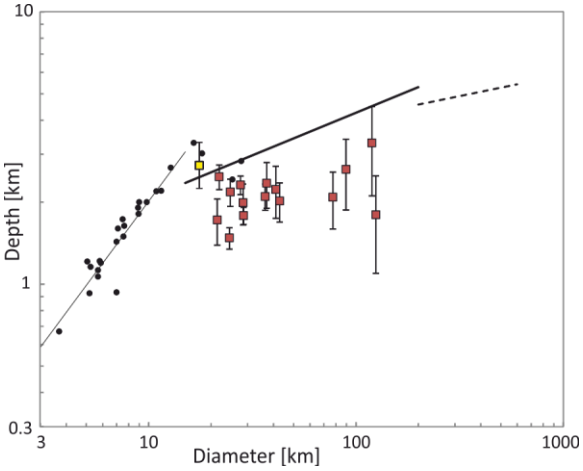

Figure 1: Depth-to-diameter relationship for craters on Ceres (squares). For reference simple and complex lunar craters (black dots) and best-fit lines for simple (thin) and complex (thick) craters, and basins (dashed) are shown [4-6]. Yellow data point may represent a simple crater.

Using the current image data the two smallest flat-floored craters without central peak development are 21.9±0.41 km and 21.4±0.30 km in diameter. In this survey no clear trend within the complex crater population is observed (Fig. 1). The data scatter is likely caused by the craters' different state of degradation resulting in various d/D ratios from 0.01–0.11.

5. Discussion

The determination of the simple to complex transition diameter is particularly important as it provides first estimates of the composition of Ceres' upper crust. The overall density of Ceres is 2077 kgm^{-3} suggesting the presence of 17-27% water by mass [7, 8]. It is commonly thought that Ceres is differentiated into a silicate core and water/ice-rich mantle. However, it is currently unclear whether the water fraction is laterally and vertically homogeneously distributed within the c.100-km-thick mantle and where liquid water (as layer(s) or lens(es)) may occur.

If Ceres's surface is primarily composed of ice, a simple-to-complex transition diameter is predicted at 10.6 km by extrapolation from icy satellites (Fig. 2). The smallest complex crater observed so far is 21.4 km in diameter (Fig. 2) suggesting that the expected transition diameter is somewhere in the range 10.6-21.4 km. Because a number of complex craters without central peak are observed in the size range 21–25 km, it may suggest that the transition diameter is closer to 21 km rather than 10.6 km. If this is the case, then Ceres' surface material cannot be composed of pure water ice and requires a rocky component, or alternatively, lateral inhomogeneity in target rocks (i.e., ice and mingled ice-rock material) is present. At EPSC, we will present an updated survey based on higher resolution data.

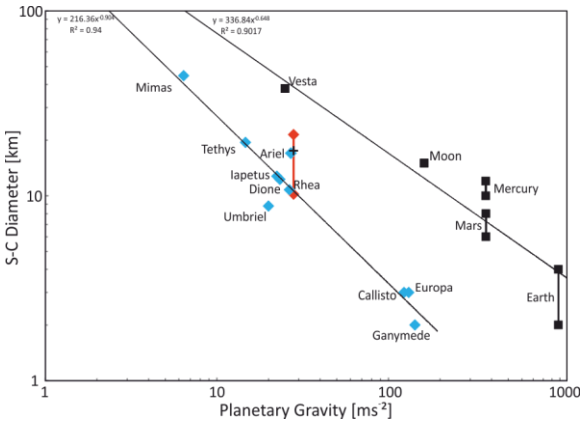

Figure 2: Simple-to-complex transition diameters for various planetary bodies as a function of their surface gravities. Ceres' transition diameter is expected to occur along the red line with the lower point resembling the predicted value and the upper point being the smallest observed complex crater so far. The black cross represents a putative simple crater. Data for planetary bodies taken from e.g. [9–13].

References

[1] Russell, C.T., and Raymond, C.A., 2012, Space Sci. Rev., 163, 3–23. [2] Sierks, H. et al., Space Sci. Rev., 163, 263–328, 2012. [3] Kneissl, T. et al., Planet. Space Sci., 59, 1243–1254, 2011. [4] Pike, R.J., Geophys. Res. Lett., 1, 291–294, 1974. [5] Pike, R.J., 11th Proc. Lunar Planet. Sci. Conf., 2159–2189, 1980. [6] Williams, K.K. and Zuber, M.T., Icarus, 131, 107–122, 1998. [7] Thomas, P.C. et al., Nature, 437, 224–226. [8] McCord, T.B. et al., Space Sci. Rev., 163, 63–76, 2011. [9] Schenk, P.M., JGR, 94, 3813–3832, 1989. [10] Schenk, P.M., Nature, 417, 419–421, 2002. [11] Moore, J.M. et al., Icarus, 171, 421–443, 2004. [12] White, O.L. et al., Icarus, 223, 699–709, 2013. [13] Vincent, J.-B. et al., Planet. Space Sci., 103, 57-65, 2014.

EPSC Abstracts
Vol. 10, EPSC2015-474, 2015
European Planetary Science Congress 2015

Active regions on 1 Ceres in Dawn Framing Camera colours

M. Hoffmann (1), A. Nathues (1), M. Schäfer (1), T. Platz, (1), C. T. Russell (2), J.-B. Vincent (1), M. V. Sykes (3), J.-Y. Li (3), V. Reddy (3), L. Le Corre (3), L. A. McFadden (4), P. Schenk (5), C. M. Pieters (6), P. Gutiérrez-Marqués (1), J. Ripken (1), T. Schäfer (1), K. Mengel (7), G. Thangjam (1), H. Sierks (1), U. Christensen (1), I. Büttner (1), I. Hall (1)

(1) Max Planck Institute for Solar System Research, Göttingen, Germany (hoffmann@mps.mpg.de); (2) Institute of Geophysics, University of California and Los Angeles, Los Angeles, CA, USA; (3) Planetary Science Institute, Tucson, AZ, USA; (4) NASA Goddard Space Flight Center, Greenbelt, MD, USA; (5) Lunar and Planetary Institute, Houston, TX, USA; (6) Department of Earth, Environmental, and Planetary Sciences, Brown University, Providence, RI, USA; (7) Technical Clausthal University of Technology, Clausthal-Zellerfeld, Germany

Abstract

Very prominent bright sites on the dwarf planet Ceres were imaged by the Dawn Framing Cameras. Continuing analysis during early phases of this mission revealed their unique visual and near-infrared spectral properties. These, their local diurnal variability, and their geologic context hint at an unprecedented phenomenon among planetary bodies.

1. Introduction

Dwarf planet Ceres is located near the H_2O „snow-line“ of the Solar System, inside of which the sublimation of water ice becomes sufficiently strong that water ice cannot be stable for a long time when exposed on the surface. Indications for water vapour were first reported by A'Hearn et al. (1992) [1], and more recently Küppers et al. (2014) [2] have reported water absorption based on data obtained by the Herschel observatory. This last is suggesting possible surface or shallow subsurface water ice or cryovolcanism. The Dawn spacecraft [3] reached Ceres in March, 2015, and has imaged its surface [4, 5] with the on-board Framing Cameras [6] during approach and high orbits dedicated to scientific imaging.

2. Bright spots

While some modest albedo variations on Ceres have already been reported from HST images [7], bright spots were already outstanding in Dawn FC images during the early approach phase. Besides one site with prominent sources of this enhanced signal, several similar but smaller features have been found (Fig. 1). The most prominent are located in small depressions inside moderately large craters (>60 km in diameter), but some may not be associated with impact features. The context of the bright spots is a surface characterized by viscous relaxation, collapsed crater centres and related linear tectonic features.

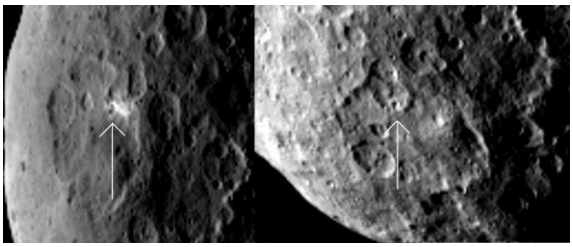

Figure 1: Diurnal change of brightness at a pit in a complex crater. Credit: NASA/JPL-Caltech/UCLA/MPS/DLR/IDA

In FC colour filter images the bright spots show not only enhanced reflectance, but also a significantly different spectral shape between 440 nm and 960 nm, which could be consistent with water ice. Mixtures with other components cannot be ruled out.
The albedo and heliocentric distance of Ceres enable maximum surface temperatures a few tens degrees below 0° Celsius. Inside this distance water sublimation on comets increases significantly from their dark surfaces. Ceres may have reservoirs of liquid water or ice overlain by an ice-rich crust [8, 9]. Impacts or tectonic processes may lead to local exposure of such material.
A comparison of images of the same features at different rotational phases, and consequently different insolation, even in broad band "clear filter" images, show large changes in reflectance in and near the cores of the bright spots. Their maximum signal is reached near local noon, and close to the terminator no contrast to the surrounding material remains visible. Also in spectral distribution some variability is detectable depending on the amount and geometry of insolation.

Figure 2: Details of the brightest feature on Ceres. Credit: NASA/JPL-Caltech/UCLA/MPS/DLR/IDA

A multi-component structure of the feature in Fig. 2 is indicated consisting of: A primary and possible minor companion, potential deposits, and a superposed extended area, which appears to change its orientation during the progressing day-time.
The crater of the brightest feature has a dark halo extending 200 km to the north-east of its host crater. Since similar and even larger dark areas are associated with some major craters without bright spots, it suggests that they are consequences of the context of the bright spot phenomenon. Since it is improbable that the bright spots have been present over the course of Ceres' history, and other similar features may have been present in the past on Ceres, these dark areas may be remnants or tracers of former similar phenomena and processes. Some smaller craters show spectra at central peaks with a trend towards the brighter, negative-sloped areas surrounding the spots.

3. Summary and Conclusions

Spectral properties and diurnal variability are consistent with insolation-dependent local activity on the surface of Ceres. While cryo-volcanism and impact-generated hydrothermal processes are possible alternatives explaining this activity, the current observational evidence by low-resolution imaging and visual-NIR spectral data rather favour local sublimation. No centres of activity have been detected near linear morphologic features yet. Temperatures at Ceres are sufficient to trigger sublimation of exposed ice layers at its heliocentric distance [10]. The possibility of sublimating areas is further supported by the morphology of impact features and current models of Ceres' interior and geologic history, as collapsed central peaks in some craters and other indications of a weak crust suggest.

References

[1] A'Hearn, M. F., and Feldman, P. D., Water vaporization on Ceres, Icarus 98, 54-60, 1992.
[2] Küppers, M., et al., Localized sources of water vapour on the dwarf planet (1) Ceres, Nature 505, 525-527, 2014.
[3] Russell, C. T., and Raymond, C. R., The Dawn Mission to Minor Planets 4 Vesta and 1 Ceres. Space Sci. Rev. 163, 3-23, 2011.
[4] Nathues, A., et al., Dawn Framing Camera clear filter imaging on Ceres approach, Proc. 46th Lunar Planet. Sci. Conf., #2069, 2015.
[5] Hoffmann, M., et al., Dawn approaches Ceres: Analysis of first FC color data. EGU2015-8830.
[6] Sierks, H., et al. The Dawn Framing Camera, Space Sci. Rev. 163, 263-327, 2011.
[7] Li, J.-Y., et al., Photometric analysis of 1 Ceres and surface mapping from HST observations, Icarus 182, 143-160, 2006.
[8] Thomas, P. C. et al. 2005, Differentiaiton of the asteroid Ceres as revealed by its shape. Nature, 437, 8 September 2005|doi:10.1038/nature03938.
[9] Castillo-Rogez, J. C., and Mc Cord, T. B., Ceres' evolution and present state constrained by shape data. Icarus 205, 443-459, 2010.
[10] Gombosi, T. I., et al., Dust and neutral gas modeling of the inner atmospheres of comets, Reviews of Geophysics 24, 667-700, 1986.

EPSC Abstracts
Vol. 10, EPSC2015-488, 2015
European Planetary Science Congress 2015

Dawn Framing Camera Color Mosaics of Ceres

M. Schäfer (1), A. Nathues (1), M. Hoffmann (1), T. Schäfer (1), M. R. M. Izawa (2), L. Le Corre (3), E. A. Cloutis (2), G. S. Thangjam (1), T. Platz (1), K. Mengel (4), C. T. Russell (5), V. Reddy (3), J. Ripken (1), P. Gutiérrez-Marqués (1), I. Büttner (1), I. Hall (1), H. Sierks (1), U. Christensen (1).
(1) Max Planck Institute for Solar System Research, Göttingen, Germany (schaeferm@mps.mpg.de), (2) University of Winnipeg, Winnipeg, Canada, (3) Planetary Science Institute, Tucson, USA, (4) Clausthal University of Technology, Clausthal-Zellerfeld, Germany, (5) University of California, Los Angeles, USA.

Abstract

We processed Dawn Framing Camera color filter images to produce global spectral mosaics of 1 Ceres. The mosaics allow analyses of compositional variations of the cerean surface. Moreover, we can derive statements about Ceres' surface absolute reflectivity using photometrically corrected FC data. During EPSC, we will show examples including global mosaics from Survey orbit images.

1. Introduction

The Dawn spacecraft entered orbit around Ceres in March, 2015 [1]. During approach and later science phases, several spectral datasets with global coverage were acquired using the Framing Camera (FC) onboard Dawn (Tab. 1). The FC is equipped with seven color filters covering the 0.4–1.0 µm wavelength region, plus one broadband filter [2]. The highest spatial resolution of FC color mosaics with complete spectral coverage of Ceres will be obtained during the High Altitude Mapping Orbit (HAMO) phase, yielding a spatial resolution of approximately 135 m/pixel.

Table 1: Dawn mission phases at Ceres with global coverage by all Framing Camera color filters.

Dawn phase	Date(s)	Resolution [m/pixel]	No. color stations*)
RC1#)	2015-02-12	~7,900	13
RC2	2015-02-19	~4,300	20
RC3	2015-05-04 – 2015-05-07	~1,260	45
Survey	2015-06-05 – 2015-06-28	~410	133
HAMO	2015-08-06 – 2015-10-11	~135	492

*) A station consists of 7 color images (all filters)
#) RC – Rotation Characterization

2. FC data processing

The FC color data is acquired in so-called 'stations' of seven images, i.e., all appendant color images are taken in the shortest possible time intervals. After calibration of the data to radiances and removal of the in-field stray light component (data level 1C), the subsequent processing is using the USGS Integrated Software for Imagers and Spectrometers (ISIS 3) [3]. Initially, every image is converted to I/F reflectance involving their respective heliocentric distances. Afterwards, every station is treated individually. At first, this comprises the precise co-registration of a single color image with the corresponding shaded relief map, which is based on the Ceres DEM. Subsequently, the remaining images of the station are co-registered with the single image. This ensures a consistent fit of all filters with the DEM, which is important for the accuracy of the following photometric corrections. These are based on individual Hapke Henyey-Greenstein model parameters for each FC filter. Finally, the spectral cubes of all stations are spatially mosaicked to create a global mosaic. Our approach yields maximum spectral integrity of the mosaic, as opposed to a separate processing and mosaicking of all images from single filters and subsequent stacking.

3. Ceres color mosaics

Figure 1 shows the low cerean surface reflectance exemplarily in the 0.55 µm filter. Considering the region between 50° N and 50° S latitude in Fig. 1 (in order to exclude areas of high incidence), nearly 99% of the pixels lie in between 0.03 and 0.04 reflectance at 0.55 µm. Only 0.2% of the pixels exhibit lower reflectances than 0.03, while 0.9% possess higher reflectances than 0.04. These reflectance values are consistent with most carbonaceous chondrite (CC) meteorites of CM type and some unusual aqueously altered and thermally metamorphosed carbonaceous chondrites (ATCC) as investigated by [4].

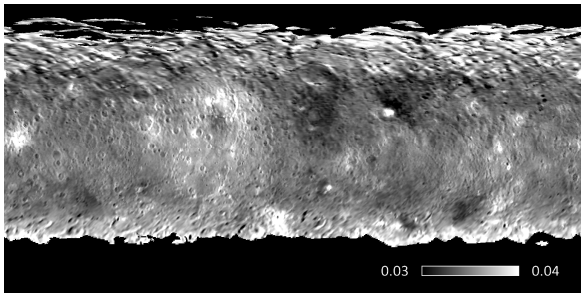

Figure 1: Global Ceres mosaic of reflectance in the FC 0.55µm filter from RC2 phase. Credits for all images: NASA/JPL-Caltech/UCLA/MPS/DLR/IDA.

Despite the FC's limited wavelength range, even early color mosaics acquired during the RC1 and RC2 phase indicate a wide diversity of cerean surface materials if viewed as simple RGB displays (Fig. 2 and 3). For Figure 2, we preferentially used areas of low solar incidence and phase angles to create the mosaic. This yields a display free of most topographic effects (e.g., crater shadows), while intensifying color differences. In contrast, Figure 3 shows a mosaic where high incidence areas were favored, in order to emphasize topographic features.

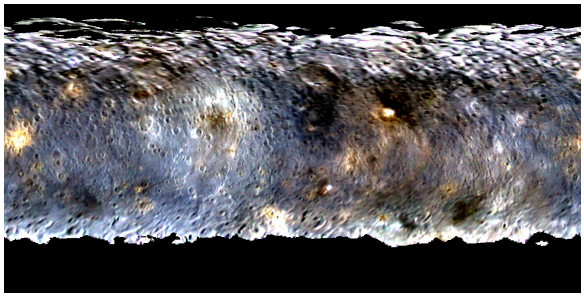

Figure 2: Global FC color image mosaic of Ceres from RC2 phase. Areas of low solar incidence have been used. R – 0.44 µm, G – 0.55 µm, B – 0.92 µm.

4. Scientific utilization (outlook)

We developed the aforementioned image processing and mosaicking approach for the FC data from Vesta, Dawn's first target. There, the spectral mosaics have proven crucial for a wide variety of geo– and mineralogical studies (e.g., [5, 6]). On Ceres, we intend to use them for the following investigations:

- Search for evidence of water ice on or near the surface.
- Investigation of the nature of the bright spots which appeared in Dawn observations during the approach phase.

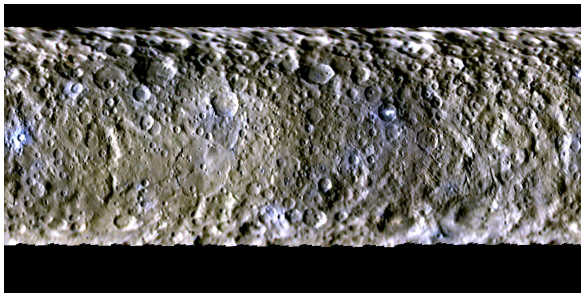

Figure 3: Global Ceres mosaic of FC color images from RC2 phase. Areas of high solar incidence have been used. R – 0.96 µm, G – 0.75 µm, B – 0.44 µm.

- Distribution of CC material on Ceres. For this, we will use FC-based spectral parameters that have been developed in [4] based on available CC laboratory spectra.
- The latter also includes the search for phyllosilicates, which are the main constituent in the matrix of aqueously altered CC meteorites (e.g., many CM). Using FC filters, [4] showed that it is possible to see both the 0.7 µm and the 0.9 µm absorption bands of Fe-bearing phyllosilicates.
- Exploration of possible cerean surface materials, e.g., serpentinization assemblages including serpentine group minerals, magnetite, carbonates and brucite. Besides, we also intend to search for salt-rich materials such as sulfate precipitates leached from CI and CM as found by [7, 8], or chloride-rich assemblages as suggested by [9].
- Signatures of exogenic materials delivered by impacts, more or less mixed with native material.
- Checking for possible temporal variations of the surface, e.g., in the case of near-surface ice.

References

[1] Russell, C. T. & C. Raymond, Space Sci. Rev., 163, 3-23, 2011. [2] Sierks, H. et al., Space Sci. Rev., 163, 263-327, 2011. [3] Anderson, J. A. et al.: ISIS Cartographic Tools for the Dawn FC and VIR Spectrometer. AGU Fall Meeting, abstract #U31A-0009, 2011. [4] Schäfer, T. et al.: Dawn FC color data: Carbonaceous Chondrites and Aqueous Alteration Products as Potential Ceres Analog Materials. Icarus, 2015, submitted. [5] Nathues, A. et al.: Detection of serpentine in exogenic CC material on Vesta from Dawn FC data. Icarus, 239, 222-237, 2014. [6] Nathues, A. et al.: Exogenic olivine on Vesta from Dawn FC color data. Icarus, in press, 2014. [7] Airieau, S. A. et al.: Planetesimal sulfate and aqueous alteration in CM and CI carbonaceous chondrites. Geoch. et Cosmoch. Acta, 69 (16), 4166-4171, 2005. [8] Izawa, M. R. M. et al.: Composition and evolution of the early oceans: Evidence from the Tagish Lake meteorite. Earth & Planet. Sci. Letters, 298 (3-4), 443-449, 2010. [9] Fries M. et al.: Do we already have samples of Ceres? 76th Annual Meteoritical Soc. Meet, abstract #5266, 2013.

EPSC Abstracts
Vol. 10, EPSC2015-490, 2015
European Planetary Science Congress 2015

Ceres: ice stability and water emission

M. Formisano(1), M.C. De Sanctis (1), G. Magni (1), M.T. Capria (1), F. Capaccioni (1), S. Marchi (5), E. Ammannito (2), D. Bockelee-Morvan (3), C.A. Raymond (4) and C.T. Russell (2)
(1)INAF-IAPS, Rome (Italy), (2) IGPP, UCLA, CA, USA, (3) LESIA, Observatorie de Paris, France, (4) JPL, Pasadena, CA, USA, (5) Southwest Research Institute, Boulder, CO, USA

Abstract

Recent observations of H_2O vapor plumes in localized regions [1] suggest the presence of ice on surface and/or on sub-surface regions of asteroid Ceres. In the hypothesis of a cometary-like emission mechanism (as already suggested by [2]), we performed several simulations in order to establish what are the likely physical conditions (in particular ice depth and thermal conductivity of crust) to fit Herschel observations [1].

1. Introduction

Ceres, target of NASA Dawn mission, is the link between outer ice satellites and inner rocky asteroid of our solar system. Recently, Herschel observed the presence of water vapor emission around Ceres, suggesting a flux of at least 10^{26} molecules for second from well localized regions, at mid-latitude [1]. This phenomenon could be explained in two main ways: the first mechanism involves the presence of long-lived radionuclides as internal heat source (as expected by theoretical models, i.e. [3, 4]); the second one requires a cometary-like behavior [2]. It was observed a certain variability of emission with the heliocentric distance [1]: this suggests that water emission could be driven by a cometary-like sublimation, due to the increase of temperature during the approach of the perihelion. So we applied a cometary model, developed by [5, 6, 7], and we studied the temperature of the first layers and the water emission.

2. The Model

The model assumes Ceres as spherical body made of a homogeneous mixture of dust and ices in well-defined proportions. At surface, the balance among solar input, energy re-emitted in space, conducted in the interior and used to sublimate ices determine the temperature. The heat diffusion through the porous mixture of ice and dust is computed, determining the water ice phase transition and the sublimation rate of the ices. The gas flow through the pore system is described by the mass conservation equation.

In Table 1 we report the main physical parameters of our model.

Albedo	0.09
Dust/ice ratio on surface	2.5
Porosity	0.4
Initial temperature	163
Crust thermal conductivity	$10^{-3}, 10^{-2}$
Emissivity	0.8
Ice depth	0, 0.02, 0.05, 0.50

Table 1: Main adopted physical parameters values in SI units.

In the assumption of a "cometary-like" behavior (valid for the external layers), we performed several simulations in order to study the effects of the different parameters on temperature and on sublimation. We explored the case of emissivity equal to 0.8 in order to simulate a "moderately-rougher" surface. Thermal conductivity values used in our model are 10^{-3} and 10^{-2} (in SI units), since they lead to "reasonable" values of thermal inertia. In fact, it is expected that Ceres could have low/medium values of thermal inertia: some studies suggest values of 15-38 (in SI units) [10, 11], others higher values, i.e. 80 [12]. We study as ice's depth influences the water emission, by setting ice front at different depth from the surface (see Table 1).

3. Summary and Conclusions

The maximum temperatures achieved are consistent with VIR measurements (Tosi et al., in preparation) and with the temperature of the warmest area (235±4K, [8]) for low values of thermal conductivity, if ice is within few cm from the surface (see Fig.1). Since the ice on surface at the equator is stable for very few orbits (as suggested by [9]) (see Fig.2), in order to fit Herschel observations (10^{26} mol/sec), we need an emitting area of about 1km^2 in agreement with

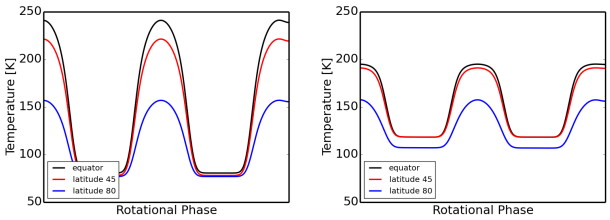

Figure 1: Temperature vs rotational phase for two different thermal conductivity values, 10^{-3} (left) and 10^{-2} (right) (in SI units), with ice at 5 cm beneath the surface.

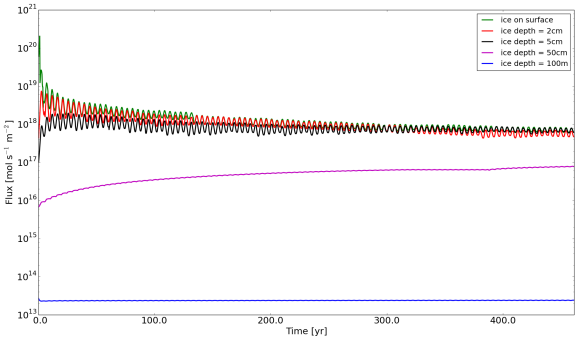

Figure 2: Flux vs time for different ice's depth at equatorial latitude, with thermal conductivity of 10^{-3} [SI].

[1] and also a continuous replenishment of water on the surface. For this purpose, an area of 1km^2 is expected to be activated every 1400-7700 years, with an excavated depth of about 200-250 m (the uncertainty depends on physical properties of the terrain). The activation rate is calculated by impact cratering (the frequency of formation of crater with at least 1 km in diameter is 4.5×10^{-11} - 2.5×10^{-10} km^{-2}yr^{-1}). If ice is below the surface of several tens of cm, water ice is stable for very long time (see Fig.2): in this case, an emitting area of 10^4 km^2 is required. If ice is very far below the surface (i.e. 100 m), an emitting area of 10^7km^2 is required, which is greater than the overall area of Ceres, so impossible. Fluxes from polar regions are very small compared to Herschel observations. The water emission could lead to a transient atmosphere around Ceres, as suggested by Magni et al. (in preparation), by applying a smoothed-particle hydrodynamic code.

Acknowledgements

This work is supported by ASI grant. The computational resources used in this research have been supplied by INAF-IAPS through the DataWell project.

References

[1] Kuppers M. et al., Nature 505, 525-527, 2014

[2] Fanale F.P and Salvail J.R., Icarus 82, 97-110, 1989

[3] McCord T.B. and Sotin C., JGR 110, E05009, 2005

[4] Castillo-Rogez J.C. and McCord T.B., Icarus 205, 443-459, 2010

[5] Lasue J., De Sanctis M.C., Coradini A., et al., Planet.Space.Sci. 56, 1977-1991, 2008

[6] De Sanctis M.C., Lasue J., Capria M.T., Astron.J. 140, 1-13, 2010

[7] De Sanctis M.C., Lasue J., Capria M.T., Icarus 207, 341-358, 2010

[8] Saint-Pe O., Combes M., Rigaut F., Icarus 107, 271, 1993

[9] Titus, N., Geophys.Res.Lett 42, doi:10.1002/2015GL063240

[10] Spencer J., Icarus 83, 27-38, 1990

[11] Chamberlain M.A. et al, Icarus 202, 487, 2009

[12] Keihm S. et al., Icarus 226, 1086-1102, 2013.

EPSC Abstracts
Vol. 10, EPSC2015-493, 2015
European Planetary Science Congress 2015

Ceres photometric properties from VIR on Dawn

M. Ciarniello (1), M. C. De Sanctis (1), E. Ammannito (1,2), F. Capaccioni (1), M. T. Capria (1), F. G. Carrozzo (1), S. Fonte (1), A. Frigeri (1), M. Giardino (1), A. Longobardo (1), G. Magni (1), E. Palomba (1), A. Raponi (1), F. Tosi (1), F. Zambon (1), C. A. Raymond (3), C. T. Russell (2) , J.-Y. Li (4) and the Dawn Science Team, (1) Istituto di Astrofisica e Planetologia Spaziali, Istituto Nazionale de Astrofisica, Rome, Italy, (mauro.ciarniello@iaps.inaf.it), (2) University of California Los Angeles, Earth Planetary and Space Sciences, Los Angeles, CA-90095, USA, (3) Jet Propulsion Laboratory, California Institute of Technology, 4800 Oak Grove Drive, Pasadena, CA-91109, USA (4) Planetary Science Institute, USA

1. Introduction

Dawn spacecraft [1] entered orbit around Ceres on 6 March 2015. During the approach phase to this dwarf planet and later, through the Survey, High Altitude Mapping (HAMO) and Low Altitude Mapping Orbits (LAMO), the Visible and Infrared Mapping Spectrometer (VIR) will perform detailed observations of the surface of the body. VIR [2] is an imaging spectrometer onboard the Dawn mission and it is composed of two spectral channels: the visible (VIS) covering the 0.25 μm – 1.0 μm wavelength range and the infrared (IR) for the 0.95 μm – 5.0 μm interval.

During the various phases of the mission, the surface of Ceres will be observed under different observation geometries. The measured signal is then affected by photometric issues that need to be minimized in order to exploit the intrinsic spectral variability of the surface, thus allowing the direct comparison between acquisitions taken under different observation conditions. In order to accomplish this task we perform a photometric reduction of the dataset by means of a simplified Hapke model, following the approach of [3].

2. Photometric model

The dataset has been compared to the Hapke bidirectional reflectance model [4] which links the photometric output to the surface single scattering albedo and geometry. Since Ceres is a relatively dark object we neglect, at a first stage, the contribution from multiple scattering, and in order to minimize the number of free parameters we do not include the Coherent Backscattering Opposition Effect (CBOE). In particular it cannot be constrained with the present dataset, because observation with very low phase angle (α < 1°-2°) are not available. The equation of the bidirectional reflectance is then:

$$I/F(i,e,\alpha) = \frac{w}{4}\frac{\mu_{0e}}{\mu_e + \mu_{0e}}[1 + B(\alpha)]p(\alpha)S(i,e,\alpha,\bar{\theta}) \quad (1)$$

where *I/F* is the measured signal, *i*, *e* and *α* are the incidence, emission and phase angles respectively, *w* is the surface single scattering albedo (SSA), *p(α)* is the single scattering phase function (SPPF), *S* is the shadowing function depending on the average surface slope $\bar{\theta}$, μ_{0e} and μ_0 are the effective cosines of the incidence and emission angles respectively and *B(α)* accounts for the Shadow Hiding Opposition Effect (SHOE). The SPPF has been modelled following [3]:

$$p(\alpha) = \frac{1 - b^2}{(1 + 2b\cos(\alpha) + b^2)^{3/2}} \quad (2)$$

and *b* represent the asymmetry parameter.
From the comparison of the Hapke model to the whole dataset it is possible to retrieve the photometric parameters of eq. 1 and it is possible to reduce the measured *I/F* to *SSA*, which is an intrinsic property of the surface (fig.1). Given the lack of data a low phase angles (α < 10°) we assume SHOE to be described by the parameters derived in [5], for the present analysis.

3. Results

Photometrically reduced data will be used to generate *SSA* maps of Ceres' across the VIR wavelengths range in order to investigate spectral variability of the surface. Simultaneously, Hapke's model parameters representing the average properties of Ceres will be determined: *b*, $\bar{\theta}$ and possibly the ones describing the SHOE if observations at low phase angle will be available.

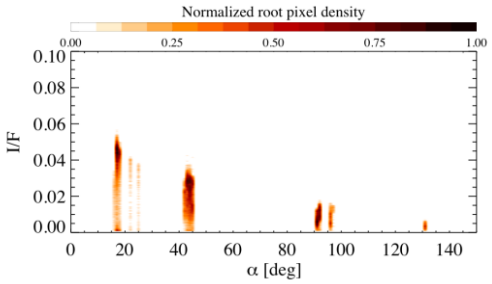

(a)

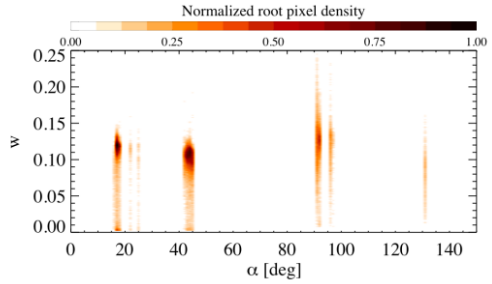

(b)

Fig.1. a) I/F at 0.*550 μm* as a function of phase angle from VIR observations of Ceres during Approach phase. b) *w* at 0.*55 μm* as a function of phase angle after photometric correction. Note that dependence on α has been eliminated. Color bars indicate the root of the pixel density normalized to the maximum value.

Acknowledgements

VIR is funded by the Italian Space Agency–ASI and was developed under the leadership of INAF-Istituto di Astrofisica e Planetologia Spaziali, Rome-Italy. The instrument was built by Selex-Galileo, Florence-Italy. The authors acknowledge the support of the Dawn Science, Instrument, and Operations Teams. This work was supported by ASI and NASA. A portion of this work was performed at the JPL/NASA.

References

[1] Russell, C.T. et al., Science, 336, 684, 2012.
[2] De Sanctis M.C. et al., Space Sci. Rev., DOI 10.1007/s11214-010-9668-5 , 2010.
[3] Ciarniello et al., submitted to A&A
[4] Hapke, 1993, Theory of reflectace and emittance spectroscopy. Cambridge University Press.
[5] Helfenstein, P., Veverka, J.: Physical characterization of asteroid surfaces from photometric analysis, In: Asteroids II, 557-593, 2002.

EPSC Abstracts
Vol. 10, EPSC2015-522, 2015
European Planetary Science Congress 2015

Surface compositional heterogeneity of (4) Vesta from Dawn FC using a 3 dimensional spectral approach

G. Thangjam (1), A. Nathues (1), K. Mengel (2), M. Hoffmann (1), M. Schäfer (1), P. Mann (3), E. A. Cloutis (3), H. Behrens (4), T. Platz (1), T. Schäfer (1), H. Sierks (1), U. Christensen (1), C. T. Russell (5).
(1) Max Planck Institute for Solar System Research, Göttingen, Germany (thangjam@mps.mpg.de), (2) Clausthal University of Technology, Germany, (3) University of Winnipeg, Canada, (4) University of Hannover, Germany, (5) University of California, Los Angeles, USA.

Abstract

The historic journey of the Dawn spacecraft in 2011-2012 was a turning point in understanding asteroid (4) Vesta. The surface composition and lithology were analysed and mapped in earlier studies using Dawn imageries [1], [2]. We introduce here a 3 dimensional spectral approach to analyze and map the surface composition using Dawn Framing Camera (FC) color data. Various laboratory spectra of available HEDs and their mixtures, including new spectra measured in this work, were used. Band parameters were reviewed and modified wherever necessary to make the best use of the data. We particularly focused on carbonaceous-chondrite-bearing and olivine-bearing lithologies. An attempt has been made to distinguish glass/impact-melt lithologies.

1. Introduction

Asteroid (4) Vesta is one of the most massive objects in the main belt which is presumed to be intact since the early solar system formation. It was the first target of the Dawn mission with an objective to study and reveal planetary evolution in the early solar system. The surface composition and mineralogy of Vesta is very important in order to understand its evolution. Such analyses and mapping were presented in earlier studies [1], [2]. Besides the overall HED lithology, other components are contributing to Vesta's heterogeneity, i.e., dark materials [3], [4], bright materials [5], [6], orange/glass/shock/impact-melt materials [7], [8], olivine-rich materials [8], [9], [10], [11]. Motivated by the current understanding of such heterogeneity, we introduce here a 3 dimensional spectral analysis approach and its applications.

2. Laboratory spectra

Various spectra of HED meteorites, CM2 chondrites, olivine, and olivine-orthopyroxene mixtures were collected from RELAB, USGS and HOSERLab [1], [10]. In addition we used spectra of eucrite-rich howardite NWA1949, diogenite-rich howardite DA779, Jbilet Winselwan (CM2 chondrite), olivine, and their mixtures in varying proportions. These samples/mixtures were prepared in a grain size range (less than 65 microns). The spectra were measured at HOSERLab (University of Winnipeg) using an ASD Fieldspec Pro HR spectrometer, relative to Spectralon® standard. The spectra were taken in the wavelength range from 0.35 to 2.5 microns, at i=30° and e=0°. All spectra were resampled to FC bandpasses [12]. Figure 1 shows resampled spectra which are normalized to 0.75 microns.

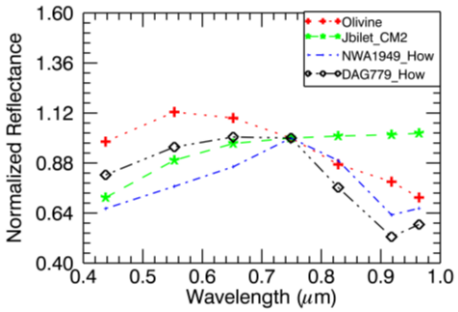

Figure 1. Normalized reflectance spectra of samples measured in this work (NWA1949, DAG779, Jbilet Winselwan, and olivine).

3. Analysis and preliminary results

We reviewed the existing FC band parameters and modified these, wherever necessary, to make the best use of the data. The parameters used here are:

1. VS: visible slope or gradient in % per 100 nm in the visible region, using the peak reflectance as upper wavelength limit [13], [14]
2. Ref: peak reflectance value in the visible region
3. BS: 1-µm band strength (i.e., the ratio between maximum and minimum reflectance values in the visible region and the near-infrared region, respectively)
4. MR: Mid Ratio, (0.75µm/0.83µm)/(0.83µm /0.92µm) [10]
5. BT: Band Tilt, (0.92µm/0.96µm) [1], [10], [15].

Significant changes were observed when applying our revised band parameters. For example, Figure 2 shows RGB composite images of Arruntia crater. The image on the left uses standard Clementine color ratios, while the right one uses our parameters. Red and blue represent spectral slope in the visible region, and green approximates 1-micron band depth.

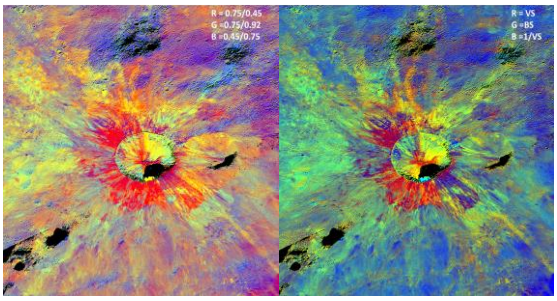

Figure 2. Clementine ratio RGB composite image (left), and revised composite image (right) of Arruntia crater (diameter ~ 12 km). R, G and B in the labels are ratios or parameters. Red and blue represent spectral slope in the visible region, while green indicates 1-micron band depth.

Three band parameter values were used to plot and discriminate lithologies in a three-dimensional space. Polyhedrons were created for each lithology, i.e., howardites, eucrites, diogenites, olivines, CM2's, olivine-HED mixtures, olivine-orthopyroxene mixtures and CM2-HED mixtures (Figure 3). A Macibini eucrite glass spectrum was also included in this plot as a single scattered point. The plots were analyzed for separability of the polyhedrons (lithologies). These polyhedrons were applied to map Vestan lithologies using FC data (~60 m/pixel). The analysis and mapping were done in MATLAB and IDL/ENVI software.

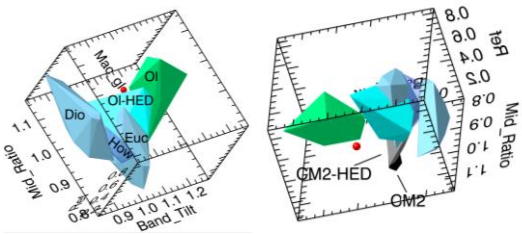

Figure 3. Two different views of a 3-dimenional band parameters space BT-MR-Ref. Each polyhedron represents a lithology (Euc - eucrite, Dio - diogenite, How- howardite, Ol - olivine, Ol-HED - olivine and HED mixtures/samples, CM2 - CM2 chondrite, CM2-HED - CM2 chondrite and HED mixtures/samples, Mac_gl - Macibini eucrite glass)

Acknowledgements

We are thankful to RELAB and USGS spectral library for the spectra used in this work. T.G. would like to thank Cornelia Ambrosi, Silke Schlenczek, Dietlind Nordhausen, Walter Goetz, Harald Steininger, Fischer Henning, for their help in preparing samples/mixtures, and also Nagaraju Krishnappa, Ladislav Rezac, Jayant Joshi, Dick Jackson, Megha Bhatt, for their help in programming.

References

[1] Thangjam, G. et al.: Meteorit. Planet. Sci., 48, 2199-2210, 2013.
[2] Ammannito, E. et al.: Meteorit. Planet. Sci., 48, 2185-2198, 2013.
[3] Reddy, V. et al.: Icarus 221, 544-559, 2012.
[4] Nathues, A. et al.: Icarus 239, 222-237, 2014.
[5] Longobardo, A. et al.: Icarus 240, 20–35, 2014.
[6] Zambon, F. et al.: Icarus 240, 73-85, 2014.
[7] Le Corre, L. et al.:, Icarus 239, 222-237, 2013.
[8] Ruesch, O. et al.: JGR, 119, 2078–2108, 2014.
[9] Ammannito, E. et al.: Nature, 504, 122-125, 2013.
[10] Thangjam, G. et al.: Meteorit. Planet. Sci. 49, 1831-1850, 2014.
[11] Nathues, A. et al.: Icarus, in press, (doi:10.1016/j.icarus.2014.09.045).
[12] Sierks, H. et al.: Space Sci. Rev., 163, 263-327, 2011.
[13] Luu, J. and Jewitt, D.: Astron. J. 99, 1985-2011, 1990.
[14] Doressoundiram, A. et al.: in The Solar System Beyond Neptune, 91-104, 2008.
[15] Isaacson, P.J. and Pieters, C.M.: JGR, 106, 28001-28022, 2009.

EPSC Abstracts
Vol. 10, EPSC2015-525, 2015
European Planetary Science Congress 2015

Color variations on Ceres derived by Dawn/VIR: Implications for the surface composition

F. Zambon (1), M. C. De Sanctis (1), F. Tosi (1), A. Longobardo (1), E. Palomba (1), G. Carrozzo(1), J. -Ph. Combe (2), J.-Y. Li (3), L. A. McFadden (4), S. Marchi (5), R. Jaumann (6), S. Schoeder (6), M.Ciarniello (1), A. Raponi (1), A. Frigeri (1) , E. Ammannito (7), C. T. Russell (7), C. A. Raymond (8)
francesca.zambon@iaps.inaf.it

(1) Istituto di Astrofisica e Planetologia Spaziali, Istituto Nazionale de Astrofisica, Rome, Italy, (2) Bearfight Institute, 22 Fiddler's Road, Winthrop, WA 98862, (3) Planetary Science Institute | 1700 E. Ft. Lowell Rd., Suite 106, Tucson, AZ 85719, USA, (4) NASA/GSFC Greenbelt , MD 20771, (5) Southwest Research Institute 1050 Walnut St, Suite 300, Boulder, CO 80302, (6) Institute of Planetary Research, German Aerospace Center (DLR), Rutherfordstrasse 2, D-12489 Berlin, Germany, (7) University of California Los Angeles, Earth Planetary and Space Sciences, Los Angeles, CA-90095, USA, (8) Jet Propulsion Laboratory, California Institute of Technology, 4800 Oak Grove Drive, Pasadena, CA-91109.

Introduction

Ceres, the second target of the Dawn mission [1], with a diameter of ~952 km, is the largest object in the main asteroid belt [2], and classified as a dwarf planet. More than two years after departure from Vesta, Dawn finally arrived to Ceres. During the approach phase, the spacecraft acquired data with unprecedented spatial resolution. Previous work based on Hubble Space Telescope (HST) data, highlight regions with different albedo variation in the UV-VIS range [3] (Fig. 1). The Visible and InfraRed (VIR) mapping spectrometer onboard Dawn covers the overall wavelength range between 0.25 and 5.1 μm [4]. VIR will enable the first comprehensive compositional mapping of Ceres, focusing on the possible presence of water ice, salts, organics and volatiles, and surface thermal properties [5].

Dataset analysis

Here we present the first map of Ceres obtained from VIR data acquired during the Rotation Characterization 2 (RC2) observation phase in February 2015 (Fig. 2). The spatial resolution is ~11 km/pixel, better than the Hubble Space Telescope (HST). The map has been obtained by mosaicking seven VIR cubes, filtered for incidence angle $0°<i<50°$ and phase angle $0°<p<50°$. The map represents spectral ratios scaled to 0.64 μm indicating regions of different colors across Ceres. Red regions have a higher value of 0.9/0.64, or a weaker or absent absorption at 0.9 μm than do the green and blue regions. Blue regions have higher value of 0.44/0.64 or a weaker UV absorption than red or green regions.

First results from VIR

The RGB image in Fig.1 obtained from HST observations of Ceres shows regions with different spectral properties in the UV-VIS range based on three wavelengths (223 nm (blue), 335 nm (green) and 535 nm (red)), which correspond to different albedo variation [3]. The numbers in Fig.1 indicate regions of interest observed by HST with different colors relative to Ceres' average. At large scale two macro-regions have been identified, (between 0° and 120° in longitude and between 120° and 300° in longitude), as well as smaller dark and bright areas. In the VIR map in Fig. 2, we observe the same dichotomy and a similar but not identical distribution of the dark and bright regions. The bright spot #1 and #5 appear on both the maps. The two spots seem to have different thermal characteristics [5], which could indicate different physical properties, and therefore their different nature. In particular spot #5 is located in a region (a stripe with a range of longitude between 215° and 250°), which is considered potentially active by [6]. The Framing Camera color filter mosaics obtained from RC2 reveal darker regions corresponding to the longitude range between 120° and 300°, which appear magenta in VIR map [4], and may consist of carbonaceous chondritic material [7].

During the RC3 and Survey, VIR will acquire data with a spatial resolution of 3.4 km/px and 1.1 km/px,

respectively. New maps will be produced with the high resolution data. Moreover thermal analysis [6] combined with a detailed spectral analysis will reveal more on the composition and physical characteristics of Ceres' surface.

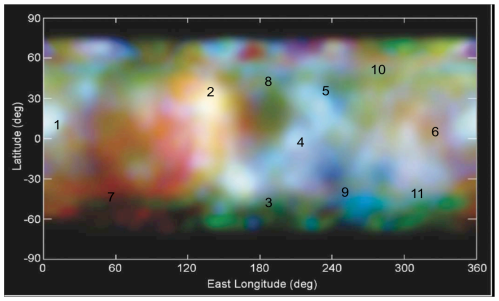

Fig. 1: RGB Hubble albedo deviation map obtained by Li et al. 2006 [3]. R: 0.555 µm, G: 0.33 µm B: 0.22 µm. The numbers indicate the regions of interest identified.

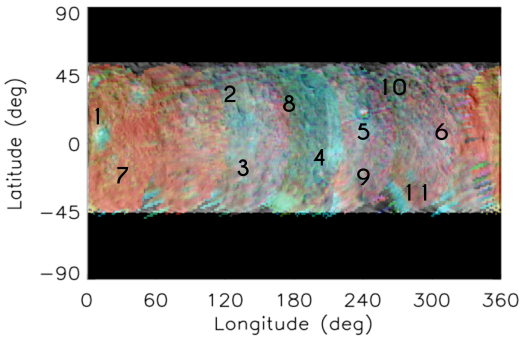

Fig 2: RGB maps of Ceres derived by RC2 VIR data overlapped to the corresponding Framing Camera map. R: 0.9 µm/0.64 µm, G: 0.55 µm/0.64 µm, B: 0.44 µm/0.64 µm. The numbers indicate the region identified in the Hubble map.

Acknowledgements

This work was supported by the Italian Space Agency (ASI), ASI-INAF Contract I/004/12/0. Support of the Dawn Science, Instrument and Operations Teams is gratefully acknowledged.

References

[1] Russell, C. T. and Raymond, C. A., The Dawn Mission to Vesta and Ceres, 2011, Space Science Reviews. [2] Tedesco, E. F. Cellino, A., Zappalà, V., The Statistical Asteroid Model. I. The Main-Belt Population for Diameters Greater than 1 Kilometer, 2005, The Astronomical Journal. [3] Li et al. , Photometric analysis of 1 Ceres and surface mapping from HST observations, 2006. [4] De Sanctis et al., The VIR Spectrometer, 2011, Space Science Reviews. [5] Tosi et al, Preliminary temperature maps of dwarf planet Ceres as derived by Dawn/VIR, 2015 LPSC. [6] Kueppers et al. Localized sources of water vapour on the dwarf planet (1) Ceres, 2014, Nature. [7] Nathues et al., Dawn Framing Camera at Ceres: results from approach to HAMO orbit,, 2015. LPSC.

EPSC Abstracts
Vol. 10, EPSC2015-537, 2015
European Planetary Science Congress 2015

Ceres spectral modelling with VIR data onboard Dawn: Method and first results

A. Raponi[1], M. Ciarniello[1], M.C. De Sanctis[1], E. Ammannito[1,2], F. Capaccioni[1], M.T. Capria[1], F. G. Carrozzo[1], A. Frigeri[1], S. Fonte[1], M. Giardino[1], A. Longobardo[1], G. Magni[1], E. Palomba[1], F. Tosi[1], F. Zambon[1], C. A. Raymond[3], C. T. Russell[2] and the Dawn Science Team, [1]Istituto di Astrofisica e Planetologia Spaziali, Istituto Nazionale de Astrofisica, Rome, Italy (andrea.raponi@iaps.inaf.it), [2]University of California Los Angeles, Earth Planetary and Space Sciences, Los Angeles, CA-90095, USA, [3]Jet Propulsion Laboratory, California Institute of Technology, 4800 Oak Grove Drive, Pasadena, CA-91109

Abstract

The Dawn spacecraft [1] is at Ceres, the closest of the IAU-defined dwarf planets to the Sun and the only one found in the inner Solar System.
Despite it has been one of the most intensely observed objects in the asteroid belt, many issues about its surface and internal composition remain unanswered.
Topic of this work is the interpretation of Ceres' surface composition based on the data coming from the VIR instrument [2] onboard Dawn. We have attempted to reproduce the composition modeled by previous works, focused on Earth-based observations.

1. Introduction

The Visible InfraRed (VIR) mapping spectrometer combines high spectral and spatial resolution in the VIS (0.25-1μm) and IR (0.95-5μm) spectral ranges. VIR will provide a very good coverage of the surface during its orbital mission at Ceres. The calibration of the instrument has been improved after departure from its first target, the large asteroid Vesta. Reliable models can be performed on the basis of the measured spectra.

2. Method

In order to model the measured spectra, we have taken into account Hapke's radiative transfer model [3], which allows one the inference of the composition, the relative abundances of the spectral end-members, and the grain size. The optical constants of the spectral end-members are obtained by applying the methodology described in [4] to IR spectra reflectance obtained from the RELAB database.

The observed spectra of Ceres surface are affected by thermal emission that prevents a comparison with laboratory data. Thus to model the whole wavelength range measured by VIR, the thermal emission is modeled together with the reflectance, thanks to the link between emissivity (ε_λ) and the single scattering albedo (w): $\varepsilon_\lambda = H(\mu,w) \times \gamma(w)$, being μ the emission angle and H the Ambartsumian-Chandrasekhar function [3].
Calibrated spectra are first cleaned by removing artefacts. The best fit is obtained with a least square optimization algorithm. The S/N is calculated and is used to weight the different parts of the spectra during the fitting procedure. For further details on the method, see reference [5].

3. Results

The possible end-members responsible for the spectral features on Ceres are those suggested by [6,7,8,9,10]. Amorphous carbon [11] is used as featureless, dark component. The best fit is obtained with the following composition: 86% amorphous carbon, 8% brucite, 6% cronstedtite, all with about 50 μm grain size. A few percent of saponite, dolomite and magnesite marginally improve the fit. The model can fairly reproduce the spectra in the range 2.0 - 4.5 μm, except in the range 2.5 – 2.9 μm in which there is a strong absorption band. This latter range is not modeled in literature, being severely hindered by Earth's atmosphere.

Acknowledgements

VIR is funded by the Italian Space Agency–ASI and was developed under the leadership of INAF-Istituto di Astrofisica e Planetologia Spaziali, Rome-Italy. The instrument was built by Selex-Galileo, Florence-Italy. The authors acknowledge the support of the Dawn Science, Instrument, and Operations Teams. This work was supported by ASI and NASA. A portion of this work was performed at the JPL/NASA.

References

[1] Russell, C.T., et al., The Dawn Mission to minor planets 4 Vesta and 1 Ceres. Springer, ISBN: 978-1-4614-4902-7, 2011.

[2] De Sanctis M.C. et al., Space Sci. Rev., DOI 10.1007/s11214-010-9668-5 , 2010.

[3] Hapke B., Cambridge Univ. Press., 1993, 2012

[4] Carli, C.; Ciarniello, M.; Capaccioni, F.; Serventi, G.; Sgavetti, M. Spectral variability of plagioclase-mafic mixtures (2): Investigation of the optical constant and retrieved mineral abundance dependence on particle size distribution, Icarus, 235, 207-219, 2014

[5] Raponi, A. PhD Thesis, arXiv:1503.08172, 2015.

[6] Lebofsky, L.A., Feierberg, M.A., Tokunaga, A.T., Larson, H.P., Johnson, J.R.,. Icarus 48, 453–459. 1981.

[7] Feierberg, M.A., Lebofsky, L.A., Larson, H.P., Geochim. Cosmochim. Acta 45, 971–981, 1981.

[8] King, T.V.V., Clark, R.N., Calvin, W.M., Sherman, D.M., Brown, R.H.,Science 255, 1551–1553, 1992 .

[9] Rivkin, A.S., Volquardsen, E.L., Clark, B.E., Icarus 185, 563–567, 2006.

[10] Milliken R.E., Rivkin A.S., Nat. Geosci. 2, 258–261, 2009.

[11] Zubko, V. G., Mennella, V., Colangeli, L., Bussoletti, E., Monthly Notices of the Royal Astronomical Society 282, 1321–1329, 1996.

EPSC Abstracts
Vol. 10, EPSC2015-617, 2015
European Planetary Science Congress 2015

Photometric correction of VIR spectra of Ceres: empirical approach

A. Longobardo (1), E. Palomba (1), M.C. De Sanctis (1), M. Ciarniello (1), F. Tosi (1), J.-Y. Li (2), F.G. Carrozzo (1), F. Zambon (1), A. Raponi (1), E. Ammannito (3), C.A. Raymond (4), C.T. Russell (3)

(1) IAPS-INAF, via Fosso del Cavaliere 100, 00133, Rome; (2) Planetary Science Institute, Tucson, AZ, USA; (3) UCLA, Institute of Geophysics, CA, USA; (4) JPL, California Inst. Techn., Pasadena, CA, USA;

Abstract

The application of the photometric empirical model, already tested for the Vesta asteroid and for the 67P/CG comet, is extended for the first data of Ceres provided by the Dawn/VIR imaging spectrometer.

1. Introduction

The NASA's Dawn mission [1] inserted on 6th March in the orbit of the (1) Ceres dwarf planet.
The Visible and Infrared (VIR) mapping spectrometer on board Dawn [2] is composed of a single optical head, including two channels, working in the visible (0.2-1 μm) and in the infrared (1-5 μm) wavelength range, respectively.
Currently, VIR acquired Ceres images having a spatial resolution down to 1 km, but better resolution will be achieved in the next mission phases.
An important operation to perform on VIR data is the photometric correction, aimed at removing the trend of reflectance with incidence, emission and phase angles. This not only is a fundamental process of data reduction (since makes it possible to compare observations taken at different illumination and viewing angles), but also allows the study of physical and optical properties of the asteroid surface, which drive the reflectance vs illumination angles behaviour, such as regolith grain size, surface roughness, presence of contaminants, role of multiple and single scattering (e.g. [3], [4], [5]).
The application of an empirical photometric model on Ceres data provided by VIR is the aim of this work.

2. Approach

The correction is based on the method already applied on VIR data of Vesta [5] and currently being also tested on VIRTIS data of 67P/CG [6].
The procedure, based on a statistical analysis of the whole dataset, does not need the assumption of theoretical photometric models and can be very helpful in studying the photometric behaviour of spectral parameters, such as band depths or slopes.
It applies on calibrated reflectance spectra on four steps:

1. Removal of incidence and emission effects, by dividing the radiance factor for the most appropriate disk function among those present in literature (e.g. Lambert, Lommell-Seeliger, Akimov).
2. Building of ten reflectance families, defined by reflectance values corresponding to 10%, 20%... 90% of brightest pixels at each phase angle.
3. For each reflectance family, retrieval of the curve describing reflectance as function of phase angle by means of a least squares fit.
4. For each pixel, retrieval of the reflectance at standard illumination conditions (i.e. normal illumination or incidence and phase at 30°).

3. Preliminary results

The method has been currently applied only to data obtained during the Approach phase to the target.
These results suggest a similar reflectance-phase angle behaviour for reflectance at different wavelengths in the visible range (Fig. 1). This would be consistent with what observed on other asteroids, where the steepness of photometric curve is almost constant through visible spectrum, except at wavelengths contained in absorption bands (e.g. [5], [7]).
A confirmation of these results can be obtained by considering in the data at better spatial resolution that will be obtained during the Dawn orbit on Ceres.

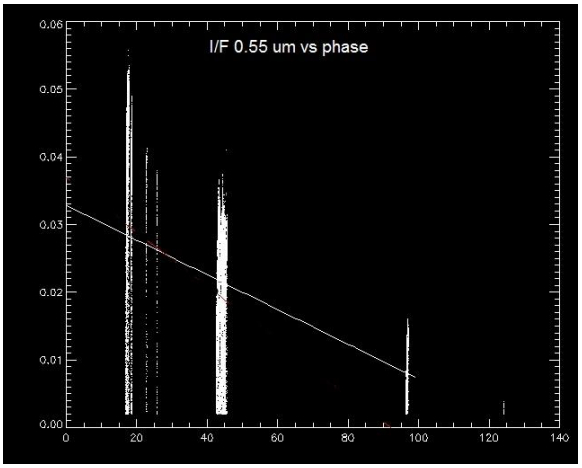

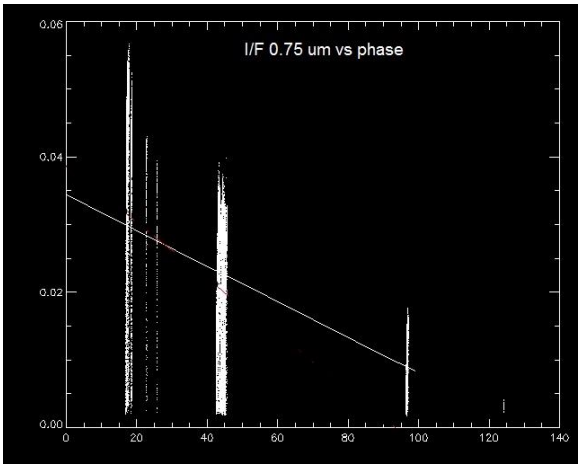

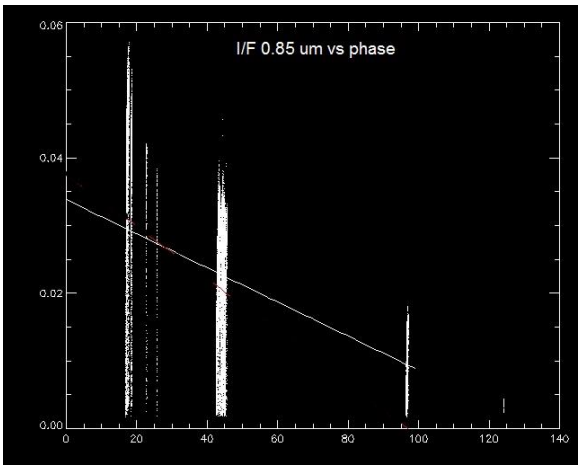

Figure 1. Reflectance as function of phase angles for three different wavelengths (0.55, 0.75 and 0.85 μm). The white line is a linear fit corresponding to the 50% of brightest pixels.

Acknowledgements

VIR is funded by the Italian Space Agency–ASI and was developed under the leadership of INAF-Istituto di Astrofisica e Planetologia Spaziali, Rome-Italy. The instrument was built by Selex-Galileo, Florence-Italy. The authors acknowledge the support of the Dawn Science, Instrument, and Operations Teams. This work was supported by ASI and NASA.

References

[1] Russell, C.T., et al. (2011). Springer, ISBN: 978-1-4614-4902-7.

[2] De Sanctis M.C. et al. (2011). *SSR, 163,* 329-369

[3] Hapke, B. (1984). *Icarus* 59, 41-59.

[4] Schröder, S.E et al. (2013). *Planetary and Space Science*, doi: 10.1016/j.pss.2013.06.009.

[5] Longobardo, A. et al. (2014). *Icarus*, doi: 10.1016/j.icarus.2014.02.014.

[6] Longobardo, A. et al. (2015). *EPSC abstract*, Rosetta session.

[7] Clark B.E. et al. (1999) *Icarus, 140,* 1, 53-65.

EPSC Abstracts
Vol. 10, EPSC2015-638, 2015
European Planetary Science Congress 2015

Artefacts removal in VIR/DAWN data

F.G. Carrozzo[1], M.C. De Sanctis[1], A. Raponi[1], E. Ammannito[1,2], M. Giardino[1], S. Fonte[1], F. Tosi[1], F. Capaccioni[1], M.T. Capria[1], M. Ciarniello[1], A. Frigeri[1], A. Longobardo[1], G. Magni[1], E. Palomba[1], F. Zambon[1], C.T. Russell[2], C.A. Raymond[3].
Istituto di Astrofisica e Planetologia Spaziali, Istituto Nazionale de Astrofisica, Rome, Italy; [2]University of California Los Angeles, Earth Planetary and Space Sciences, Los Angeles, CA-90095, USA; [3]Jet Propulsion Laboratory, California Institute of Technology, 4800 Oak Grove Drive, Pasadena, CA-91109

Introduction

VIR is a imaging spectrometer on board Dawn spacecraft acquiring hyperspectral images in the 0.25-5.1 spectral range [1]. After the success of the Dawn mission in the study of the asteroid Vesta, the spacecraft departed toward the dwarf planet Ceres and is currently in its orbit.

All VIR spectra display residual artifacts due to the systematic instrumental uncorrected effects. In order to highlight the spectral bands hidden by spectral artifacts, we propose here a denoising method to remove these artifacts from the VIR spectra. Other authors have studied the denoising of planetary spectra with different approach [2] or similar one [3].

The method that we are applying is in a test phase, but the obtained results are encouraging. We tested this method on various cubes of different mission phases during Vesta observations and the results are presented in this paper.

Method and Results

In general, the method consist of two stages: 1) creation of the artifacts matrix; 2) application of the artifacts matrix to the VIR cubes.

In the VIR spectra we assume that the reflectance (R) of each pixel is a combination of signal due to the surface contribution (S), artifacts (A) and noise (N): R=S+A+N.

In VIR data, detector artifacts change from sample to sample (column dependency). For this reason it is necessary to understand what are the residual artifacts for each sample. In order to study these effects we use the survey mission phase of Vesta to compute the artifacts profiles.

Starting from this dataset we extract a mean spectrum that characterizes the systematic residuals for each sample. The algorithm consists of four steps summarized in the following:

1. one thousand spectra are randomly selected using the data of survey mission phase of Vesta;

2. the median value are computed for each wavelengths;

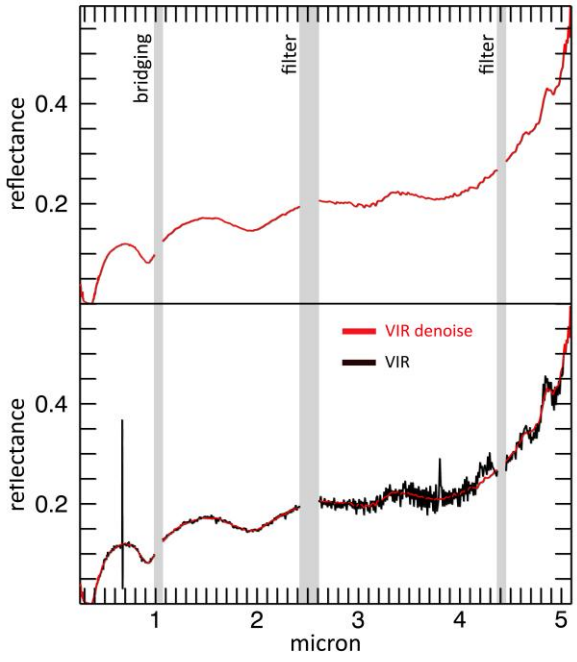

Figure 1. In the bottom panel are displayed a spectrum of Vesta acquired by VIR spectrometer (black curve) and the same spectrum after the denoising (red curve). In the top panel is displayed only the denoised spectrum for clarity.

3. a polynomial function is computed to fit the average spectrum;

4. the artifacts profile is extracted as ratio between the average signal and the fit at each sample.

The output file of this procedure is a 2D-matrix [number of samples, number of wavelengths] that we call “artifacts matrix”. It represents the percentage of signal to remove in the VIR spectra that have a wavelength dependency. In the second and last stage we remove the column-dependent artifacts from the reflectance values applying the artifacts matrix to the VIR reflectance cubes. This algorithm is able to remove the systematic residual artifacts but it cannot include the random spatial frequency residuals. In this last case a despiking procedure is necessary.

We are applying the artifacts matrix to the observations obtained during the various Vesta mission phases. In Figure 1 we show a spectrum of Vesta after the artefacts have been removed.

Acknowledgements

This work was supported by the Italian Space Agency (ASI), ASI-INAF Contract I/004/12/0. Support of the Dawn Science, Instrument and Operations Teams is gratefully acknowledged. The computational resources used in this research have been supplied by INAF-IAPS through the DataWell project.

References

[1] De Sanctis, M.C. et al. (2011). SSR, 163, 329-369.

[2] Parente, M. (2008). LPSC XXXIX, abstract #2528.

[3] Raponi, A. PhD Tesis, arXiv:1503.08172, 2015.

EPSC Abstracts
Vol. 10, EPSC2015-640, 2015
European Planetary Science Congress 2015

A numerical model of the physical and chemical evolution of Vesta.

H. Mizzon[1], M. Monnereau[1], M.J. Toplis[1], T.H. Prettyman[2], H.Y. McSween[3], C.A. Raymond[4], C.T. Russell[5], [1]Université de Toulouse - Institut de Recherche en Astrophysique et Planétologie, Toulouse, France (hugau.mizzon@irap.omp.eu), [2]Planetary Science Institute, Tucson, AZ, [3]University of Tennessee, Knoxville, TN, [4]Jet Propulsion Laboratory, Pasadena, CA, [5]University of California Los Angeles, CA.

1. Introduction

Vesta is a 262 km radius asteroid that has been proposed as the parent body of the Howardite-Eucrite-Diogenite family of meteorites. The observations of the Dawn spacecraft confirm the idea that this protoplanet underwent magmatic differentiation, providing evidence for regions of the upper crust rich in basaltic (eucritic) lithologies, while regions that have experienced excavation related to large impacts (i.e. Rheasilvia) are richer in pyroxene-dominated (diogenitic) lithologies [1,2]. One of the most striking results of the Dawn mission is the absence of olivine at the near-surface, even in the deep Rheasiliva basin. This observation has been used to question the chondritic nature of bulk Vesta and/or question its status as an intact protoplanet [3].

From a geochemical point of view, the HED meteorites are consistent with chondritic precursors [4], but petrological models have met difficulties explaining both eucrites and diogenites in a unified way [5]. These models comprise two extreme endmember scenarios: the first considers the partial melting of the primitive mantle of Vesta, followed by melt extraction [6], while the second involves the solidification of an initially entirely molten magma ocean [7]. In the latter case, major-element chemistry of eucrites and diogenites can be reproduced [7], but not the extreme range of trace element concentrations observed in diogenites [8]. More importantly, the physics of melt migration seems to preclude the existence of a global magma ocean, assuming that ^{26}Al is the only heat source capable of extensively producing melt in early small bodies. This is because plagioclase is one of the first phases to melt, thus early formed liquids are Al-rich. Rapid migration of such liquids redistributes ^{26}Al, limiting melt production where liquid has been lost [9,10]. This idea was explored by [11], who qualitatively suggested that the first melts formed would migrate to the surface (as eucrites), while the lower mantle would become enriched in refractory olivine through its downward compaction. This last point potentially explains the lack of this mineral near Vesta's surface. The aim of work presented here is to quantitatively explore this idea by computing the mineralogy as a function of depth and time, using a set of numerical solutions of conservative equations and an appropriate phase diagram.

2. The Model

Our model is based on the idea that mineralogy can be monitored by coupling compaction equations with a phase diagram [*e.g.* 12]. For modelling Vesta, we assumed instantaneous accretion, an initial temperature of 292K and a homogeneous composition derived from H type chondrites [4]. Each time step involves the following: 1) Coupled mass and momentum conservation equations computing the proportion of the different phases (solid, liquid) for all components considered (iron metal, iron sulfide, olivine, pyroxene and anorthite). These equations [13] describe the two phase flow between a high viscosity matrix (a mixture of solid silicates and metal here), and a low viscosity mobile fluid (molten silicates). 2) Temperature is then solved accounting for ^{26}Al decay with conductive cooling, without considering the effect of latent heat. Knowing the composition and the amount of available energy, a phase diagram provides the equilibrium temperature, the amount of melt, and the compositions of the liquid and solid. 3) The equilibrium temperature and the amount of melt is used to correct the initial estimations of the phase proportions and account for the effect of release or consumption of latent heat on the temperature. This enthalpy method is extensively described by [14], and a similar computation for planetesimals with pure components can be found in [15]. We considered a binary phase diagram for iron metal and iron sulfides. Because the eucrites and diogenites are

volatile depleted, the silicate composition can be well approximated by a set of three minerals: anorthite $CaAl_2Si_2O_8$, olivine $(Fe,Mg)_2SiO_4$ and pyroxene $(Ca,Fe,Mg)_2Si_2O_6$. We have therefore used a simplified forsterite – anorthite - silica phase diagram adapted for the effect of additional iron from [16].

In general liquid moves up towards the surface, locally reaching high concentrations. We assumed that when a critical liquid fraction is attained (taken to be 80%) the layer behaves like a magma ocean (i.e. there is no thermal gradient across the layer). Because the liquid is concentrated in ^{26}Al, this layer thermally erodes the subsurface, thinning the overlying conductive lid. We also make the assumption that the conductive lid is recycled into the magma ocean when its thickness is less than 10 km, taking account of a loss of cohesion by thermal expansion, by impacts, or by the effect of the pressure exerted by the underlying magma ocean.

3. Results

A simulation run for our bulk composition and an accretion time 0.7 Myr after CAI formation, shows that the first melt reaches the surface within 1.2 Ma of CAI formation, a time at which the lower mantle has reached a melting degree of barely 10%. Melting in the lower mantle proceeds until it is completely depleted in aluminum. For this reason silicate melting stops at about 4.0 Myr after CAIs, leaving an olivine residue with only a few percent of pyroxenes in the lower mantle. In the meantime, near the surface a competition between heating by ^{26}Al and magma-ocean cooling takes place. The liquid layer is fed both by liquid coming from below and by local ^{26}Al overheating. When the melt fraction is sufficient, the composition is stirred and homogenized in this convective layer, but more importantly, the surface lid is regularly recycled by volcanism, which significantly cools the magma ocean and makes it crystalize. This process repeats itself until the energy provided by ^{26}Al decay cannot produce further melt. When the magma ocean cools to the point where convection is stopped, the more refractory pyroxenes crystallize at its base while the surface solidifies with a near-eutectic composition. The resulting upper crust is $An_{50}Px_{50}$, which is in good agreement with normative eucrite composition [17]. The underlying rock compositions are 90 – 100% pyroxenes, consistent with diogenites.

In this 1D model the composition of eucrite and diogenite layers and their thickness (Figure 1) are independent of accretion time as long as the latter is < ~0.8 Myr after CAI formation. This does not exclude regional variations of crustal thickness, indicated by geophysical data [18], that may occur due to 3D interactions.

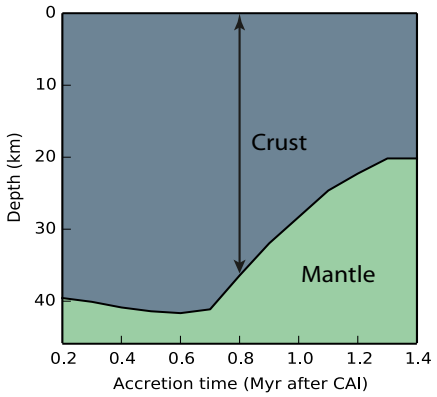

Figure 1: The crust, considered here as the less refractory material brought to the surface by melt migration is represented in grey, while the underlying olivine rich mantle residue is coloured in green. Increasing the accretion time, makes the ^{26}Al energy supply decrease. This results in less melting of the mantle and in a thinner crust.

References: [1] Prettyman T.H. et al (2013), MAPS, 48(11), 2211-2236. [2] DeSanctis et al (2012), Science, 336, 697-700. [3] Clenet H. et al (2013), Nature, 511, 303-305 [4] Toplis et al, (2013), MAPS, 48(11), 2300-2315. [5] Mittlefelhdt D. W., (2012), MAPS, 47(1), 72-98. [6] Stolper E, (1977), 41(5), 587-611 [7] Mandler B. E. and Elkins-Tanton L. T., (2013), MAPS, 48(11), 2333-2349. [8] Barrat J. A. and Yamaguchi A., (2014), MAPS, 49(3), 468-472. [9] Wilson L. and Keil K., (2012), Chemie der Erde, 72, 289-321 [10] Moskovitz N. and Gaidos E., (2011), MAPS, 46(6), 903-918. [11] Neumann et al, (2014), EPSL, 396, 267-280. [12] Ribe N., (1985), EPSL, 73, 361-376. [13] Bercovici D. and Ricard Y., (2003), GJI, 152, 581-596 [14] Katz F. K., (2008), JPetrol., 49(12), 468-472. [15] Sramek O. et al (2012), Icarus, 217, 339-354. [16] Morse S. A. (1980) *Springer-Verlag.* [17] Delaney J. S., (1984), Proc. Lunar Planet Sci Conf, JGR, 89, 251-288. [18] Raymond C.A. et al. (2015) LPSC.

EPSC Abstracts
Vol. 10, EPSC2015-715, 2015
European Planetary Science Congress 2015

Correlation between the mineralogic and geologic maps of Vesta: spatial analysis and perspectives towards the mapping of Ceres

A. Frigeri[1] , M.C. De Sanctis [1] , E. Ammannito [2] , R. A. Yingst [3] , D. A. Williams [4], F. Capaccioni [1] ,F. Tosi [1] , E. Palomba [1] , F. Zambon [1] , R. Jaumann [5] , C.M. Pieters [6] , C.A. Raymond [7] , C.T. Russell [2] and the Dawn Team;

[1] Istituto di Astrofisica e Planetologia Spaziali, Istituto Nazionale di Astrofisica, via del Fosso del Cavaliere, 00133 Roma, Italy (alessandro.frigeri@iaps.inaf.it); [2] Institute of Geophysics and Planetary Physics, University of California at Los Angeles, Los Angeles, California, USA; [3] Planetary Science Institute, Tucson, Arizona, USA; [4] Arizona State University, Tempe, AZ; [5] DLR, Berlin, Germany; [6] Department of Geological Sciences, Brown University, Providence, Rhode Island, USA; [7] NASA Jet Propulsion Laboratory, California Institute of Technology, Pasadena, California, USA;

1. Introduction

Between July 2011 and September 2012, the NASA/Dawn mission has mapped the surface of Vesta with images from the Framing Camera (FC [1]), spectral data from the Visible and Infrared Mapping Spectrometer (VIR [2]), and elemental data from the Gamma Ray and Neutron Detector (GRaND [3]). The successful acquisition of imagery from FC and VIR allowed us to produce global image mosaics reaching 20 meters per pixel and global mineralogic maps at 100 meters per pixel. A global geologic map of Vesta has been recently published [4,5]. Geologic units and structures have been identified and put into their stratigraphic context using FC image-mosaic and the digital terrain model derived from stereo image processing. The VIR spectra have been synthesized into spectral parameters or indicators [6] that have been used to produce quadrangle and global maps showing the mineralogic diversity across Vesta, through the variation of the compositional and the physical state of the pyroxene-rich lithologies, which are typical of Vesta[7]. Herein we present the work done to explore the spatial correlation between the mineralogic and geologic map of Vesta (Figure 1).

2. Geoprocessing

We have designed a Geographic Information System (GIS) approach to spatially correlate the geologic map and the spectral parameters maps of Vesta. For this work the mineralogic and geologic maps of Vesta have been imported into a widely-used Free Open Source GIS (the Geographic Resources Analysis Support System, or GRASS[8]) using a common coordinate reference system. The digital GIS maps are stored in a Open Gis Consortium (OGC) compatible format to facilitate interoperability between different GIS packages. Within the GIS environment, specialized tools allow us to spatially correlate different maps, do statistical analyses and

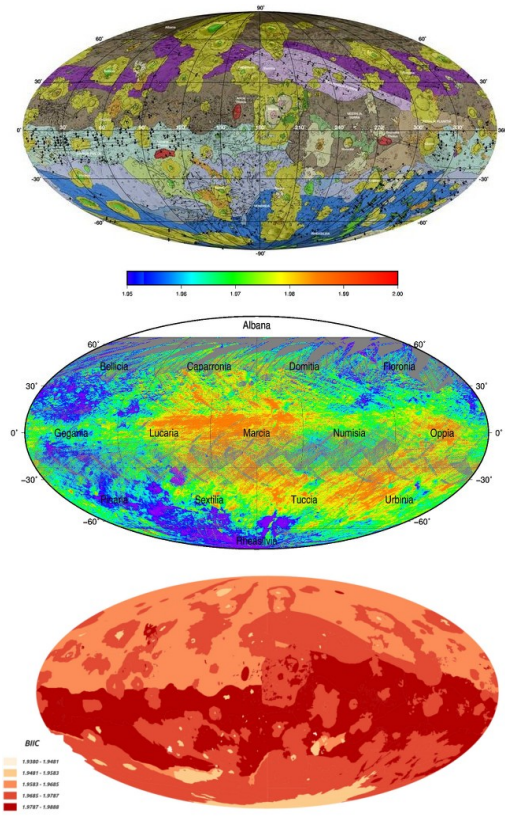

Figure 1: Top: the geologic map of Vesta. Middle: the pyroxene-related Band II center spectral parameter map. Bottom: the geologic units classified on the basis of Band II center.

develop specific geoprocessing pipelines involving different types of geospatial data.

Figure 1-bottom shows the map resulting from the correlation of the geologic map and the pyroxene-related spectral parameters Band II center, which is the position of the absorption band around 2 microns. Lowest values are found for the Rheasilvia related units at the south pole, mid-values are found within the northern emisphere, while higher values are typical of equatorial units.

3. Discussion and New Perspectives

This work of comparison of the geologic map of Vesta and the mosaics of spectral parameters extracted from VIR data aims to explore the level of spatial correlation between two kind of maps made with different approaches. The geologic map is the result of an interpretative process, while the spectral parameters map is the result of an automated processing. The basic element of a geologic map is the geologic unit. Geologic units are made up of bodies of rock that are interpreted to have been formed by a particular process or set of related processes over a discrete interval of time, so the morphology and the topography are the primary sources for the crafting of a geologic map. Spectral parameter maps are the result of a data reduction process made by experienced spectroscopists and allow the non-spectroscopists to focus on the spatial variation of a single aspects of a complex spectra, representing a perfect element for the study of the spatial correlation with other dataset, as the gelogic map of this study. Figure 1 shows that although globally there is no one-to-one correlation between geologic units and spectral parameters, the re-classification of the geologic units on the base of their spectral fingerprint (Figure 1, bottom) represent an additional way to explore the geologic characteristic of Vesta. The availability of global geologic and mineralogic maps published in late 2014 / early 2015 represents the first opportunity to observe the spatial correlation globally for Vesta, using the most up-to-date dataset. Dawn is currently collecting data from Ceres, and the first geologic mineralogic maps are being prepared. Our study made on Vesta is going to be replicated on Ceres, but this time we can apply our experience early in the mapping process, providing new views for a more detailed interpretation of the geologic history of the dwarf planet Ceres.

References

[1] Sierks, H. et al. The Dawn Framing Camera.*Space Science Reviews*, 163:263-327, Dec. 2011.

[2] De Sanctis et al. The VIR Spectrometer. *Space Science Reviews*, 163:329-369, December 2011.

[3] Prettyman et al. Dawn's Gamma Ray and Neutron Detector. Space Science Reviews 163, 371–459. doi:10.1007/s11214-011-9862-0, 2011

[4] Williams et al. Introduction: The geologic mapping of Vesta. Icarus 244, 1 – 12. 2014

[5] D. A. Williams et al., LPSC Abstract #1126. 2015

[6] Ammannito, et al. 2013. Vestan lithologies mapped by the visual and infrared spectrometer on Dawn. Meteoritics & Planetary Science 48, 2185–2198. 2013

[7] McCord, T.B. et al. Asteroid Vesta: Spectral Reflectivity and Compositional Implications. Science 168, 1445–1447. 1970

[8] M. Neteler and H. Mitasova (2008), Open Source GIS: A GRASS GIS Approach. Third edition. Springer, New York.

EPSC Abstracts
Vol. 10, EPSC2015-742, 2015
European Planetary Science Congress 2015

Preliminary Geologic Mapping of the Ac-S-1 Hemisphere of Ceres from NASA's Dawn Mission

Mest, S.C. (1), **D.A. Williams** (2), D.L. Buczkowski (3), J.E.C. Scully (4), D.A. Crown (1), R.A. Yingst (1), R. Jaumann (5), C.T. Russell (4), C.A. Raymond (6), C.M. DeSanctis (7), A. Frigeri (7), E. Kersten (5), S. Marchi (8), A. Nathues (9), D.P. O'Brien (1), K.A. Otto (5), T. Platz (9), F. Preusker (5), T. Roatsch (5), M. Schäfer (9), P.M. Schenk (10), K. Stephan (5).
(1) Planetary Science Institute, Tucson, AZ, USA, mest@psi.edu; (2) School of Earth & Space Exploration, Arizona State University, Tempe, AZ, USA; (3) Johns Hopkins University Applied Physics Laboratory, Laurel, MD, USA; (4) UCLA, Institute of Geophysics, Los Angeles, CA, USA; (5) DLR, Planetary Research Berlin, Germany; (6) NASA Jet Propulsion Laboratory, California Institute of Technology, Pasadena, CA, USA; (7) Istituto di Astrofisica e Planetologia Spaziali, Istituto Nazionale de Astrofisica, Rome, Italy. (8) Southwest Research Institute, Boulder, CO, USA; (9) Max Planck Institute for Solar System Research, Göttingen, Germany; (10) Lunar and Planetary Institute, Houston, TX, USA.

Abstract

NASA's Dawn spacecraft [1], launched in September 2007, spent ~1 year (2011-2012) investigating Vesta and recently (March 6, 2015) arrived at dwarf planet Ceres. The first images of Ceres' surface were acquired by Dawn's Framing Camera (FC) [2] as it made optical navigation and rotation characterization observations during the Approach phase. The Dawn Science Team will conduct a geological mapping campaign at Ceres during the Nominal Mission, which will include iterative mapping using data obtained during each orbital phase. Iterative geologic mapping was previously successfully conducted during Dawn's mission to Vesta [3,4]. This abstract describes the preliminary geologic mapping results for quadrangle Ac-S-1 (55-90°N, 0-360°E), the northern hemisphere of Ceres.

1. Geologic Mapping of Ceres

Geologic maps are research products that document the nature and distribution of surface terrains, as well as tools that help interpret the geologic history of a planetary surface. Compilation of a geologic map may utilize photogeologic, spectral and topographic analyses to organize planetary features into discrete process-related map units. These units are defined and characterized by their physical (albedo, morphology, structure, color, topography) and chemical (mineralogy) attributes related to the putative geologic processes that produced them (e.g., volcanism, tectonism, impact cratering, weathering-erosion-deposition). Relative ages of map units are determined by principles of stratigraphic relations (superposition, lateral continuity, cross-cutting, embayment, intrusion, etc.) and analyzing crater size-frequency distribution statistics.

Iterative geologic mapping of dwarf planet Ceres will be accomplished during the Nominal Mission. The goals of mapping include (1) providing increasingly improved geologic context to the full science team as FC images are acquired at increasing spatial resolution during discrete orbital phases of the mission, and (2) providing geologic context to the Visible and Infrared Spectrometer (VIR) and the Gamma-Ray and Neutron Detector (GRaND) teams to aid in interpreting their compositional information.

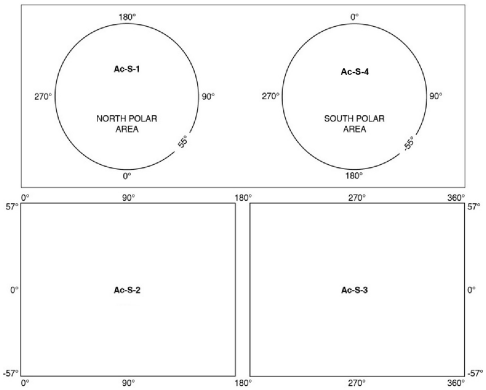

Fig 1: Hemispheric geologic mapping quadrangles for dwarf planet Ceres.

Similar to Vesta [5], the first iteration geologic map of Ceres will be a preliminary map generated from FC images acquired during the Approach and Survey orbital phases [6]. This map will provide a global assessment of Ceres' geology, including its geologic units and structures, and identification of potential surface processes. This preliminary map will be accomplished using a hemispheric 4-quadrangle

system (Fig. 1). This abstract presents an overview of the geology of Ac-S-1 (55-90°N, 0-360˚E), the northern hemisphere of Ceres.

2. First Geological Results

At the time of this writing, images for approximately two-thirds of the northern hemisphere have been acquired (currently unreleased data). Dawn FC images [7] show that the surface of the north hemisphere quadrangle (Ac-S-1) is heavily modified by impact craters (Fig. 2). In this region, the surface is densely cratered, and there are numerous examples of superposition of crater forms. Current observations of the northern hemisphere show the distribution of craters appears fairly homogeneous. Craters range in size from the limits of resolution (several kilometers at this scale) to a few hundred kilometers. Morphologically, most craters appear circular, shallow, and flat-floored, but there are some craters with polygonal shapes (generally hexagonal), which may have implications for the target material [see 8,9]. Most of the smaller-diameter craters appear to have sharp, clearly defined rims, whereas rims for larger craters, although most are clearly defined, are not as sharp and appear flattened to the level of the surrounding terrain. Numerous craters contain central peaks, and at this scale there does not appear to be any post-formation modification of crater walls, such as by slumping, terracing or mass wasting. Distinct ejecta blankets are not apparent at this resolution.

Apart from impact craters, intercrater regions appear relatively smooth at this scale, and albedo variations are not apparent. Large-scale structural features are not evident in the northern hemisphere; however, some localized ridges, scarps and other topographic high areas are visible, and could represent tectonic deformation of Ceres' crust, or the remnants of the rims of ancient impact craters/basins that have been heavily modified by subsequent processes. Some small dome-like features are also apparent, but will have to be confirmed by later imaging

3. Future Work

As data are acquired during the RC3 and Survey phases of Dawn's mission to Ceres, mosaics will be created from these data and detailed mapping of contacts, structures and other geologic features will begin.

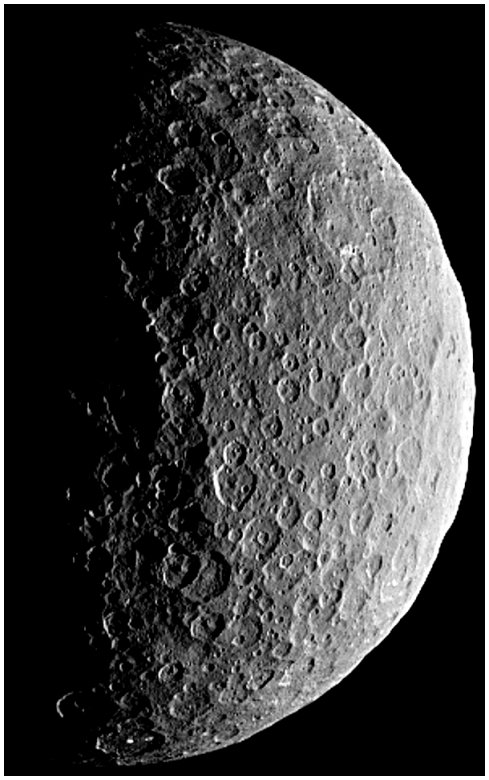

Fig. 2: Dawn FC image of Ceres looking at the northern terrain on the sunlit side. This image was acquired during Optical Navigation 7 (OpNav7) while Dawn was ~22,000 km above Ceres' northern hemisphere. Image resolution = 2.1 km/pixel; NASA/JPL-Caltech/UCLA/MPS/DLR/IDA.

References:

[1] Russell, C.T., and Raymond, C.A., The Dawn mission to Vesta and Ceres, Space Sci. Rev., 163, 3-23, 2011.

[2] Sierks, H., et al., The Dawn Framing Camera, Space Sci. Rev., 163, 263-328, 2011.

[3] Williams, D.A., R.A. Yingst, and W.B. Garry, Introduction: The geologic mapping of Vesta, Icarus, 244, 1-12, 2014.

[4] Yingst, R.A., et al., Geologic mapping of Vesta, PSS, 103, 2-23, 2014.

[5] Yingst, R.A., et al., A preliminary global geologic map of Vesta based on Dawn Survey orbit data, *AGU*, P43B-0248, 2011.

[6] Williams, D.A., et al., Complete global geologic map of Vesta from Dawn and mapping plans for Ceres, LPSC 46, Abstract #1126, 2015.

[7] Roatsch, T., et al., High-resolution Ceres survey atlas derived from Dawn FC images, abstract EPSC2015-62, 2015.

[8] Otto et al., Polygonal craters on dwarf-planet Ceres, EPSC2015-284, 2015.

[9] Schenk et al., Impact craters on Ceres: Evidence for water-ice mantle?, abstract submitted to this EPSC, 2015.

EPSC Abstracts
Vol. 10, EPSC2015-763, 2015
European Planetary Science Congress 2015

Ceres: structures from afar and near.

G.G. Kochemasov; IGEM of the Russian Academy of Sciences, Moscow, RF, kochem.36@mail.ru

"Orbits make structures" – basic statement of the wave planetology [1-3]. Moving in non-circular keplerian orbits with periodically changing accelerations cosmic bodies are warped by inertia-gravity waves. Their lengths and amplitudes are proportional to orbiting periods or inversely proportional to orbiting frequencies. They have standing character and four crossing directions: ortho- and diagonal. An etalon is Earth with 1/365 days frequency and corresponding πR/4 tectonic granule size.

Ceres has 1/4435 days orbital frequency and 1/9.07 hours rotation frequency. To both parameters correspond tectonic granules too large and too small to be observed (3.3πR and πR/3863). The wave modulation (division and multiplication of the higher fr. by the lower fr.) gives two side frequencies: 1/85212 and 1/965410. To them correspond tectonic granules πR/38.8 and πR/440.8 (R=475 km), thus about 38.4 km and 3.4 km. Now both sizes are discerned: larger granules from larger distance as 'blobs" at wave intersections (HST image, Fig. 1; Dawn's distant image, Fig. 2) and small circles in strings and grids covering the whole imaged surface, Fig. 3.

Earlier the wave modulation approach was used to explain anomalies (extra craters) in the lunar crater size – frequency curve [4] and for explaining appearance and size of the saturnian storms making the "leopard skin" picture [5]. Recently, a bifurcation nature and sizes of debris on the Churyumov-Gerasimenko comet core surface were also explained by this method [6]

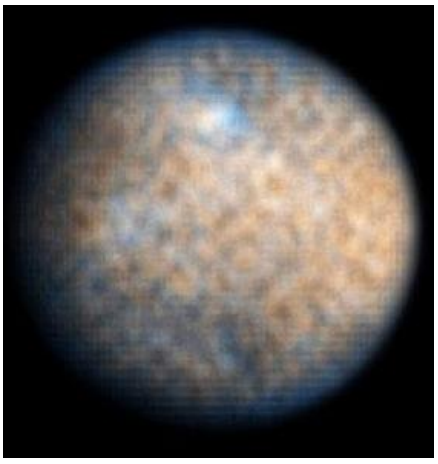

Fig.1.

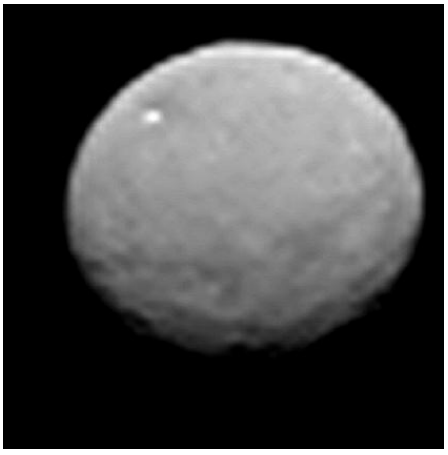

Fig.2.

Fig. 1. Color view of Ceres (HST image), PIA10235. In visible and ultraviolet light between Dec. 2003 and Jan. 2004. Diameter 950 km. Image credit: NASA/ESA/J. Parker, P. Thomas, L. McFadden, M. Mutchler & Z. Levay

Fig. 2. DAWN image of Ceres. FC21B0032726_smooth_700-237000km.jpg.

Fig. 3. A portion of Ceres from distance of 22000 km, view_of_the_bright_spots_in_the_cra.jpg.

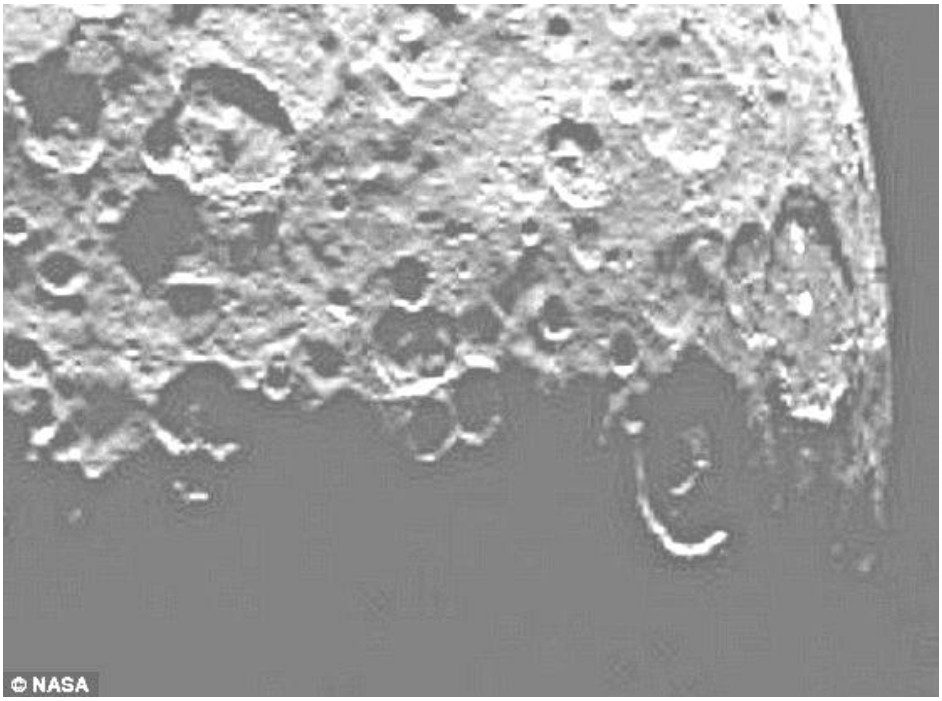

Fig. 3.

References: [1] Kochemasov, G.G.: Concerted wave supergranulation of the Solar system bodies, 16th Russian-American microsymposium on planetology, Moscow, Vernadsky Inst. (GEOKHI), Abstracts, 36-37, 1992.
[2] Kochemasov, G.G.: Sectoral tectonics of the Earth's eastern hemisphere and its crucial role in localization of giant ore deposits, prominent rift systems and large flood basalt provinces, Global Tectonics and Metallogeny, V. 6, # 3 & 4, 195-197, 1998.
[3] Kochemasov, G.G.: Tectonic dichotomy, sectoring and granulation of Earth and other celestial bodies, Proceedings of the International Symposium on New Concepts in Global Tectonics, "NCGT-98 TSUKUBA", Geological Survey of Japan, Tsukuba, Nov 20-23, 1998, p. 144-147, 1998
[4] Kochemasov G.G. (2001) On one condition of further progress in lunar studies // First Convention of Lunar Explorers, 8th to 10th March, 2001, Palais de la Découverte, Paris, France; Programme and Contributed Abstracts; ESTEC, eds: D. Heather and B. Foing, 58 pp (p.26).
[5] Kochemasov G.G. (2007) Calculating size of the Saturn's "Leopard Skin" spots // Lunar and Planetary Science Conference (LPSC) XXXVIII, Lunar and Planetary Inst., Houston, USA, March 2007, Abstract # 1040 (CD-ROM).
[6] Kochemasov G.G. (2015) A wave modulation nature of the 3D structural lattice of the Churyumov-Gerasimenko comet icy core // 46th LPSC, 2015, Abstr. # 1088.

EPSC Abstracts
Vol. 10, EPSC2015-931, 2015
European Planetary Science Congress 2015

Spectral diversity of Ceres surface as measured by VIR

E. Ammannito[1], M.C. DeSanctis[2], F. Capaccioni[2], M.T. Capria[2], G. Carrozzo[2], M. Ciarniello[2], J-P. Combe[3], A. Frigeri[2], S. Fonte[2], M. Giardino[2], R. Jaumann[4], S.P. Joy[1], A. Longobardo[2], G. Magni[2], T.B. McCord[3], L.A. McFadden[5], H.McSween[6], E. Palomba[2], C. M. Pieters[7], C. A. Polanskey[8], A. Raponi[2], M.D. Rayman[8], C. A. Raymond[8], F. Tosi[2], F. Zambon[2], C. T. Russell[1] and the Dawn Science Team.

1) University of California Los Angeles, Earth Planetary and Space Sciences, Los Angeles, CA-90095, USA, 2) Istituto di Astrofisica e Planetologia Spaziali, Istituto Nazionale de Astrofisica, Rome, Italy, 3) Bear Fight Institute, Winthrop, WA, USA; 4) Institute of Planetary Research, DLR, Berlin, Germany; 5) NASA, GSFC, Greenbelt, MD, USA; 6) Department of Earth and Planetary Sciences, University of Tennessee, Knoxville, TN; 7) Department of Geological Sciences, Brown University, Providence, RI 02912, USA; 8) Jet Propulsion Laboratory, California Institute of Technology, 4800 Oak Grove Drive, Pasadena, CA 91109 (eleonora.ammannito@igpp.ucla.edu)

1. Introduction

The Dawn spacecraft (1) has been acquiring data of dwarf planet Ceres since January 2015 (2). During the approach maneuver (January to April 2015), there were nine opportunities – called OpNavs or RCs - to point the optical instruments towards Ceres and to acquire spectral information of its surface. These opportunities differ in resolution, illumination conditions and sub-spacecraft point (Table 1). In late April/early May 2015, the instruments performed an observation campaign while the spacecraft was in orbit around Ceres at an altitude of about 13600km. In this mission phase – called RC3 – the instruments acquired Limb and High Phase images while the spacecraft was in the night side of the orbit and nadir images while it was in the day side. In three consequent orbits scheduled to start respectively early in June (Survey, 4400 km altitude); early in August (HAMO, 1470 km altitude); early in December (LAMO, 375 km altitude) the instruments will acquire data in the dayside section of the orbit at increasing resolution.

2. VIR measurements at Ceres

The spectrometer VIR (spectral range: 250-5000nm) (3) acquired data during all OpNavs and RCs. It will continue its measurements during Survey, HAMO and LAMO (4). VIR is observing compositional variability all across the surface of Ceres since data acquired in RC2 (March 2015) (5). The spectral diversity of Ceres is confirmed by color filters data acquired by the Dawn camera (6) (7). The variability is particularly evident in changes of the shape of the spectra in the range from 500nm to 4000nm. Outside this range, the data have not been considered in this first step of the analysis because they are difficult to handle: in the short wavelengths side (250nm-500nm) due to a drop in the sensitivity of the instrument; in the long wavelengths side (4000nm-5000nm) due to the thermal emission from Ceres (8).

The spectral slope in addition to center and depth of absorption bands in the considered spectral range have been computed and mapped. In figure 1 there is an example of a VIR image acquired during RC3. In the image there are still several artifacts evident as vertical columns. However, it is possible to identify an underlying variability that sometime is associated with high reflectance regions (circle A) but not always (circle B). In figure 1 central panel (RGB in the VIS range), regions in orange have a higher level of reflectance in wavelengths around 550nm in comparison with the 1000nm range. On the contrary, the bluish regions have a smoother behavior all along the 550-1000nm spectral range. The image also has an extended reddish region in the left side; however, considering the acquisition geometry, this is likely a residual of the photometric correction. The Green channel used in the composition of the image (ratio 965/830) does not show a significant variability in this specific cube indicating a weak correlation between the spectral shape in this section of the VIR sensitivity range and the properties of the surface of Ceres. On the contrary, in the bottom panel (RGB in the IR range) most of the variability is in the Green (ratio 2660/1200) and Blue (ratio 2730/2660) channels. This is an indication that in the IR range, wavelengths above 2500nm are the most correlated with the composition of Ceres.

Table 1: Characteristic of the VIR observations during the approach of the Dawn spacecraft to Ceres. OpNav is short for Optical Navigation, RC is short for Rotational Characterization. OpNavs are activities of about one to two hours, RCs last enough time to give the instruments the possibility to acquire data for a full rotation of Ceres.

	VIR Resolution (km)	Phase Angle (deg)	Sub-Solar Latitude (deg)
OpNav1	95	27	-28
OpNav2	60	23	-26
OpNav3	37	19	-22
RC1	22	17	-16
RC3	11	47	8
OpNav4	10	92	29
OpNav5	13	126	34
OpNav6	8	126	57
OpNav7	6	81	77

3. Figures

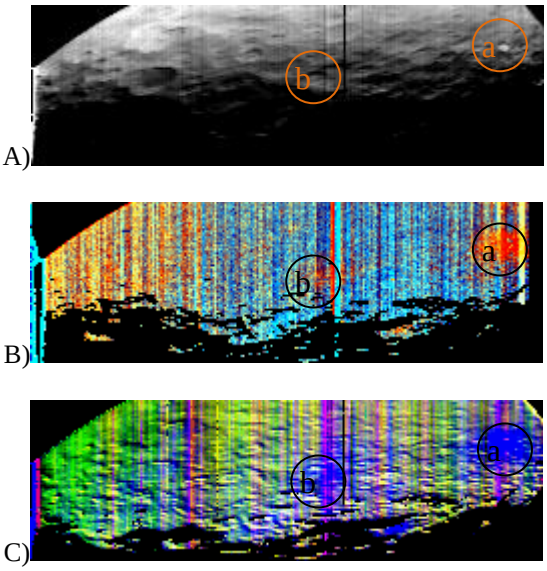

Figure 1: Images of a Spectral Cube acquired during RC3 (about 3.4km/px). Top image is I/F at 1200nm in grey scale. Central panel is an RGB combination of band ratios in the VIS range (R: 550/830, G: 965/830, B: 965/550). Bottom panel is an RGB combination of band ratios in the IR range (R: 2000/1200, G: 2660/1200, B:2730/2660). All the wavelengths are in nm.

4. Summary and Conclusions

In summary, according to VIR measurements, Ceres surface has a compositional variability already evident in the 3.5Km/px spectral images acquired in RC3. Analysis of the spectra is still going on and for a detailed compositional assessment higher resolution data are needed. However, already in the RC3 images, it is clear that the 3000nm range is the section of the spectrum that has the highest correlation with the composition of the surface although variations are present also at shorter wavelengths. This is a confirmation of the intriguing nature of the spectrum of Ceres in the 3000nm range already evident in pre-Dawn observations (9).

Acknowledgements

VIR is funded by the Italian Space Agency–ASI and was developed under the leadership of INAF-Istituto di Astrofisica e Planetologia Spaziali, Rome-Italy. The instrument was built by Selex-Galileo, Florence-Italy. The authors acknowledge the support of the Dawn Science, Instrument, and Operations Teams. This work was supported by ASI and NASA. A portion of this work was performed at the JPL/NASA.

References

[1] Russell, C. T. and Raymond, C. A., The Dawn Mission to Vesta and Ceres, 2011, Space Science Reviews. [2] Russell, C. T. et al. Dawn arrives at Ceres: results of Survey orbits, 2015, EPSC. [3] De Sanctis M.C. et al., The VIR Spectrometer, 2011, Space Science Reviews. [4] De Sanctis M.C. et al., Ceres hyperspectral observations by VIR on Dawn: First Results, 2015, EPSC. [5] Zambon, F. et al. Identification of Homogeneous Units on Ceres. First Results by Dawn, 2015, LPSC [6] Sierks et al., The Dawn Framing Camera, 2011, Space Science Reviews. [7] Nathues, A. et al. Dawn Framing Camera at Ceres: results from Approach to HAMO orbit, 2015, EPSC [8] Tosi, F. et al, Preliminary temperature maps of dwarf planet Ceres as derived by Dawn/VIR, 2015 LPSC. [9] Rivkin, A. The Surface Composition of Ceres, 2011, Space Science Reviews.